FOLIA VETERINARIA

The scientific journal of the
UNIVERSITY OF VETERINARY MEDICINE AND
PHARMACY IN KOŠICE — Slovakia

ISSN 0015-5748
eISSN 2453-7837

2

LXII • 2018

FOLIA VETERINARIA is a scientific journal issued by the University of Veterinary Medicine and Pharmacy in Košice, Komenského 73, 041 81 Košice, Slovakia.
The journal is published quarterly in English (numbers 1—4) and distributed worldwide.

Contact: tel.: +421 915 984 669
e-mail: folia.veterinaria@uvlf.sk

Electronic Publisher: De Gruyter Poland, Bogumila Zuga 32A
01-811 Warsaw, Poland

ISSN 2453-7837 on-line
ISSN 0015-5748 print
EV 3485/09

Publisher's identification number: IČO 00397474

June 2018

FOLIA VETERINARIA

PUBLISHED BY
THE UNIVERSITY OF VETERINARY MEDICINE AND PHARMACY IN KOŠICE
SLOVAKIA

Folia Veterinaria
Vol. 62, 2, 2018

VYDÁVA
UNIVERZITA VETERINÁRSKEHO LEKÁRSTVA A FARMÁCIE V KOŠICIACH
2018

FOLIA VETERINARIA, 62, 2, 2018

CONTENTS

sciendo

DOI: 10.2478/fv-2018-0011

FOLIA VETERINARIA, 62, 2: 5—12, 2018

ECHINOCHASMUS SWABIENSIS N. SP. (DIGENEA: ECHINOSTOMATIDAE) FROM BLACK KITE (*MILVUS MIGRANS MIGRANS*) IN SWABI DISTRICT, PAKISTAN

Suleman, S.[1], Khan, M. S.[2], Zhu, X. Q.[3], Dharejo, A. M.[4] Uwalaka, E. C.[5], Shah, M.[6], Adediran, O. A.[7]

[1]Department of Zoology, Hazara University, Mansehra
[2]Department of Zoology, University of Swabi, Khyber Pakhtunkhwa
Pakistan
[3]Lanzhou Veterinary Research Institute, Chinese Academy of Agricultural Sciences
Lanzhou, Gansu Province 730046
China
[4]Department of Zoology, University of Sindh, Jamshoro
Pakistan
[5]Department of Veterinary Parasitology and Entomology
Micheal Okpara University of Agriculture, Umudike
Nigeria
[6]Center for Animal Sciences and Fisheries, University of Swat
Pakistan
[7]Department of Veterinary Parasitology, University of Ibadan
Nigeria

emmauwalaka@gmail.com

ABSTRACT

A new species of the genus *Echinochasmushas* been described from the small intestine of the black kite (*Milvus m. migrans*) collected from Swabi, Khyber Pakhtunkhwa, Pakistan and identified as *E. swabiensis n.* sp. The new species is different from its congeners in its body size; it has 22 collar spines which includes two corner spines on one side, four on the other side and eight marginal plus ventral spines on each side. There areteg-umental-scale like spines interspersed on the anterior margin of the ventral sucker with a smaller, terminal oral sucker. The pharynx is nearly twice as large as the oral sucker, while the ventral sucker is nearly six times as large as the oral sucker. The suckers' width ratio is 1 : 4.7 to 1 : 5.6. The vitelline follicles are compact and denser at the lateral sides masking the caeca. This species has been added to the record of trematodes circulating among avian species, especially in the study area.

Key words: Digenea; *Echinochasmus swabiensis*; fluke; *Milvus migrans*; Pakistan; Swabi

INTRODUCTION

The family Echinostomatidae is the largest family of parasitic trematodes, parasitizing birds and mammals in-

cluding man [2, 5, 12, 15, 19, 21, 22, 23]. They are characterized by having a head collar with spines and their cercaria encyst in invertebrates like mollusks, insect larvae, freshwater snails, crustaceans, and the gills of tadpoles and fishes [6, 9, 18, 24, 25]. Echinochasminae is one of ten subfamilies of the family Echinostomatidae distinguished by having a well-developed head collar with interrupted spines arranged in either a single row or sometimes in a double row [4, 21, 25].

The genus *Echinochasmus* Dietz, 1909, is characterized by a well-developed head collar bearing 20—24 or 30—34 spines with the teguments covered by scale like spines, long pre-pharynx, large pharynx, dextral ovary, vitelline field confluent in post-testicular region, a cirrus pouch lying anterior to the ventral sucker or overlapping it, and a uterus which is short with few large eggs when gravid [11, 25].

Species of the genus *Echinochasmus* Dietz, 1909 are cosmopolitan in distribution and parasitize birds and mammals [11, 12, 17, 21, 25]. Different authors have reported different species of the genus *Echinochasmus* from various avian hosts [10, 13, 16, 20]. Different reports also exist in Pakistan [1, 3, 7, 8, 23]. This study is aimed at investigating the presence of flukes in the small intestine of the black kite and describes their morphological characterization. This study is the latest addition to the genus *Echinochasmus* recovered from the black kite.

MATERIALS AND METHODS

Twelve apparently healthy, adult Black kites (*Milvus m. migrans*, Boddaert) were trapped alive (July 2012 to March 2014) from various localities of Swabi (34° 7' 48" N and 72° 28' 11" E), Khyber Pakhtunkhwa, Pakistan and brought to the laboratory of parasitology at Hazara University, Mansehra, Pakistan. These birds were anesthetized and necropsied for the presence of trematode parasites. The entire digestive system with other visceral organs including lungs, liver and heart were removed and placed in separate petri-dishes containing physiological saline. These organs were examined with the aid of a dissection microscope. Four specimens were found in the contents of the intestine of a single bird. The flukes were removed, placed in saline solution until dead and then fixed in AFA solution (70 % ethanol, 92 ml; formaldehyde, 6 ml; and acetic acid, 2 ml) under tolerable pressure of glass slides. They were then stained in Mayer's carmalum, dehydrated in graduated series of ethanol (70—100 %), clarified in xylene and mounted permanently in Canada balsam for further study. Line drawings were prepared with the aid of a drawing tube and photomicrographs were taken by using an Olympus DP12 camera. All measurements were given in millimetres. By using trematodes identification keys and the available literature [11, 12, 22, 25] the recovered specimens were placed in the genus *Echinochasmus* Dietz, 1909. Holotype specimens were deposited in the Laboratory of Parasitology, at Hazara University, Mansehra, Pakistan.

RESULTS

Table 1. Taxonomic summary

Subfamily	**Echinochasminae (Odhner, 1910)**
Species	*Echinochasmus swabiensis* n. sp
Host	Black kite (*Milvus m. migrans*, Boddaert)
Site of specimen collection	Small intestine
Locality type	Yar Hussain, Swabi
Number of specimen	4 from a single host, 12 samples examined
Frequency of appearance	8.33 %
Accession number	HUPE-1

The morphology of *Echinochasmus swabiensis n.* sp. was based on four specimens of these trematodes. The more clear permanently mounted slides were used for the morphological studies. The head end of these specimens presented the characteristic features of the genus *Echinochasmus* Dietz, 1909, with a small, triangular mouth opening and reniform head collar bearing 22 large spines in a single dorsally interrupted row (Figs. 1b and 1d).

The worms were small, thin, elongated, with a gradually tapering anterior end and somewhat broadly rounded posterior end. The total body length was 2.85—2.95 mm with a maximum width of 0.525—0.575 mm, at the region of acetabulum or its posterior border (Fig. 2a). The anterior body was 0.95—0.1 mm long while the posterior body was 1.9—1.95 mm long, so that the anterior body and posterior body length ratio was 1 : 2. The tegument was covered by scale like spines, interspersed only up to the region of the ventral sucker.

The oral sucker was terminal, slightly protruding and much smaller than the pharynx (Fig. 2a), measured 0.058—0.063 × 0.075—0.08 mm in size; nearly half of the size of the pharynx (Fig 2a). The head collar was 0.13—0.20 × 0.29—0.3 mm in size, bearing 2 corner spines on one side, while 4 on the other side with 8 marginal plus ventral spines on each side; so that one side consisted of 12 spines, while the other had 10 spines (Fig. 2b). The collar spines were 0.047—0.06 × 0.018—0.022 mm in size. The corner spines were smaller, 0.028—0.03 × 0.013—0.02 mm in size, while the marginal and ventral spines were 0.04—0.075 × 0.02—0.023 mm and 0.073—0.075 × 0.022—0.023 mm in size, respectively (Fig. 2d).

The pre-pharynx was present but varied in length from 0.05 to 0.063mm, due to the contraction of the neck of the flukes (Fig. 2a). The pharynx was nearly twice as large as the oral sucker (Fig. 2a), globular to nearly oval, measured 0.13—0.134 × 0.13—0.15 mm in size, followed by 0.33 to 0.5 mm long esophagus which was divided into two intestinal caeca at a distance of 0.45—0.59 mm from the anterior end of the body. The intestinal bifurcation occurred a short distance ahead of the ventral sucker and the intestinal caeca were masked by the lateral fields of the vitellaria (Fig. 2c). The ventral sucker was six times larger in length than the oral sucker, rounded to oval with well-developed muscular walls, 0.35—0.38 × 0.35—0.45 mm in size and was situated in the second quarter of the body at a distance of 0.65 to 0.83 mm from the anterior end of the body. The width of the suckers had a ratio of 1 : 4.7 to 1 : 5.6.

The two testes were with entire margins, post-equatorial, median, lying one behind the other, contiguous and separated by a smaller gap and were sub-equal in size. The anterior testis was transversely elongated, somewhat rectangular, 0.11—0.25 × 0.26—0.35 mm in size and was situat-

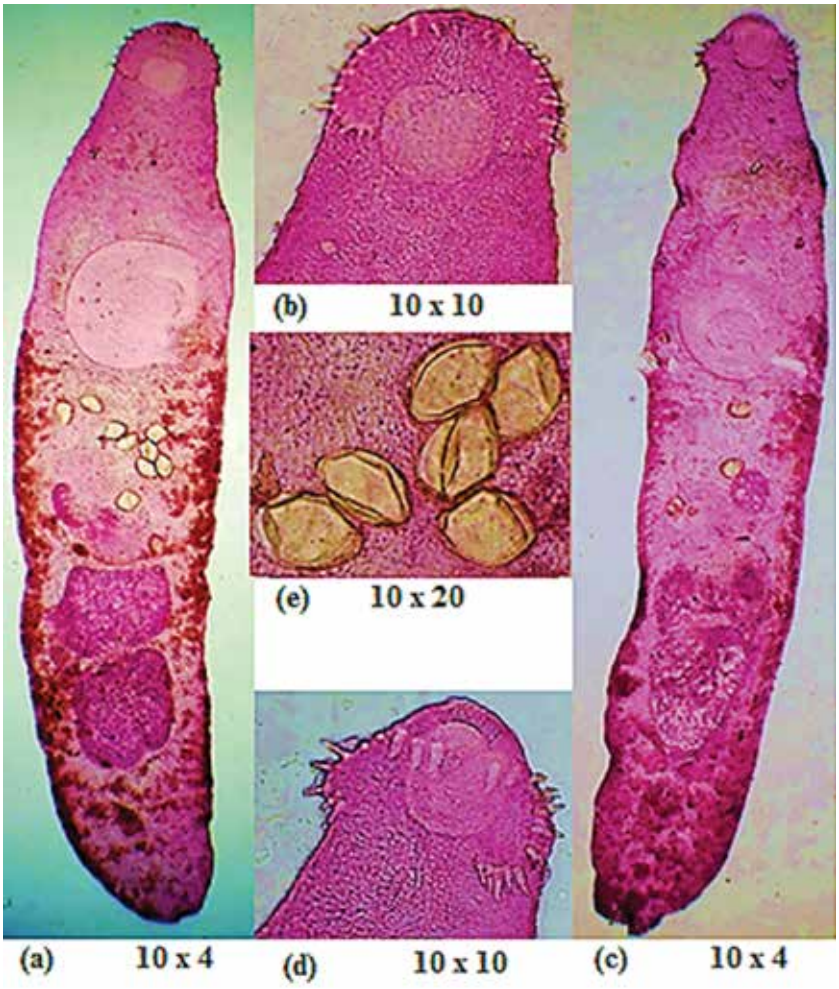

Fig. 1. Photomicrographs of *Echinochasmus swabiensis n.* sp. and (c) — entire specimens; (b) and (d) — head collars; (e) — eggs

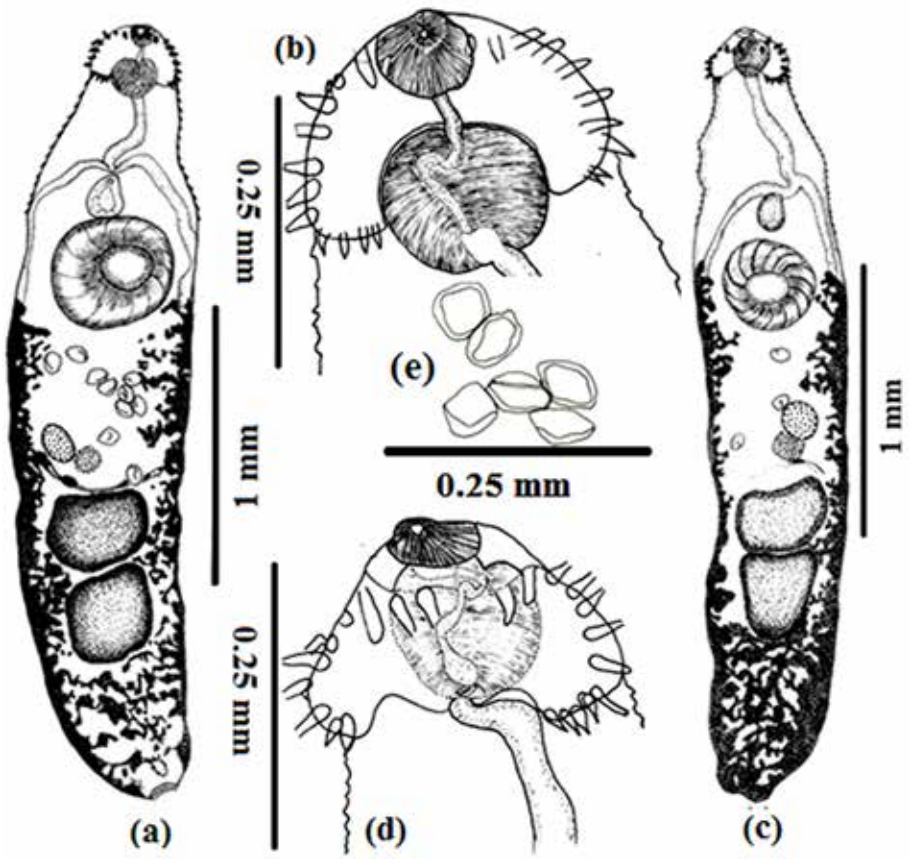

Fig. 2. Diagrams of *Echinochasmus swabiensis n.* sp.
and (c) — whole specimens; (b) and (d) — head collars;(e) — eggs

ed at a distance of 0.6 to 0.65 mm from the posterior border of the ventral sucker (Fig. 2a and 2c). The posterior testis was longer than wide, quadrilateral or nearly triangular with tapered posterior end and measured 0.325—0.372 × 0.3—0.322 mm in size. The distance between the posterior border of the posterior testis and the posterior end of the body was 0.47 to 0.575 mm. The vasa efferentia were inconspicuous. The cirrus pouch was small, nearly oval, 0.15—0.164 × 0.1—0.13 mm in size and was situated between the intestinal bifurcation and ventral sucker or overlapping the anterior border of the ventral sucker. The cirrus was inconspicuous and the genital pore laid between the intestinal bifurcation and the ventral sucker (Fig. 2c).

The ovary was rounded to oval in shape, equatorial or post-equatorial and laid slightly at one side of the body; 0.28 to 0.3 mm away from the posterior border of the ventral sucker (Fig. 2a). It was much smaller than the testes and measured 0.145—0.15 × 0.1—0.125 mm in size. The shell gland was smaller than the ovary, sub-median, situated in the close proximity of the ovary. The vitelline reservoir with transverse vitelline ducts was situated posterior to the shell gland and anterior to the anterior testis. The vitellaria consisted of small follicles which were compact and denser at the lateral sides, masking the caeca. The vitelline folds commencing from about the mid portion of the ventral sucker or its posterior border, ran laterally and met freely behind the posterior testis. The uterus consisted of a few folds containing few, yellowish, large eggs, 0.058—0.078 × 0.046—0.06 mm in size (Fig. 1a and 2a). The excretory bladder had a chamber like appearance and opened into the terminal or sub-terminal excretory pore (Fig. 2c).

DISCUSSION

The genus *Echinochasmus* was proposed by Dietz, 1909 with the type species *E. coaxatus*, in Europe, Central Asia, Siberia [25, 11].

Our studied species is larger in size (2.85—2.95 × 0.525—0.575) than *E. liliputanus* (Looss, 1896) Odh-

ner, 1910 (0.5—0.8×0.2), *E. japonicas* Tanabe, 1926 (0.6—0.9×0.16—0.18), *E. microacetabulum* Leonov, 1958 (0.702—0.936×0.28—0.34), *E. milvi* Yamaguti, 1939 (0.7—1.2×0.27—0.32), *E. zubedakhaname* Nasir, Dietz, 1968 (0.850—1.675×0.225—0.555), *E. donaldsoni* Beaver, 1941 (0.88—1.84×0.256—0.32), *E. dietzevi* Issaitschikoff, 1927 (1.13—1.47×0.39—0.55), *E. bagulai* Verma, 1935 (1.0—1.75×0.25—0.5), *E. megavitellus* Lal, 1939 (1.05×0.45), *E. haliasturis* Odening, 1962 (1.1—1.9×0.8—0.9), *E. vindhianae* Vasudev, 1973 (1.82—1.92×0.38—0.45), *E. spinosus* (Odhner, 1910) Skrjabin, Bashkirova, 1956 (2.02—2.25×0.4—0.5), *E. coaxatus* Dietz, 1909 (2.13—2.56×0.65—0.81) and *E. spinulosus* Rudolphi, 1809 (1.09—2.7×0.41—0.43). It is however smaller in size than *E. euryporus* Looss, 1896 (3—4×0.85), *E. novalichesensis* Tubangui, 1932 (2.32—3.25×0.48—0.75), *E. botauri* Baer, 1923 (3.25×0.65), *E. amphiboles* Kotlan, 1922 (4.16—5.16 ×0.765), *E. tobi* (6.5—7.5×1.1—1.3), *E. fanielicus* (Odhner, 1910), Prudhoe, 1944 (8.65×1.55) and *E. antigonus* Gupta, 1955 (11.75—12.92×1.2—1.43).

Our studied species is also bigger in size than the species recovered from other avian hosts in Pakistan. These species include *E. jamshorensi* (0.432×0.124), *E. mohiuddini* (0.780—1.613×0.215—0.416), *E. passeri* (0.725×0.285) and *E. mazharuddini* (0.81—0.88×0.39—0.42) described by [3, 7, 8] and [23], respectively.

Using the number of spines as morphological characteristics, our studied species has a resemblance with *E. cohensi* Rao, 1951, *E. euryporus, E. gorsakii*, 1939, *E. microacetabulum, E. milvi, E. mordax* (Looss, 1899), Price, 1931, *E. muraschkinzewi* Bashkirova, 1941, *E. spinosus, E. spinulosus, E. vindhianae*, in having 22 spines; while it differs from *E. accipiteri* Bhutta, Khan, 1975, *E. japonicus, E. botauri, E. beleocephalus, E. bagulai, E. novalichesensis, E. megavitellus, E. oligolecithosus* Mendheim, 1940, *E. tobi, E. militaris* Leonov, 1958, *E. liliputanus, E. coaxatus, E. famelicus* (Odhner, 1910), Prudhoe 1944, *E. amphibolus, E. ruficapensis, E. perfoliatus* Ratz, 1908, *E. africanum* Stiles, 1901, *E. jamshorensi, E. mohiuddini* which has 24 spines; *E. zubedakhaname, E. donaldsoni, E. dietzevi* which has 20 spines; *E. passeriwith* 26 spines; and *E. mazharuddini* with 28 spines.

The eggs of our specimen under study (58—78×46—60 μm or 0.058—0.078×0.046—0.06 mm) (Fig. 1e and 2e) are larger in size than those of *E. zubedakhaname* (42—67×32—40) and *E. euryporus* (67×42); while they are smaller than the eggs of *E. gorsakii* (72—90×51—57), *E. oligolecithosus* (73—83×54—76), *E. milvi* (78—84×51—57), *E. botauri* (84—97×46—65), *E. colymbi* Shigin in Skrjabin, Bashkirova, 1956 (87×60), *E. novalichesensis* (95.6—108×58.2—70.7), *E. amphiboles* (97.2—102.6×59.4—67.5), *E. tobi* (102—117×60—72), *E. antigonus* (104—126×57—68) and *E. famelicus* (110—120×70—80).

Our studied species' eggs differ from the eggs of *E. beleocephalus* (73—81×34—43), *E. vindhianae* (67×40) and *E. spinosus* (74—80×40) in width and from the eggs of *E. muraschkinzewi* (81—96×43—47), *E. cohensi* (84—89×49—52.5) and *E. mirus* Mendheim, 1940 (92—100×4856) in length.

The type species, *E. coaxatus* Dietz, 1909, is sub-equal to our studied species in the size of the pharynx and ovary, resembling it in the extension of the vitellaria but differs in having a maximum width in the region of the testes; 24 larger collar spines (0.0768—0.0816×0.019—0.0216) with 3 corner spines and 9 marginal spines on each side; cuticle spines scattered up to the posterior level of the acetabulum; oral sucker two times as large as the oral sucker of our studied species; smaller ventral sucker; longer prepharynx and esophagus; larger testes lie mid-way between the ventral sucker and rear end of the body. Moreover, the ratio in size of the oral sucker to the acetabulum is about 1:2.6 in *E. coaxatus* and 1 : 4.7 to 1 : 5.6 in our studied species.

E. mordax (Looss, 1899), Price, 1931 resembles this new species in the number of spines; size of oral sucker and eggs, and extension of the vitellaria; but differs in body shape and arrangement of the collar spines (2 corner and 9 marginal spines on each side); having a smaller body with a maximum width at the level of the cirrus sac; smaller pharynx and ventral sucker; tegument spines distributed up to the level of the posterior testis but very dense in between the ventral sucker and head; smaller and globular testes; cirrus sac oval extending dorsally from the intestinal fork to 2/3 of the length of the acetabulum; the size of the ventral sucker is nearly equal to the size of the pharynx of the present studied species.

E. bagulai Verma, 1935, differs in having a smaller body with a maximum width at about the middle of the testes; 24 collar spines with 4 corner spines and 8 marginal spines on each side; the spines on the cuticle extend to the posterior end of the body; the pharynx has the same mean diameter as the oral sucker; the acetabulum is three times as large as the oral sucker and situated at the commence-

ment of the middle third of the body. The oral sucker is larger, while the pharynx and acetabulum are smaller and have 9 to 15 numbers of eggs.

E. vindhianae Asudev, 1973 collected from an Indian Tawny eagle, Aquila rapaxvindhiana is similar in having 22 collar spines; maximum width at the level of the acetabulum; caeca are masked by the vitelline follicles and the vitelline fields extending anteriorly up to the mid-level of the acetabulum but differs in having 3 corner spines and 8 marginal spines on each side of the head collar; the oral sucker and pharynx are sub-equal in diameter; shorter esophagus; intestinal fork occurs at a distance of 0.37—0.44 mm from the anterior end of the body; suckers width a ratio of 1 : 4.2; and the testes are oval in shape and situated in the middle of the body.

E. novalichesensis Tubangui, 1932, collected from the small intestine of Hyptaenidiatorquata in Novaliches, Rizal, Luzon, differs in having somewhat larger body with a maximum width across the anterior testis; larger head collar bearing 24 spines with 3 corner spines and 9 marginal spines on each side; tegumental spines distributed up to the level of the anterior testis; suckers width a ratio of 1 : 2.7; much smaller pharynx; oval and elongated cirrus pouch; ovary equatorial or pre-equatorial; shell gland median and larger than ovary.

E. spinulosus Rudolphi, 1809, syn. *Monilifer spinulosus* Diets, 1910, differs in having a smaller body; 2 corner spines and 9 marginal spines on each side of the head collar; much smaller pharynx (sub-equal to the size of oral sucker); much smaller ventral sucker; suckers with a width ratio of 1 : 2.8 to 1 : 3.2; vitelline fields commencing from the level of the testes and vitelline ducts arise from the anterior end of the vitelline fields; ovary smaller in size and situated just before the anterior testis. Differences are also found in the shape of the testes.

E.macrocaudatus Ditrich et al., 1996, differs in having a smaller body; tegumental spines covered 2/3 of the dorsal surface and ventral surface of the body; smaller collar spines, varies in number, 22 (11+11), 23 (11+12), 24 (12+12); larger, sub-terminal oral sucker; a smaller ventral sucker; smaller pharynx; suckers width a ratio of 1 : 1.68; ventral sucker situated at about 2/5 of the body length; prepharynx short or absent; cirrus sac elongated and anterodorsal to the acetabulum with a large seminal vesicle.

Our studied species is closely related with *E. schwartzi* Price, 1931, in general body shape, extension of the vitellaria and position of ventral sucker and gonads, but differs in having a smaller body with a maximum width at the region of the anterior testis; smaller (0.037—0.051 × 0.011—0.015) 22 collar spines (2 corner and 9 marginal on each side), tegumental spines covered the body up to the posterior margin of the posterior testis; sub-terminal, larger oral sucker; cirrus sac piriform, extending to the posterior border of the ventral sucker and smaller ovary. The size ratio of the oral sucker to acetabulum is about 1:2 in *E. schwartzi* and 1 : 4.7 to 1 : 5.6 in our species.

E. zubedakhaname Nasir, Diaz, 1968, reported by Argumedo, Macedo [14] in 1991 differs in having a smaller body with a maximum width at the level of the testes; tegumental spines covered the body up to the posterior margin of the posterior testis; head collar consists of 20 smaller spines, with 3 corner spines and 7 marginal spines on each side; larger oral sucker, longer esophagus and smaller pharynx; smaller, equatorial ventral sucker; suckers width a ratio of 1 : 1.9 to 1 : 2.5; cirrus sac elongated and situated lateral to the anterior margins of the acetabulum; ovary larger, postero-lateral to the acetabulum; vitelline fields extra-caecal and exceeds the anterior margin of acetabulum.

Our specimen also differs from the species reported from Pakistan in size and shape of the body; number and arrangement of collar spines; distribution of vitellaria; size, shape and position of gonads and other organs.

E. mohiuddini [7] differs in size and shape of the body; number and arrangement of collar spines; size and position of the pharynx; shape, size and position of cirrus sac and shape and size of the testes. *E. passeri* [8] differs in general body shape; number and arrangement of collar spines; size of oral sucker, pharynx and ventral sucker; sucker width the ratio (1 : 2.06); length of pre-pharynx and esophagus; shape, size and position of gonads; extension and distribution of vitellaria. *E. mazharuddini* [23] differs in having a smaller body with maximum width at the level of the testes; a smaller head collar bearing 28 spines including 4 corner spines; longer pre-pharynx; smaller ventral sucker (twice as large as the oral sucker); larger cirrus sac; larger, pear-shaped ovary, overlapped with the acetabulum and anterior testis; smaller testes; extension and distribution of the vitellaira. Moreover, the post-testicular space is 0.122—0.139 mm long in *E. mazharuddini* while 0.47 to 0.575 mm long in our species. *E. jamshorensi* [3] differs in having a smaller body; smaller head collar bearing 24 spines; larger

oral sucker; smaller pharynx; much smaller ventral sucker; smaller cirrus sac; smaller gonads and longer post-testicular space.

CONCLUSIONS

The variations in our studied specimens from the previously described species of the genus *Echinochasmus*, strengthen the statement that the specimens discovered in our investigation are new to science. This also calls for more research into this particular family especially in the area of its systematics and epidemiology. The new species is named as *Echinochasmus swabiensis*.

Etymology: Name of new species refers to the locality of the host.

"Nomenclatural acts": *This work and the nomenclatural acts it contains have been registered in the Zoo Bank. The Zoo Bank Life Science Identifier (LSID) for this publication is:LSIDurn:lsid:zoobank.org:pub:7F675C67-1A8B-4CC3-B143-653CD3EDD107.*

REFERENCES

1. **Bhutta, M. S., Khan, D., 1975:** Digenetic trematodes of vertebrates from Pakistan. *Bull. Dept. Zool. Univ. Punjab*, 8, 1—175.
2. **Chai, J. Y., Lee, S. H., 2002:** Food borne intestinal trematode infections in the republic of Korea. *Parasitol. Int.*, 51, 129—154.
3. **Channa, M. A., Khan, M. M., Shaikh, A. A., Dharejo, A. M., 2009:** *Echinochasmu sjamshorensi*, new species (Trematoda: Echinostomatidae) from Pond Heron, Ardeolagrayii (Aves: Ardeidae) of Jamshoro, Sindh, Pakistan. *Proc. Parasitol.*, 48, 151—158.
4. **Choi, S., Lee, D., Park, H., Oh, M., Jeon, H. K., Lee, Y., Eom, K. S., 2014:** Three *Echinostome* species from wild birds in the Republic of Korea. *Korean J. Parasitol.*, 52, 513—520.
5. **Choi, M. H., Kim, S. H., Chung, J. H., Jang, H. Y., Joon, H. E., Chung, B. S., 2006:** Morphological observations of *Echinochasmus japonicas* cercariae and the *in vitro* maintenance of its life cycle from cercariae to adults. *J. Parasitol.*, 92, 236—241.
6. **Detwiler, J. T., Zajac, A. M., Minchella, D. J., Belden, L. K., 2012:** Revealing cryptic parasite diversity in a definitive host: echinostomes in muskrats. *J. Parasitol.*, 98, 1148—1155.
7. **Dharejo, A. M., Bilqees, F. M., Khan, M. M., 2007:** *Echinochasmus mohiuddini*, new species (Trematoda: Echinostomatidae) from Paddy Bird *Ardeolagrayii* (Ardeidae) of Hyderabad, Sindh, Pakistan. *Proc. Parasitol.*, 39, 285—288.
8. **Dharejo, A. M., Birmani, N. A., Khan, M. M., 2010:** *Echinochsmus passeri*, new species (Digenea: Echinostomatidae) from gallbladder of House Sparrow, Passer domesticus (Aves: Passeridae) of Hyderabad, Sindh, Pakistan. *Proc. Parasitol.*, 50, 139—145.
9. **Dimitrov, V., Kanev, I., Bezprozvanich, V., Radev, V., 1998:** Argentophilic structures of the miracidium of *Echinochasmus perfoliatus* (Trematoda: Echinosmatidae). *Parasite*, 5, 185—188.
10. **Faltynková, A., Gibson, D. I., Kostadinova, A., 2008:** A revision of Petasiger Dietz, 1909 (Digenea: Echinostomatidae) and a key to its species. *Syst. Parasitol.*, 71, 1—40.
11. **Gibson, D. I., Jones, A., Bray, R. A., 2005:** *Keys to the Trematoda*, Vol. 2., CABI Publishing and the Natural History Museum, Wallingford and London, UK, 745 pp.
12. **Kostadinova, A., Jones, A., 2005:** Superfamily Echinostomatoidea. In **Jones, A., Bray, R. A., Gibson, D. I.:** *Keys to the Trematoda*, Vol. 2., CABI Publishing and the Natural History Museum, Wallingford and London, UK, 5—8.
13. **Kudlai, O., Kostadinova., A, Pulis, E. E., Tkach, V. V., 2015:** A new species of *Drepanocephalus* Dietz, 1909 (Digenea: Echinostomatidae) from the Double-crested Cormorant *Phalacrocoraxauritus* (Lesson) (Aves: Phalacrocoracidae) in North America. *Syst. Parasitol.*, 90, 221—230.
14. **Argumedo, R. L., Macedo, L. A., 1991:** Trematodos de aves IV. Estudio de *Echinochasmus zubeddakhanamae* (Trematoda: Echinostomatidae) recuperados experimentalmente. *Annales Inst. Biol. Univ. Nac. Auton. Mex. Ser. Zool.*, 62, 11—14.
15. **Leles, D., Cascardo, P., dos Santos Freire, A., Maldonado, A., Sianto, L., Araujo, A., 2014:** Insights about echinostomiasis by paleomolecular diagnosis. *Parasitol. Int.*, 63, 646—649.
16. **Overstreet, R. M., Cook, J. O., Heard, R. W., 2009:** Trematoda (platyhelminthes) of the Gulf of Mexico. In **Felder, D. L., Camp, D. K.:** *Gulf of Mexico-Origins, Waters and Biota Biodiversity*. Texas A and M University Press, College station, Texas, 419—486.
17. **Platt, T. R., 2006:** First report of *Echinochasmus* sp. from the snapping turtle (*Chelydraserpentina* L.) from Reelfoot Lake, Tennessee, USA. *Comp. Parasitol.*, 73, 161—164.
18. **Scholz, T., Ditrich, O., Vargas-Vázquez, J., 1996:** *Echinochasmus leopoldinae* n. sp. (Trematoda: Echinostomatidae) and data on its life-cycle. *Syst. Parasitol.*, 33, 157—165.
19. **Seo, B. S., Lee, S. H., Chai, J. Y., Hong, S. J., 1985:** Studies on intestinal trematodes in Korea XX. Four cases of natural hu-

man infection by *Echinochasmus japonicus*. *Korean J. Parasitol.*, 23, 214—220.

20. Supelveda, M. S., Spalding, M. G., Kinsella, J. M., Forrester, D. J., 1996: Parasitic helminthes of the Little Blue Heron, Egrettacaerulea, in Southern Florida. *J. Helminthol. Soc. Wash.*, 63, 136—140.

21. Tkach, V. V., Kudlai, O., Kostadinova, A., 2016: Molecular phylogeny and systematics of the Echinostomatoidea Looss, 1899 (Platyhelminthes: Digenea). *Int. J. Parasitol.*, 46, 171—185.

22. Toledo, R., Radev, V., Kanev, I., Gardner, S., Fried, B., 2014: History of echinostomes (Trematoda). *Acta Parasitol.*, 59, 555—567.

23. Ujan, H. M., Birmani, N. A., Shaikh, A. M., 2014: *Echinochasmus mazharuddini* n. sp. (Digenea: Echinostomatidae) from the Bank Myna *Acridotheres ginginianus* L. (Passeriformes: Sturnidae) in Sindh province, Pakistan. *J. Entomol. Zool. Stud.*, 2, 226—232.

24. Wojdak, J. M., Clay, L., Moore, S., Williams, T., Belden, L. K., 2013: *Echinostoma trivolvis* (Digenea: Echinostomatidae) second intermediate host preference matches host suitability. *Parasitol. Res.*, 112, 799—805.

25. Yamaguti, S., 1971: *Synopsis of Digenetic Trematodes of Vertebrates*. Vol. II., Keigaku Publishing Co., Tokyo, Japan, 698 pp.

Received August 9, 2017

Accepted November 14, 2017

sciendo

DOI: 10.2478/fv-2018-0012

FOLIA VETERINARIA, 62, 2: 13—18, 2018

PROTECTIVE ROLE OF *AGRIMONIA EUPATORIA* L. IN HEAVY METAL INDUCED NEPHROTOXICITY

Marcinčáková, D.[1], Falis, M.[1], Schusterová, P.[2]
Váczi, P.[1], Marcinčák, S.[3], Legáth, J.[1]

[1]Department of Pharmacology and Toxicology
[2]Deparment of Microbiology and Immunology
[3]Department of Food Hygiene and Technology
University of Veterinary Medicine and Pharmacy, Košice
Slovakia

dana.marcincakova@uvlf.sk

ABSTRACT

The aim of this study was to evaluate the potential protective role of *Agrimonia eupatoria* L. in heavy metal induced nephrotoxicity. Rabbit kidney epithelial cells (RK13) were used as the model cell line. They were exposed to three different heavy metal compounds: cadmium chloride dihydrate $CdCl_2.2H_2O$ (15 and 20 mg.l^{-1}), potassium dichromate K2Cr2O7 (1, 10 mg.l^{-1}), and zinc sulfate heptahydrate $ZnSO_4.7H_2O$ (50, 150 mg.l^{-1}) simultaneously with agrimony (ethanolic extract, 100 mg.l^{-1}). The cell response was recorded using the xCELLigence system or real-time cell analysis (RTCA) as a cell index (CI) and expressed as cell adherence (%) compared to control cells without treatment. The potential nephroprotective effects were recorded in cells treated with chromium (1 a 10 mg.l^{-1}) and agrimony, where the cell adherence increased from 95.11 ± 11.25 % and 7.24 ± 0.33 % to 103.26 ± 1.23 % and 68.54 ± 4.89 % (P < 0.05) respectfully and also with a combination of agrimony and zinc (150 mg.l^{-1}), where the adherence increased from 57.45 ± 1.98 % to 95.4 ± 6.95 %. During the cell exposure to cadmium in combination with agrimony, the protective effect was not recorded; the adherence of cells was even decreased (P < 0.05).

Key words: agrimony; cell response; cytotoxicity; heavy metals; kidney; xCELLigence system

INTRODUCTION

In recent years, there has been an increased concern about ecological and global public health impact related to environmental contamination by heavy metals. Their wide use in industrial, agricultural, domestic and technological applications has resulted in a rapidly increased human exposure. Environmental pollution has become very prominent in point source areas, such as mining, foundries and smelters, and other metal-based industrial operations. Reported sources of heavy metals in the environment include geogenic, industrial, agricultural, pharmaceutical, domestic effluents, and atmospheric sources [6, 15]. Heavy metal-induced toxicity and carcinogenicity involves many

mechanistic aspects, some of which have not been clearly elucidated or understood. However, each metal is known to have unique features and physico-chemical properties that result in its specific toxicological mechanisms of action [15].

The first target organ of heavy metals and other xenobiotics toxicity is the kidney, due to the high capacity of renal epithelium to transport and accumulate these toxins [3]. Renal cells are often exposed to higher concentrations of xenobiotics, because they play the most important role in the excretion of various drugs and toxic substances. According to the nature, dose, route, and duration of exposure, the kidney displays diverse alterations in renal function ranging from mild tubular dysfunction to severe renal failure [14].

The trend of today is to search and explore potentially protective medicinal resources in phytotherapy. Because of its widespread use in folk medicine, agrimony (*Agrimonia eupatoria*, L.) provokes a great deal of scientific interest. Agrimony is well-known for its use as a raw material for the extraction of medicinal ingredients or production of drugs in the pharmaceutical industry. The plant is recognized for its traditional use in folk medicine and possesses anti-inflammatory, neuroprotective, antidiabetic, antiobesity, hepatoprotective, and anticancer properties. It also has a positive effect on the alleviation of urinary tract disorders [1, 2, 4, 10, 18].

Nowadays, in the development of new drugs in preclinical research and toxicological testing, cell-based assays have been used as suitable substitute methods for animal experiments. Viability and cytotoxicity assays are performed to determine the effect of various agents added to the cells with respect to their viability after the treatment. The xCELLigence system or real time cell analysis (RTCA) was used for label-free and dynamic monitoring of cell responses to cytotoxicants. Cellular status changes (cell number, viability, morphology, and adherence) were continuously monitored by measuring the electrical impedance. The presence of the cells leads to an increase in the electrode impedance. The more cells are attached to the sensor, the higher the impedance that could be monitored by RTCA. Because the test is label free, the RTCA assays allows real-time, automatic and continuous monitoring of the cellular status changes throughout the process of the cell-toxicant interactions [16, 17].

In our study, we evaluated the protective role of ethanolic extract of agrimony in nephrotoxicity induced by selected heavy metals using a model rabbit epithelial kidney cell line (RK13). The cells were exposed to heavy metals simultaneously with agrimony extract and the cell response was monitored by xCELLigence system during 24 h. While adherence is an important characteristic of RK13 cells, its loss may lead to cell death. Based on the increase or decrease of cell adherence, we evaluated the potential nephroprotective effects of agrimony.

MATERIALS AND METHODS

Plant extract

The ethanolic extract of *Agrimonia eupatoria* L. (Calendula, Nová Ľubovňa, Slovakia) in a powdered form was diluted with water to a final concentration of 100 mg.l^{-1}. This concentration was selected based on a preliminary study (data not shown) which compared the effects of different concentrations (0.01—1000 mg.l^{-1}) on cell adherence.

Heavy metals — stock solution

Chemicals of analytical grade purchased from Sigma Aldrich (Germany) were diluted and tested at the final concentrations: cadmium chloride dihydrate — $CdCl_2.2H_2O$ (15 and 50 mg.l^{-1}), potassium dichromate — $K_2Cr_2O_7$ (1, 10 mg.l^{-1}), and zinc sulfate heptahydrate $ZnSO_4.7H_2O$ (50, 150 mg.l^{-1}). These solutions were sterilised by filtration using 0.22 µm filters (Milipore, Watford, UK). The concentrations were selected based on previously published studies [8].

Cell cultivation

For this experiment a rabbit kidney epithelial cell line (RK 13) obtained from the American Type Culture Collection (ATCC®CCL-37TM) was used. The cells were cultivated in Earl's Minimal Essential Medium (EMEM; Lonza, Valais, Switzerland) supplemented with 10 % (v/v) foetal bovine serum (FBS; Lonza, Valais, Switzerland) and 50 mg.l^{-1} gentamicin (Sigma Aldrich; St. Louis, USA) in a humidified atmosphere of 5 % CO2 at 37 °C. The cells were subcultured twice weekly and the passage number range was maintained between 20 and 25. In the experiments, RK13 cells were cultured in complete cultivation medium without antibiotics.

xCELLigence system

The xCELLigence system or real time cell analysis

(RTCA) was used for monitoring of the cell response during treatment with heavy metals simultaneously with agrimony.

The RTCA system included three components: the analyser and E-plate station; the integrated software; and a 16-well E-plate. The E-plate station was placed inside the CO_2 incubator and connected to the analyser outside the incubator through a thin cable. The E-plate containing the cells was placed onto the E-plate station inside the incubator and the experimental data were collected automatically by the analyser under the control of an integrated software. Cell attachment, spreading, and proliferation were continuously monitored using the xCELLigence system. The principles of RTCA technology has been described previously [12, 16, 17].

Briefly, 100 µl of medium was added into the 16-well E-plates for the background measurement. Subsequently, 1.5×10^4 cells/well in 50 µl of RK13-cell medium were seeded in the 16-well E-plates (Roche, Applied Science, Mannheim, Germany) and inserted into the plate station kept inside of a CO_2 incubator at 37 °C with 5 % CO_2 and humidified atmosphere. After 24 h, when RK13-cells were within a log phase, the agrimony (100 mg.l^{-1}) and subsequently heavy metals in selected concentrations were added to the cells. The RK13 cells without treatment served as the control. The cell response was monitored for 24 h and was expressed as the cell index (CI) measured automatically by the RTCA system once per hour until the end of the experiment. The parameter measured to specify the effect of the tested compounds was assessed as the normalized CI. The proliferative activity or cell adherence was expressed in % values using the following formula: % = CIsample × 100/ CIcontrol [9, 11].

Statistical analysis

The data were evaluated by the GraphPad Prism 3.00 software, using one-way analysis of variance (ANOVA) followed by Dunnett's multiple comparison test. The results were presented as the means ± SD. The significance level was set to $P < 0.5$.

RESULTS AND DISCUSSION

Heavy metals are essential in many industrial and manufacturing areas important for humans. However, the biotoxic effects of their over-exposure may be potentially life-threatening. Heavy metals are accumulated in the kidney and liver; for this reason, it is more accurate to estimate the degree and duration of exposition to them, by measuring their concentrations in renal and hepatic tissues rather than in the blood. The kidney is the target of heavy metals and the proximal tubule has been recognized for a long time, as the main site of accumulation and damage [14].

Natural substances are often used as protection against toxicants or in symptomatic therapy, because of their effectiveness and relatively low risk of adverse effects. Agrimony as a plant has a long tradition of use as a folk medicine and has shown great potential in the treatment and also in the protection of organisms against various diseases [1, 4, 10, 18].

In our work, we evaluated the potential protective role of ethanolic extract of agrimony during the exposure to heavy metals. The impact of heavy metals in combination with agrimony on the RK13 cell line may be seen in Figures 1—3. A significant increase in the proliferation in comparison to control cells (without treatment) was observed after the addition of agrimony alone (100 mg.l^{-1}) that indicated its supportive effect ($P < 0.05$). The exposure to chromium in the tested concentration caused a significant decrease in the proliferation compared to the control (95.11 ± 11.25 % and 7.24 ± 0.33 %), but after the simultaneous exposure also to agrimony, the adherence values were significantly improved (103.26 ± 1.23 %, 68.54 ± 4.89 %; Fig. 1).

The main effects after higher amounts of chromium intake, was tubular and glomerular damage and necrosis. The evidence of kidney damage from chronic exposure to lower levels was unclear. The toxicity has not been shown even in animals with chronic exposure, but there were biochemical changes indicating tubular damage [5].

The impact on human health after zinc intoxication has been described rarely. Toxicity *in vivo* is relatively low, because of quick dispersion in an organism. On the cellular level, zinc can be an important regulator of apoptosis and also death of neurons after brain damage [13].

In our experiment, the exposure of RK13 cells to the concentration of zinc used demonstrated in the beginning a decrease and subsequently an increase in cell adherence. The experimental cells did not reach the adherence of the control cells (Fig. 2). After exposure to the combination of zinc (50 mg.l^{-1}) and agrimony the adherence significantly decreased from 97.38 ± 7.79 %, recorded after exposure to

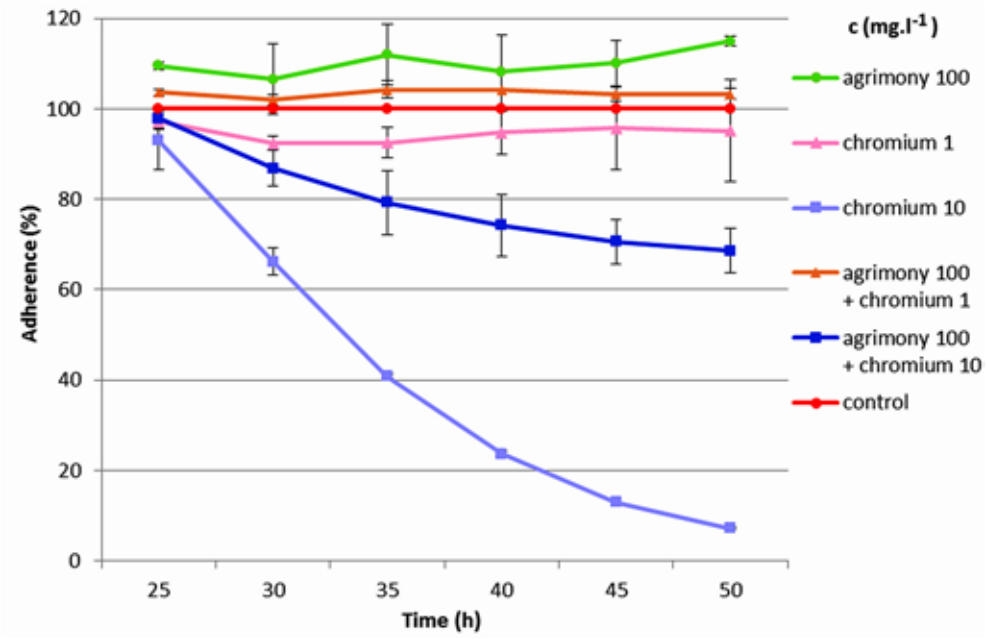

Fig. 1. Dynamic changes in cell adherence (%) after exposure to chromium and agrimony

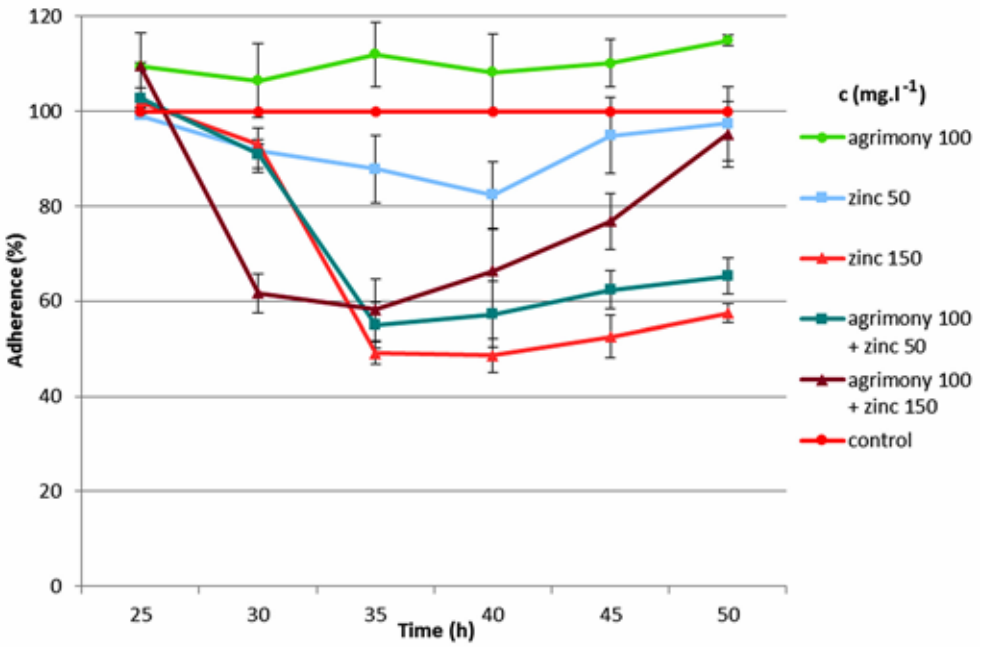

Fig. 2. Dynamic changes in cell adherence (%) after exposure to zinc and agrimony

zinc alone, to 65.28 ± 3.89 % ($P < 0.5$). However, the combination of agrimony and zinc (150 mg.l^{-1}) caused an increase in cell adherence to 95.14 ± 6.95 % from 57.45 ± 1.98 % measured after the addition of zinc (150 mg.l^{-1}). This result may be related to the protective effect of agrimony, however there are many specifics in zinc distribution and also functions in an organism. Therefore, more cellular studies are needed.

Cadmium is a widespread environmental contaminant that can adversely affect health. A large proportion of the exposure is via the respiratory or gastrointestinal tract. Important non-industrial sources of exposure are cigarette smoke and food (from contaminated soil and water). There is a direct link between exposure and the toxic renal effect of cadmium. In the case of renal impairment, proteinuria is the most important indicator of cadmium-induced nephrotoxicity [7].

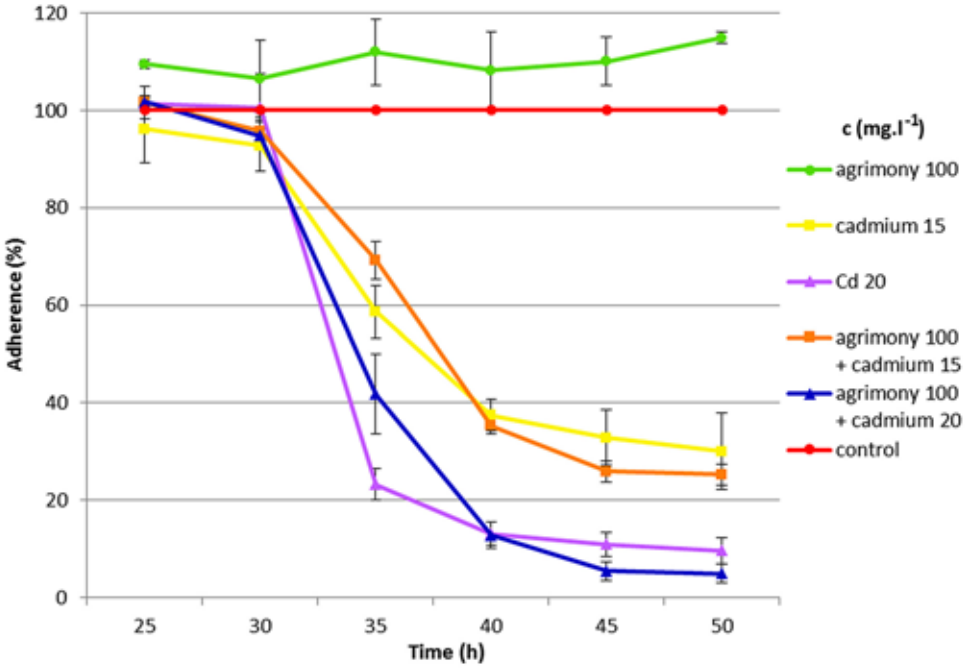

Fig. 3. Dynamic changes in cell adherence (%) after exposure to cadmium and agrimony

We confirmed a significant detrimental effect of the cadmium compound at both concentrations (15 and 20 mg.l^{-1}) after RK13 cells were exposed during 24 hours (Fig. 3). The nephroprotective effect of agrimony was not shown in combinations with cadmium. The adherence values were decreased significantly ($P < 0.05$). Cadmium is a very strong nephrotoxic agent. We observed a significant decrease in the adherence at the end of the cadmium exposure (30.04 ± 7.86 % at concentration 15 mg.l^{-1} and 9.64 ± 2.76 % at concentration 20 mg.l^{-1}) and when combined with agrimony, the adherence was even lower (25.25 ± 2.20 % and 4.93 ± 1.96 %). Thus, the nephroprotective effect of agrimony with cadmium exposure was not detected.

CONCLUSIONS

The kidney is an organ of high interest because it is the target of many xenobiotics, not only of heavy metals. Together with the liver, the kidneys play an important role in the elimination of toxic substances from the body. There is a high risk of glomerular necrosis or renal cells damage. The trend of today is to search and explore potentially protective or medicinal phytotherapeutic resources. The *in vitro* testing performed in our study showed a potential nephroprotective role of agrimony during the simultaneous exposure of renal epithelial cells to chromium and zinc.

Considering our results, we can state that due to its chemical constituents, agrimony has prospective pharmacological and other effects that may play a role in the development of new drugs.

ACKNOWLEDGEMENTS

This study was supported by the National Reference Laboratory for Pesticides of the University of Veterinary Medicine and Pharmacy in Košice, Slovakia, and by the Ministry of Education and Science of the Slovak Republic under the contract VEGA No. 1/0408/17.

REFERENCES

1. **Ad'hiah, A. L., Al-Bederi, O. N. H., Al-Sammarraie, K. W., 2013:** Cytotoxic effects of *Agrimonia eupatoria* L. against cancer cell lives *in vitro*. *J. Assoc. Arab. Univ. Basic Appl. Sci.*, 14, 87—92.
2. **Al-Snafi, A. E., 2015:** The pharmacological and therapeutic importance of *Agrimonia eupatoria*. *Asian Journal of Pharmaceutical Science and Technology*, 5, 112—117.

3. **Barbier, O., Jacquillet, G., Tauc, M., Cougnon M., Poujeol, P., 2005:** Effect of heavy metals on, and handling by, the kidney. *Nephron Physiol.*, 99, 105—110.
4. **Chan, S. M., Khoo, K. S., Sit, N. W., 2015:** Interactions between plant extracts and cell viability indicators during cytotoxicity testing: implications for ethnopharmacological studies. *Trop. J. Pharm. Res.*, 14, 1991—1998.
5. **Goyer, P. A., 2001:** *Casarett and Doull's Toxicology: The Basic Science of Poisons. Toxic Effects of Metals*. 6th edn., McGraw-Hill, USA, 811—867.
6. **He, Z. L., Yang, X. E., Stoffella, P. J., 2005:** Trace elements in agroecosystems and impacts on the environment. *J. Trace Elem. Med. Biol.*, 19, 125—140.
7. **Johri, N., Jacquillet, G., Unwin, R., 2010:** Heavy metal poisoning: the effects of cadmium on the kidney. *Biometals*, 23, 783—792.
8. **Marcinčáková, D., Falis, M., Legáth, J., Csank, T., Kšonžeková, P., Pistl, J., Milek, M., 2013:** Monitoring of selected heavy metals cytotoxicity on xCELLigence real-time cell analyser. In *Proceedings from the 33rd International Symposium: Industrial Toxicology,* 2013, June, 19—21, Faculty of Chemical and Food Technology of the Slovak University of Technology, Bratislava, Slovakia, 165—168.
9. **Martinez-Serra, J., Gutierrez, A., Muñoz-Capó, S., Navarro-Palou, M., Ros, T., Amat, J. C., et al., 2014:** xCELLigence system for real-time label-free monitoring of growth and viability of cell lines from hematological malignancies. *Onco-Targets and Therapy*, 7, 985—994.
10. **Muruzović, M. Ž., Mladenović, K. G., Stefanović, O. D., Vasić, S. M., Čomić, L. R., 2016:** Extracts of *Agrimonia eupatoria* L. as sources of biologically active compounds and evaluation of their antioxidant, antimicrobial, and antibiofilm activities. *J. Food Drug Anal.*, 24, 539—547.
11. **Özdemir, A, Ark, M., 2013:** xCELLigence Real Time Cell Analysis System: a new method for cell proliferation and cytotoxicity. *Niche*, 2, 15—17.
12. **Pan, T. H., Huang, B., Xing, J. Z., Zhang, W. P., Gabos, S., Chen, J., 2012:** Recognition of chemical compounds in contaminated water using time-dependent multiple dose cellular responses. *Anal. Chim. Acta*, 724, 30—39.
13. **Plum, L. M., Rink, L., Haase, H., 2010:** The essential toxin: impact of zinc on human health. *Int. J. Environ. Res. Public Health*, 7, 1342—1365.
14. **Reyes, J. L., Molina-Jijón, E., Rodríguez-Muñoz, R., Bautista-García, P., Debray-García, Y., Namorado, M. D. C., 2013:** Tight junction proteins and oxidative stress in heavy metals-induced nephrotoxicity. *Biomed. Res. Int.*, http://dx.doi.org/10.1155/2013/730789.
15. **Tchounwou, P. B., Yedjou, C. G., Patlolla, A. K., Sutton, D. J., 2012:** Heavy metal toxicity and the environment. *Molecular, Clinical and Environmental Toxicology*, Springer Basel, 133—164.
16. **Xing, J. Z., Zhu, L., Jackson, J. A., Gabos S., Sun, X. Wang, X., Xu, X., 2005:** Dynamic monitoring of cytotoxicity on microelectronic sensors. *Chem. Res. Toxicol.*, 18, 154—161.
17. **Xing, J. Z., Zhu, L., Gabos, S., Xie, L., 2006:** Microelectronic cell sensor assay for detection of cyotoxicity and prediction of acute toxicity. *Toxicology in Vitro*, 20, 995—1004.
18. **Yoon, S. J., Koh, E. J., Kim, C. S., Zee, O. P., Kwak, J. H., Jeong, W. J., Kim, J. H., Lee, S. M., 2012:** *Agrimonia eupatoria* protects against chronic ethanol induced liver injury in rats. *Food Chem. Toxicol.*, 50, 2335—2341.

Received October 24, 2017
Accepted December 6, 2017

sciendo

DOI: 10.2478/fv-2018-0013

FOLIA VETERINARIA, 62, 2: 19—29, 2018

DIAGNOSTICS OF *MALASSEZIA* SPECIES: A REVIEW

Böhmová, E., Čonková, E., Sihelská, Z., Harčárová, M.

Department of Pharmacology and Toxicology,
University of Veterinary Medicine and Pharmacy, Komenského 73, 04181 Košice,
Slovakia

ema.bohmova@student.uvlf.sk

ABSTRACT

Yeasts from the genus *Malassezia* belongs to normal commensal skin flora of warm-blooded vertebrates. These yeasts may act as opportunistic pathogens and cause skin diseases in humans and animals under certain conditions. The identification of *Malassezia* species is based on the phenotypic or genotypic diagnostics. The methods used for the phenotypic identification is determined by: the growth on Sabouraud agar, growth on selective media (Leeming-Notman agar, Dixon agar, Chrom *Malassezia* agar), the ability to utilise different concentrations of Tween, monitoring of the growth on CEL agar (soil enriched with castor oil) and TE agar (Tween-esculine agar), and the catalase test. The genotypic identification uses molecular methods like: the pulsed field gel electrophoresis (PFGE), random amplified polymorphic DNA (RAPD), amplified fragment lenght polymorphism (AFLP), denaturing gradient gel electrophoresis (DGGE), and the DNA sequence analysis.

Key words: genotypic; identification; phenotypic; yeasts

INTRODUCTION

Malassezia yeasts are lipophilic organisms known for more than a century as a part of the natural human skin microflora, as well as the agents of some skin diseases. Yeasts have also been considered as the agents of occasional systemic infections since the 1980s [5].

After the first isolation from an Indian rhinoceros, *Malassezia* yeasts were subsequently found in wild mammals (bears, wolves, coyotes, foxes, seals, sea lions, llamas, porcupines, elephants, armadillo, monkeys, ferrets, leopards), as well as in domestic animals (dogs, cats, horses, cattle, sheep, goats, pigs). *Malassezia* yeasts were also isolated from various species of birds, therefore it is assumed that these yeasts may be found in all warm-blooded vertebrates [20] and their distribution in nature is currently being examined by molecular techniques [5].

Until the late 1980s, only two species were known within the genus, *Malassezia furfur* and *Malassezia pachydermatis* [9].

It took a long time to understand the importance of lipids for the growth of *Malassezia* yeasts, so it was difficult to maintain cultures *in vitro* [5]. *M. furfur* was considered

as lipid-dependent yeast, occurring in humans, whereas the lipophilic but not lipid-dependent species *M. pachydermatis*, was found in domestic carnivores, particularly in dogs [9, 28]. Later, other species have been found and described and the range of animal hosts greatly extended [20]. *M. sympodialis*, the third accepted species isolated from human skin, was discovered a century after *M. furfur*. The genus *Malassezia* was revised in 1996 on the basis of morphological, physiological and rRNA studies and four new lipid-dependent species were described, *M. globosa*, *M. obtusa, M. restricta* and *M. slooffiae* [26]. Many reports have shown that the skin of healthy animals, in addition to *M. pachydermatis*, may have also been colonized by the lipid-dependent species [9] as *M. obtusa, M. globosa, M. slooffiae, M. furfur and M. sympodialis* were found in cattle and goats. A new species *M. caprae* was also isolated from goats. *M. equina* was found in horses [20] and *M. nana* was isolated from cats and cattle [34].

Nowadays, *Malassezia* can be isolated from almost all domestic and wild animals [9]. Molecular methods helped reveal new types of *Malassezia* also in humans, such as *M. dermatis*, *M. yamatoensis* and *M. japonica* [5]. Currently, *Malassezia genus* includes 16 species (Table 1) which colonize human or animal skin [10].

Malassezia yeasts are primarily located in the sebaceous glands, which provide lipids necessary for their growth [19]. The sebaceous glands are mostly found on the face, head, chest and back which made these places the most affected by yeast infections [61]. The *Malassezia genus* is typical in its morphology and affinity to lipids in the medium [5]. All members of this genus, except for *M. pachydermatis*, need for their growth medium supplementation with long chain fatty acids (C12—C24). *M. pachydermatis* is able to grow without the addition of lipids in the medium, but more vigorous growth can be seen in the presence of lipids. Species, requiring the addition of lipids in the medium are called lipid-dependent [61].

The most frequently isolated zoophilic species is *M. pachydermatis*, which is often associated with the inflammation of the external ear canal and various types of

Table 1. Currently described *Malassezia* species, authors, year of the description and their main hosts

Malassezia species	Discovery	Main host/others
M. furfur (Robin, Baillon)	1889	man/cow, elephant, pig, monkey, pelican
M. pachydermatis (Weidman, Dodge)	1925	dog, cat/carnivores, birds
M. sympodialis (Simmons & Guého)	1990	man/horse, pig, sheep
M. globosa (Midgley et al.)	1996	man/cheetah, cow
M. obtusa (Midgley et al.)	1996	man
M. restricta (Guého et al.)	1996	man
M. slooffiae (Guillot et al.)	1996	man, pig/goat, sheep
M. dermatis (Sugita et al.)	2002	man
M. japonica (Sugita et al.)	2003	man
M. nana (Hirai et al.)	2004	cat, cow/dog
M. yamatoensis (Sugita et al.)	2004	man
M. caprae (Cabañes and Boekhout)	2007	goat/horse
M. equina (Cabañes and Boekhout)	2007	horse/cow
M. cuniculi (Cabañes and Castellá)	2011	rabbit
M. brasiliensis (Cabañes et al.)	2016	parrot
M. psittaci (Cabañes et al.)	2016	parrot

dermatitis in animals [13]. It usually occurs in dogs, cats and less frequently it can be isolated from other animals. This yeast is opportunistic and may become pathogenic when environmental changes of the skin surface occur or in the immunosuppressed hosts. In some breeds of dogs the growth of yeasts can be supported by different types of hypersensitivity (such as flea bite allergy, food hypersensitivity and atopy) and long term antimicrobial therapy or therapy with corticosteroids [9].

IDENTIFICATION OF *MALASSEZIA* SPECIES

Malassezia yeasts can be identified either by culture methods based on their morphological characteristics and biochemical properties or by non-culture, molecular methods [1, 30]. When using conventional culture methods, the samples are collected from healthy or affected skin, scalp, hair, nails or any other human or animal sources. The samples, cultured on special selective media in Petri dishes, are incubated in a moist environment. *Malassezia* yeasts as cutaneous mycobiota are ecologically adapted to a lower temperature and optimum cultivation temperature for them is around 32—34 °C. The vitality of yeasts on culture media decreases rapidly so it is necessary to transfer samples regularly on fresh medium every one or two months [5, 42].

Culture media supplemented with different sources of lipids are often used because of the lipophilic properties of this genus [11]. Sabouraud dextrose agar, the culture medium without the addition of lipids, is used to differentiate the lipid-dependency of the species [38]. *M. pachydermatis*, a less demanding species, is able to grow on this medium (Fig. 1) [5, 6].

Other media were developed and successfully used as a selective media for *Malassezia* species, e. g. Dixon agar, Leeming-Notman agar (Fig. 2) and Ushijima agar [1]. All of these complex media contain ox bile which is a sufficient compound for good growth of *Malassezia* yeasts. Some of the media use Tween 40 (Leeming-Notman agar) or Tween 60 (Dixon agar) but Tween 60 seems to be more efficiently utilized, thus it is better for the growth of most species [5].

Fig. 1. The growth of *Malassezia pachydermatis* on Sabourad dextrose agar

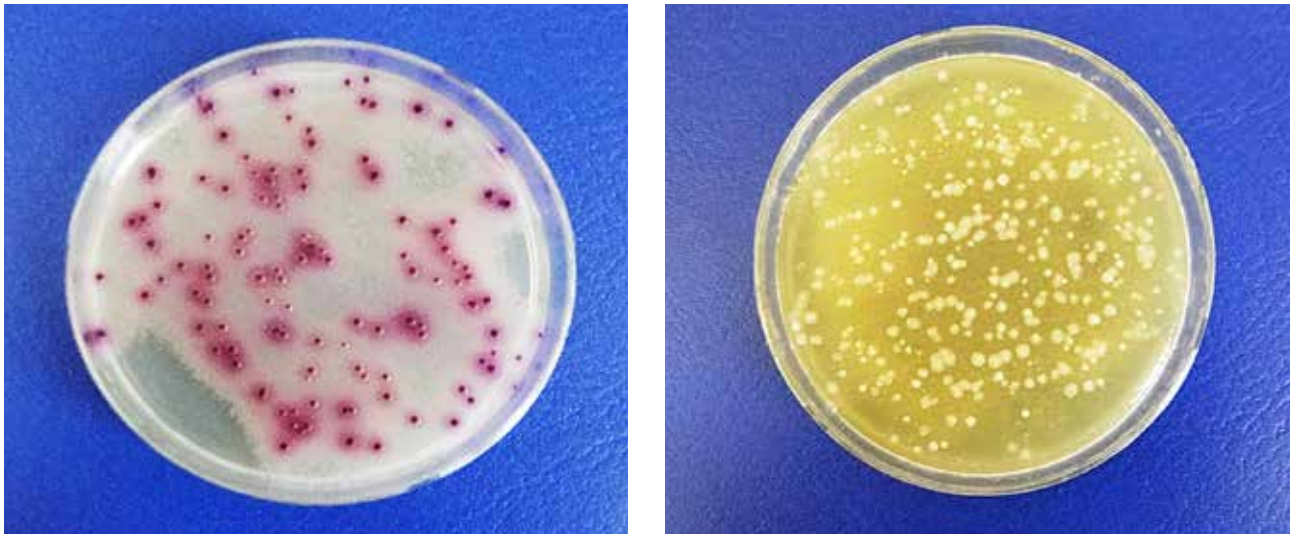

Fig. 2. The growth of *M. pachydermatis* on Leeming-Notman agar and modified CHROMagar *Candida*

By using chromogenic *Candida* agar (CHROMagar Candida) (Fig. 2), enriched with lipid components, it was possible to culture and differentiate 9 *Malassezia* species on the basis of the colony morphology [1, 37]. CHROMagar is also used for the differentiation of the genus *Malassezia* and *Candida*.

The specific media used for *Malassezia* cultivation are Cremophor EL agar and Tween 60-esculin agar. Cremophor EL agar is used to determine the ability of species to utilize the polyethoxylated castor oil and Tween-esculin agar for determining the ability of isolates to hydrolyse esculin and utilize Tween 60 [38].

The culture methods may not be objective because of the difference in growth rates and the cultivation requirements of individual species, therefore, the focus is currently on molecular techniques [32].

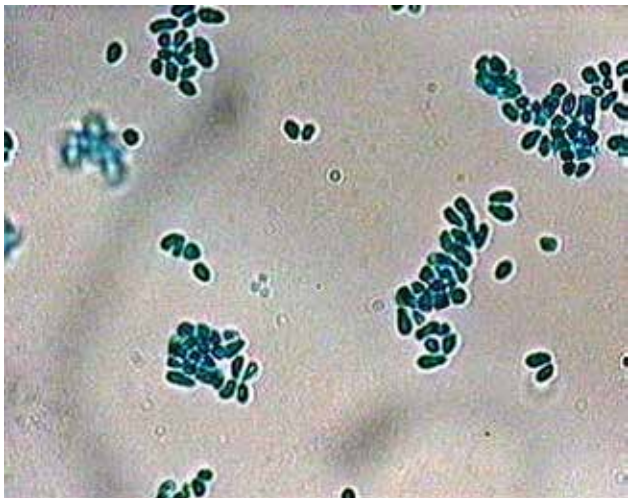

Fig, 3. Microscopic view of *Malassezia pachydermatis* **cells Magn. ×400**

PHENOTYPIC IDENTIFICATION

Individual species from the genus *Malassezia* can be identified by macroscopic and microscopic morphology and also by certain physiological properties [24]. Macroscopic diagnosis includes an identification of the shape, texture and colour of the colonies; microscopically they are examined by cell morphology and budding [52].

The size of colonies is determined by measuring well isolated single colonies and the isolates are divided into three groups: small (1 mm: *M. globosa, M. slooffiae* and *M. restricta*), intermediate (1—2 mm: *M. obtusa*) and large (2—5 mm: *M. pachydermatis, M. sympodialis, M. dermatis, M. furfur and M. japonica*) [38]. Unipolar cells with round to ovoid shape can be observed by microscopic examination [34, 54]. The *M. globosa* cells are typically spherical [14] (Fig. 3).

Although there are morphological differences between *Malassezia* species, their identification is usually determined also upon the basis of their physiological characteristics [14, 52]. Physiological tests used for the identification of *Malassezia* species are based on: the monitoring of catalase reaction (decomposition of 3 % hydrogen peroxide); on the ability of yeasts to utilize different concentrations of Tween (i.e. T20, T40, T60 and T80) and Cremophor EL (castor oil) as a source of lipids [38, 14]; the β-glucosidase activity [38, 44]; the ability to produce pigments [24] and fluorochromes in the presence of tryptophan as a main source of nitrogen [45]; and production of the urease enzyme (ability to hydrolyze urea to ammonia and carbon dioxide) [38]. The urease activity test is not used to distinguish *Malassezia* species but to eliminate cultures that are contaminated by bacteria or ascomycetous yeasts, such as *Candida* spp. which are quite common on the skin [5].

Malassezia furfur

M. furfur forms smooth or slightly wrinkled single colonies about 4—5 mm in diameter. The colonies are creamy coloured, dull, with straight or lobate margins. The texture of the colonies is soft. Colonies of *M. furfur* are easily distinguishable from other *Malassezia* species on CHROMagar where they form characteristic large pale pink and wrinkled colonies [38]. The cells are morphologically variable, with ovoid, globose or cylindrical shape and budding is on a broad base. Some strains are able to occasionally produce filaments [2, 5, 29, 61].

Malassezia furfur can be identified: by its ability to grow up to 41 °C; by a strong catalase reaction; the absence or a very weak β-glucosidase activity; and equal growth in the presence of Tweens 20, 40, 60, 80 and CremophorEL as a lipid sources [4, 27]. The optimum temperature for the growth is near 34 °C, but good growth occurs at 37 °C, and the maximum temperature for growth is 41 °C. In contrast to *M. globosa, M. obtusa, M. restricta, M. slooffiae* and *M. sympodialis*, this species is able to utilize glycine as a nitrogen source [50].

Malassezia pachydermatis

M. pachydermatis forms convex single colonies 1—5 mm in diameter, pale yellowish, dull, smooth, lightly wrinkled, with an entire straight margin. Cells are ovoid, ellipsoidal to cylindrical with monopolar budding on a broad base. This species does not produce filaments.

In all rDNA genotypes there occurs differences in catalase and β-glucosidase expression and Tweens 20, 40, 60, 80 and Cremophor EL (CrEL) growth reactions. All isolates grow well at 37 °C with the maximum at 40—41 °C and some primary cultures show a certain lipid-dependence [4, 5, 20, 53, 59, 61].

Malassezia sympodialis

M. sympodialis forms flat or elevated single colonies, approximately 5—8 mm in diameter, pale cream, glistening, smooth, with an entire or folded margin. Cells are small, with ovoid to globose shape and monopolar budding on a narrow base. This strain, able to grow at 40 °C, is characterized by the presence of a catalase reaction and a strong β-glucosidase activity, and good growth in the presence of Tweens 40, 60 and 80. With CrEL, growth is usually absent but fresh isolates can develop a ring of tiny colonies [2, 5, 26].

Malassezia globosa

M. globosa forms raised, wrinkled single colonies, 3—4 mm in diameter, pale yellowish, rough, shiny or dull, with a slightly lobate margin. Yeast cells are spherical, so this species is easily recognized morphologically with monopolar budding on a narrow base. This species is able to produce short filaments [2, 23, 26]. The yeast has a strong catalase activity but does not split esculin. Growth is limited at 37 °C, and no growth occurs on the five lipid substrates [2, 5, 39].

Malassezia obtusa

M. obtusa forms flat to convex, smooth single colonies, on average 1.5—2 mm in diameter, glistening or dull, butyrous, and with entire or slightly lobate margins. The cells are cylindrical with monopolar budding on a broad base. Filaments may be present. This species has a maximum temperature at 38 °C and cannot utilize any of the five lipids used in the tests as the only lipid supplement in the medium. *M. obtusa* combines the positive reactions of catalase and β-glucosidase [4, 5, 26].

Malassezia restricta

M. restricta forms small, flat or raised single colonies, 1—2 mm in diameter on average, pale yellowish-brown, dull, smooth, with a lobate margins. The shape of the cells is globose or ovoid, and budding is monopolar on a relatively narrow base. *M. restricta* does not produce any filaments. This species lacks catalase and β-glucosidase activity, does not grow at 37 °C or with any of the Tween lipid supplements. Growth with CrEL is always absent. Growth of the colonies is very restricted [2, 5, 26, 31].

Malassezia slooffiae

M. slooffiae forms flat or raised single colonies with a roughened surface, about 3—4 mm in diameter, pale yellowish-brown, shiny, butyrous and with finely folded margins. The cells are short and cylindrical with monopolar budding on a broad base. The species is not known to produce any filaments. This species is able to grow at 40 °C, and shows a catalase reaction, but absence of β-glucosidase activity. *M. slooffiae* may be misidentified as *M. furfur*, but the main difference is that growth of *M. sloofiae* with CrEL is absent. Growth with Tween 80 is always very weak in comparison with the other three Tweens [4, 5, 26, 35].

Malassezia dermatis

M. dermatis forms flat or convex single colonies, 5—6 mm in diameter, pale yellowish, glistering or dull, butyrous and with an entire or finely folded margin. The shape of the cells is globose, ovoid or ellipsoidal. Budding is monopolar on a moderately broad base. The production of filaments has not been observed. *M. dermatis* does not grow at 40 °C and can be identified by its lack of catalase and β-glucosidase activity. Growth occurs with all four Tweens but with Tween 80 it may be weaker, similar to that of *M. caprae*. CrEL is not assimilated [5, 54].

Malassezia japonica

M. japonica forms flat slightly wrinkled single colonies about 2—3 mm in diameter, pale yellowish-cream, dull and butyrous with a straight or folded margin. Cells are ovoid to cylindrical, with budding which is monopolar on a broad base. The production of hyphae has not been observed. *M. japonica* grows at 37 °C, with strong catalase and β-glucosidase reactions. From all four Tweens, only 60 and 80 are well assimilated. Tweens 20, 40 and CrEL are assimilated weakly [5, 56].

Malassezia nana

M. nana forms convex single colonies, 1.5—2 mm in diameter, yellowish, dull, smooth, butyrous, with entire to narrowly folded margins. The shape of the cells is globose to ovoid with monopolar budding on a relatively narrow base. *M. nana* does not produce any filaments.

This species grows at 37 °C, Tweens 40, 60 and 80 are well assimilated and CrEL is not utilized [2, 5, 34].

Malassezia yamatoensis

M. yamatoensis forms flat to convex single colonies about 3—4 mm in diameter, pale yellowish, shiny, smooth or wrinkled, with an entire margin. The shape of cells is ovale or cylindrical with monopolar budding on a broad base. This strain can be identified by its ability to grow at 37 °C, a strong catalase reaction and lack of β-glucosidase activity. These characteristics distinguish the species from *M. sympodialis*. Growth appears in the presence of all four Tweens and CrEL [5].

Malassezia caprae

M. caprae forms small moderately convex single colonies about 1—2 mm in diameter, whitish or cream-colored, smooth, butyrous with an entire or lobate margin. Cells are globose or ovoid with budding on a broad base. The species does not produce hyphae. *M. caprae* can be identified by: its weak growth at 37 °C, the presence of a catalase reaction, β-glucosidase activity, and good growth in the presence of all four Tweens. Growth may be weaker with Tween 80 [5, 8].

Malassezia equina

M. equina forms single colonies, about 1—3 mm in diameter, cream-colored, glistening to dull, wrinkled, butyrous, with a folded to fringed margins. The cells are ovoid or ellipsoidal with monopolar budding on a narrow base. Filaments have not been observed. *M. equina* grows at maximum temperature of 37 °C. The catalase reaction is strong, but this species lacks the β-glucosidase expression. Tweens 40, 60 and 80 are well assimilated. CrEL is not assimilated, but sometimes a weak precipitate can occur [5].

Malassezia brasiliensis

M. brasiliensis forms large convex colonies elevated in the centre with an average diameter of 2.5 mm, whitish to cream-colored, smooth, dull and butyrous with entire margins. The cells are ovoid or ellipsoidal with buds formed monopolarly on a broad base [10].

Malassezia psittaci

M. psittaci forms large moderately convex colonies, about 2.5 mm in diameter. They look similar to the colonies of *M. brasiliensis* with the whitish to cream colour and smooth, shiny, butyrous appearance. The yeast cells are globose to ovoid [10].

Phenotypic methods are usually time-consuming, multistep processes, requiring a number of cultural techniques and usually are unable to clearly differentiate newly identified species. Also, there are significant differences in the evaluation and description of *Malassezia* biochemical properties by various authors [2, 26, 38] and this complicates the phenotypic identification. The occurence of strains with atypical physiological and biochemical properties is increasing and for these reasons it is essential to support the phenotypic identification by molecular analysis [14].

GENOTYPIC IDENTIFICATION

The number of molecular methods have been developed and successfully used as tools to diagnose and differentiate *Malassezia* species, to better understand the epidemiology of *Malassezia* and their connection with diseases [14].

To overcome the limitations of culture-based techniques which do not always allow identification and typing of each *Malassezia* species, a range of molecular biology methods are used, such as: nested polymerase chain reaction (PCR) [49], real-time PCR [58], pulsed-field gel electrophoresis (PFGE) [53], random amplified polymorphic DNA analysis (RAPD — random amplification of polymorphic DNA (RAPD) [21], amplified fragment length polymorphism (AFLP) [32], denaturing gradient gel electrophoresis (DGGE) [60], single strand conformation polymorphism (SSCP) [17], terminal fragment length polymorphism (tFLP) [23], restriction fragment length polymorphism (RFLP) [16, 41, 48] and sequencing analysis [40] (Tab. 2).

Table 2. Molecular methods used for detection and identification of Malassezia species [7]

Fingerprinting methods:
PFGE-Pulsed field gel electrophoresis
RAPD-Random amplified polymorphic DNA
AFLP-Amplified fragment lenght polymorphism
DGGE-Denaturing gradient gel electrophoresis
DNA sequence analysis:
Ribosomal DNA analysis (D1/D2 region LSU- Large subunit —rDNA)
Analysis ITS (Internal transcribed spacer regions) rDNA
Analysis IGS (Intergenic spacer regions) rDNA
Restriction analysis of PCR amplicons:
RFLP-Restriction fragment length polymorphism
tFLP-Terminal fragment lenght polymorphism
Chitin synthase gene sequence analysis

FINGERPRINTING METHODS

Pulsed-field gel electrophoresis (PFGE)

Pulsed-field gel electrophoresis is a highly discriminative molecular method based on the variable migration/separation of large genomic fragments in an agarose gel [46]. This technique characterized seven *Malassezia* spp. (i. e. *M. furfur*, *M. obtusa*, *M. globosa*, *M. slooffiae*, *M. sympodialis*, *M. pachydermatis* and *M. restricta*) and allows them to be differentiated into species on the basis of distinct karyotypes displayed by PFGE analysis [53]. PFGE is a useful diagnostic tool, but is time consuming, technically difficult and requires large amounts of genomic DNA for analysis. Therefore, it is not suitable as a rapid routine diagnostic method [14, 48].

Random amplified polymorphic DNA analysis (RAPD)

PCR based random amplification of polymorphic DNA utilizes random fragments of genomic DNA. This method has been used for the identification, differentiation and taxonomic classification of some *Malassezia* species (*M. pachydermatis, M. furfur* and *M. slooffiae*) and for the examination of epidemiological relations. Most of the *Malassezia* species can be differentiated by RAPD, but analysis can be complicated by the presence of intraspecific variations [3]. In spite of limited reproducibility of results and its technical limitations due to the need for specialized equipment and training, RAPD is a sensitive and efficient method for discrimination of closely related strains due to its high specificity. RAPD is still being used for the monitoring of *Malassezia* "carriage" on domestic animals and humans [15, 18, 21].

Amplified fragment length polymorphism (AFLP)

AFLP is a useful diagnostic tool for the identification of *Malassezia* isolates and for the detection and differentiation between clinically relevant variants within *Malassezia* spp. This technique provides highly-specific genotypic information about each strain and helps to understand the genetic relationship among *Malassezia* isolates [8, 32, 60].

AFLP is suitable and apropriate for analyses where detailed information is necessary. This method requires clonal isolates from culture so that the results are usually complicated to interpret. AFLP is relatively time-consuming and sometimes not sufficiently reliable for identification or discrimination of clinically isolated yeasts [2, 14, 18].

Denaturing gradient gel electrophoresis (DGGE)

DGGE is a molecular fingerprinting technique based on differences in the electrophoretic mobility and denaturing properties of double-stranded DNA. DGGE can fully separate and detect DNA fragments of the same size but with different base-pair sequences. The melted DNA is separated and spread through the denaturing polyacrylamide gel and is analyzed for single components [25, 33, 47, 51]. DGGE is useful for the identification of *Malassezia* isolates and is suitable for the analysis of the clinical samples that may include several different species. However, the clinical use may be limited by technical demands [4, 60].

DNA sequence analysis

The rRNA gene complex is often used in identification of clinically important yeasts. The fungal gene is composed of multiple copies of the gene regions: 18S, 5.8S, 26 (28) and 5S. 18S is a small subunit (SSU) and 28S is referred as large subunit (LSU). Other regions, ITS1 and ITS2 region (internal transcribed spacer region) and IGS1 and IGS2 region (intergenic spacer region) are inserted among the subunits. The rRNA gene complex is also used for comparison between phylogenetically distant species. Phylogenetically close species are compared through more variable region, the ITS and IGS regions [5].

Sequencing of ITS1 region of ribosomal DNA is relatively quick and specific analysis and is used for the identification of *Malassezia* species and the strains. Sequence

analysis of IGS1 is not widely used for species identification [55, 57].

RESTRICTION ANALYSIS OF PCR AMPLICONS

Restriction fragment length polymorphism (RFLP)

One of the frequently used molecular method is the polymerase chain reaction (PCR) followed by restriction analysis (RFLP). Enzyme digestion of PCR amplicons has been shown to be useful for the differentiation of *Malassezia* species.

Various authors suggested RFLP for the diagnosis of *Malassezia*. Mirhendi et al. [48] and Gaitanis and Velegraki [17] differentiated 11 species (*M. furfur, M. pachydermatis, M. sympodialis, M. obtusa, M. globosa, M. restricta, M. slooffiae, M. dermatis M. nana, M. japonica* and *M. yamatoensis*) using RFLP. PCR-RFLP analysis is less difficult and more precise than the majority of molecular methods and requires less technical equipment.

Terminal fragment length polymorphism analysis (tFLP)

Terminal restriction fragment length polymorphism (tRFLP) analysis of PCR-amplified genes is a widely used fingerprinting technique. This analysis is based on the restriction endonuclease digestion of fluorescently end-labeled PCR products. tFLP analysis is a sensitive and reproducible method suitable for the rapid and reliable identification of *Malassezia* species. It eliminates the need for prior strain cultivation in direct investigations of *Malassezia* populations on skin samples. The technique, however, is not suitable for epidemiological typing, as its ability to show heterogeneity within a species is limited [23, 32].

Chitin synthase gene sequence analysis

Sequencing of the chs-2 gene has also allowed the differentiation of *Malassezia* spp., in spite of the high similarity (95 %) in sequence among them [36]. A multilocus approach which employed the sequencing of the chs-2 gene, ITS1 and LSU has been applied to *M. pachydermatis* and defined three major *M. pachydermatis genotypes* (A, B and C). Although the multilocus sequencing provides interesting option for epidemiological investigations, it has not yet been employed for studying *Malassezia* from animals other than dogs [12, 13].

In the last few decades, advances in research and technology contributed to partial explanation of the role which *Malassezia* plays in skin diseases. By using the detailed information obtained from genetic analyses, different types of *Malassezia* spp. can be detected and identified [11, 14]. Most of molecular studies point to the presence of numerous *Malassezia* genotypes within species, suggesting a connection to the host, the geographical origin and clinical manifestations. Standardized molecular processes in combination with reliable physiological and biochemical methods are necessary for the definition of species and for consideration of genetic diversity within a species [22].

Despite the usefulness of molecular techniques, there are some disadvantages associated with them, such as: the inability to distinguish all species and questionable reproducibility, the requirements for technical equipment, and higher cost of analysis. Importantly, most of the molecular methods mentioned above require cultivation to enhance sensitivity and to perform the test [14].

Some studies have shown discrepancies between phenotypic and molecular methods for the identification of *Malassezia*. For example, Makimura et al. [43] examined 46 clinical isolates by the phenotypic methods as *M. furfur.* However, by genetic identification 22 of them were identified as *M. sympodialis* and 5 as *M. slooffiae*.

It is possible that differences between phenotypic and molecular methods may reflect the possible mistakes in sampling and culturing, which strengthen the need to perform well-controlled, comparative molecular studies of samples taken directly from the skin, as well as samples after *in vitro* cultivation [14].

CONCLUSIONS

In recent decades, yeast infections have become a significant problem in humans and also in animals. In most cases, they are opportunistic infections because *Malassezia* belongs to the normal commensal skin flora of warm-blooded vertebrates. The increasing trend in the incidence of these infections can be caused mainly because of massive use of broad spectrum antibiotics and the increasing number of immunosuppressed patients.

Identification of yeast is performed by phenotypic and molecular methods. Molecular methods are necessary for identification and differentiation of various *Malassezia* spe-

cies, which can be difficult to characterize by phenotypic methods.

In the future, the identification should focus on the use of reliable molecular methods to achieve a better understanding of the role that *Malassezia* spp. plays as a commensal and as a pathogen.

ACKNOWLEDGEMENT

This work was supported by the Slovak Research and Development Agency under the contract No. APVV-15-0377.

REFERENCES

1. **Ashbee, H. R., 2007:** Update on the genus *Malassezia*. *Med. Mycol.*, 45, 287—303.
2. **Batra, R., Boekhout, T., Guého, E., Cabanes, F. J., Dawson, Jr. T. L., Gupta, A. K., 2005:** *Malassezia Baillon*, emerging clinical yeasts. *FEMS Yeast Research*, 5, 1101—1113.
3. **Boekhout, T., Kamp, M., Guého, E., 1998:** Molecular typing of *Malassezia* species with PFGE and RAPD. *Med. Mycol.*, 36, 365—372.
4. **Boekhout, T., Guého E., 2003:** Basidiomycetous yeasts. In **Howard, D. H., (Ed.):** *Pathogenic Fungi in Humans and Animals*, 2nd edn., Marcel Dekker, Inc., New York, USA, 537—542.
5. **Boekhout, T., Guého-Kellermann, E., Mayser, P., Velegraki, A., 2010***: Malassezia and the Skin: Science and Clinical Practice*. Springer-Verlag Berlin Heidelberg, 18—50.
6. **Bond, R., Lloyd, D. H., 1996:** Comparison of media and conditions of incubation for the quantitive culture of *Malassezia pachydermatis* from canine skin. *Res. Vet. Sci.*, 61, 273—274.
7. **Brakhage, A. A., Zipfel, P. F., 2008:** *The Mycota, Human and Animal Relationships*. Berlin, Springer, 296 pp.
8. **Cabañes, F. J., Theelen, B., Castella, G., Boekhout, T., 2007:** Two new lipid-dependent *Malassezia* species from domestic animals. *FEMS Yeast Res.*, 7, 1064—1076.
9. **Cabañes, F. J., 2014:** *Malassezia* yeasts: How many species infect humans and animals? *PLoS Pathogens 10*. e1003892. doi:10.1371/journal.ppat.1003892.
10. **Cabañes, F. J., Coutinho, S. D., Puig, L., Bragulat, M. R., Castellá, G., 2016:** New lipid-dependent *Malassezia* species from parrots. *Rev. Iberoam. Mycol.*, 33, 92—99.
11. **Cafarchia, C., Latrofa, M. S., Testini, G., Parisi, A., Guillot, J., Gasser, R. B., Otranto, D., 2007:** Molecular characterization of *Malassezia* isolates from dogs using three distinct genetic markers in nuclear DNA. *Mol. Cell. Probes*, 21, 229—238.
12. **Cafarchia, C., Gasser, R. B., Latrofa, M. S., Parisi, A., Campbell, B. E., Otranto, D., 2008:** Genetic variants of *Malassezia pachydermatis* from canine skin: body distribution and phospholipase activity. *FEMS Yeast Res.*, 8, 451—459.
13. **Cafarchia, C., Latrofa, M. S., Figueredo, L. A., da Silva Machado, M. L., Ferreiro, L., Guillot, J., Boekhout, T., Otranto, D., 2011:** Physiological and molecular characterization of a typical lipid *Malassezia* yeasts from a dog with skin lesions: adaptation to a new host? *Med. Mycol.*, 49, 365—374.
14. **Cafarchia, C., Gasser, R. B., Figueredo, L. A., Latrofa, M. S., Otranto, D., 2011:** Advances in the identification of *Malassezia*. *Mol. Cell. Probes*, 25, 1—7.
15. **Duarte, E. R., Hamdan, J. S., 2010:** RAPD differentiation of *Malassezia* spp. from cattle, dogs and humans. *Mycoses*, 53, 48—56.
16. **Gaitanis, G., Velegraki, A., Frangoulis, E., Mitroussia, A., Tsigonia, A., Tzimogianni, A., et al., 2002:** Identification of *Malassezia* species from patient skin scales by PCR-RFLP. *Clin. Microbiol. Infect.*, 8, 162—173.
17. **Gaitanis, G., Veleqraki, A., Alexopoulos, E. C., Chasapi, W., Tsiqonia, A., Katsambas, A., 2006:** Distribution of *Malassezia* species in pityriasis versicolor and seborrhoeic dermatitis in Greece. Typing of the major pityriasis versicolor isolate *M. globosa*. *Br. J. Dermatol.*, 154, 854—859.
18. **Gaitanis, G., Bassukas, I. D., Velegraki, A., 2009:** The range of molecular methods for typing *Malassezia*. *Curr. Opin. Infect. Dis.*, 22, 119—25.
19. **Gaitanis, G., Velegraki, A., Mayser, P., Bassukas, I. D., 2013:** Skin diseases associated with *Malassezia* yeasts: facts and controversies. *Clin. Dermatol.*, 31, 455—463.
20. **Galuppi, R., Tampieri, M. P., 2008:** Epidemiology and variability of *Malassezia* spp. *Parasitologia*, 50, 73—76.
21. **Gandra, R. F., Simao, R. C., Matsumoto, F. E., da Silva, B. C., Ruiz, L. S., da Silva, E. G., et al., 2006:** Genotyping by RAPD-PCR analyses of *Malassezia furfur* strains from pityriasis versicolor and seborrhoeic dermatitis patients. *Mycopathol.*, 162, 273—280.
22. **Gasser, R. B., Hu, M., Chilton, N. B., Campbell, B. E., Jex, A. J., Otranto, D., et al., 2006:** Single-strand conformation polymorphism (SSCP) for the analysis of genetic variation. *Nat. Protoc.*, 1, 3121—3128.
23. **Gemmer, C. M., DeAngelis, Y. M., Theelen, B., Boekhout, T., Dawson Jr., T. L., 2002:** Fast, noninvasive method for molecular detection and differentiation of *Malassezia* yeast spe-

cies on human skin and application of the method to dandruff microbiology. *J. Clin. Microbiol.*, 40, 3350—3357.

24. **Gonzales, A., Sierra, R., Cardenes, M. E., Grajales, A., Restrepo, S., Cepero de García, M. C., Celis, A., 2009:** Physiological and molecular characterization of atypical isolates of *Malassezia furfur*. *J. Clin. Microbiol.*, 47, 48—53.
25. **Green, S. J., Leigh, M. B., Neufeld, J. D., 2009:** Denaturing gradient gel electrophoresis (DGGE) for microbial community analysis. In **Timmis, K. N. (Ed.):** *Microbiology of Hydrocarbons, Oils, Lipids and Derived Compounds*, Springer, Heidelberg, Germany, 4137—4158.
26. **Guého, E., Midgley, G., Guillot, J., 1996:** The genus *Malassezia* with description of four new species. *Antonie van Leeuwenhoek*, 69, 337—355.
27. **Guého, E., Boekhout, T., Ashbee, H. R., Guillot, J., van Belkum, A., Faergemann, J., 1998:** The role of *Malassezia* species in the ecology of human skin and as pathogens. *Med. Mycol.*, 36, 220—229.
28. **Guillot, J., Guého, E., Chermette, R., 1994:** Confirmation of the nomenclatural status of *Malassezia pachydermatis*. *Antonie van Leeuwenhoek*, 67, 173—176.
29. **Guillot, J., Guého, E., Prevost, M. C., 1995:** Ultrastructural features of the dimorphic yeast *Malassezia furfur*. *J. Mycol. Med.*, 5, 86—91.
30. **Guillot, J., Guého, E., Lesourd, M., Midgley, G., Chevrier, G., Dupont, B., 1996:** Identification of *Malassezia* species. A practical approach. *J. Mycol. Med.*, 6, 103—110.
31. **Gupta, A. K., Kohli, Y., Summerbell, R. C., 2000:** Molecular differentiation of seven *Malassezia* species. J. Clin. Microbiol., 38, 1869—1875.
32. **Gupta, A. K., Boekhout, T., Theelen, B., Summerbell, R., Batra, R., 2004:** Identification and typing of *Malassezia* species by amplified fragment length polymorphism and sequence analyses of the internal transcribed spacer and large-subunit regions of ribosomal DNA. *J. Clin. Microbiol.*, 42, 4253—4260.
33. **Hayes, V. M., Wu, Y., Osinga, J., Mulder, I. M., Van Der Vlies, P., Elfferich, P., et al., 1999:** Improvements in gel composition and electrophoretic conditions for broad-range mutation analysis by denaturing gradient gel electrophoresis. *Nucleic Acids Res.*, 27, 29.
34. **Hirai, A., Kano, R., Makimura, K., Duartem R. E., Hamdanm J. S., Lachancem M. A., et al., 2004:** *Malassezia nana* sp. nov., a novel lipid-dependent yeast species isolated from animals. *Int. J. Syst. Evol. Microbiol.*, 54, 623—627.
35. **Howard, D. H., 2003:** *Pathogenic Fungi in Humans and Animals*. 2nd edn., New York, Dekker, 790 pp.
36. **Kano, R., Aizawa, T., Nakamura, Y., Watanabe, S., Hasegawa, A., 1999:** Chitin synthase 2 gene sequence of *Malassezia* species. *Microbiol. Immunol.*, 43, 813—815.
37. **Kaneko, T., Makimura, K., Onozaki, M., Ueda, K., Yamada, Y., Nishiyama, Y., Yamaguchi, H., 2005:** Vital growth factors of *Malassezia* species on modified CHROMagar *Candida*. *Med. Mycol.*, 43, 699—704.
38. **Kaneko, T., Makimura, K., Abe, M., Shiota, R., Nakamura, Y., Kano, R., et al., 2007:** Revised culture-based system for identification of *Malassezia* species. *J. Clin. Microbiol.*, 45, 3737—3742.
39. **Kindo, A. J., Sophia, S. K. C., Kalyani, J., Anandan, S., 2004:** Identification of *Malassezia* species. *Indian J. Med. Microbiol.*, 22, 179—181.
40. **Lee, Y. W., Lim, S. H., Ahn, K. J., 2006:** The application of 26S rDNA PCR-RFLP in the identification and classification of *Malassezia* yeast. *Kor. J. Med. Mycol.*, 11, 141—153.
41. **Lee, Y. W., Kim, S. M., Oh, B. H., Lim, S. H., Choe, Y. B., Ahn, K. J., 2008:** Isolation of 19 strains of *Malassezia dermatis* from healthy human skin in Korea. *J. Dermatol.*, 35, 772—777.
42. **Lim, S. H., Kim, Y. R., Jung, J. W., Hahn, H. J., Lee, Y. W., Choe, Y. B., Ahn, K. J., 2012:** A comparison study between culture based technique and op-site non-culture based technique for identifying *Malassezia* yeasts on normal skin. *Korean J. Med. Mycol.*, 17, 217—229.
43. **Makimura, K., Tamura, Y., Kudo, M., Uchida, K., Saito, H., Yamaguchi, H., 2000:** Species identification and strain typing of *Malassezia* species stock strains and clinical isolates based on the DNA sequences of nuclear ribosomal internal transcribed spacer 1 regions. *J. Med. Microbiol.*, 49, 29—35.
44. **Mayser, P., Haze, P., Papavassilis, C., Pickel, M., Gruender, K., Guého, E., 1997:** Differentiation of *Malassezia* species: selectivity of Cremophor EL, castor oil and ricinoleic acid for *M. furfur*. *Br. J. Dermatol.*, 137, 208—213.
45. **Mayser, P., Tows, A., Kramer, H. J., Weiss, R., 2004:** Further characterization of pigment producing *Malassezia* strains. *Mycoses*, 47, 34—39.
46. **Melles, D. C., van Leeuwen, W. B., Snijders, S. V., Horst-Kreft, D., Peeters, J. K., Verbrugh, H. A., van Belkum, A., 2007:** Comparison of multilocus sequence typing (MLST), pulsed-field gel electrophoresis (PFGE), and amplified fragment length polymorphism (AFLP) for genetic typing of Staphylococcus aureus. *J. Microbiol. Methods*, 69, 2, 371—375.
47. **Michaelsen, A., Pinzari, F., Ripka, K., Lubitz, W., Pinar, G., 2006:** Application of molecular techniques for identification

of fungal communities colonising paper material. *Int. Biodeterior. Biodegrad.*, 58, 133—141.

48. **Mirhendi, H., Makimura, K., Zomorodian, K., Yamada, T., Sugita, T., Yamaguchi, H., 2005:** A simple PCR-RFLP method for identification and differentiation of 11 *Malassezia* species. *J. Microbiol. Methods*, 61, 281—284.
49. **Morishita, N., Sei, Y., Sugita, T., 2006:** Molecular analysis of *Malassezia* microflora from patients with pityriasis versicolor. *Mycopathol.*, 161, 61—165.
50. **Murai, T., Nakamura, Y., Kano, R., Watanabe, S., Hasegawa, A., 2002:** Differentiation of *Malassezia furfur* and *Malassezia sympodialis* by glycine utilization. *Mycoses*, 45, 180—183.
51. **Muyzer, G., Smalla, K., 1998:** Application of denaturing gradient gel electrophoresis (DGGE) and temperature gradient gel electrophoresis (TGGE) in microbial ecology. *Antonie Leeuwenhoek*, 73, 127—141.
52. **Saghazadeh, M., Farshi, S., Hashemi, J., Mansouri, P., Khosravi, A. R., 2010:** Identification of *Malassezia* species isolated from patients with seborrheic dermatitis, atopic dermatitis and normal subjects. *J. Mycol. Med.*, 20, 4, 279—282.
53. **Senczek, D., Siesenop, U., Bohm, K., 1999:** Characterization of *Malassezia* species by means of phenotypic characteristics and detection of electrophoretic karyotypes by pulsed field gel electrophoresis (PFGE). *Mycoses*, 42, 409—414.
54. **Sugita, T., Takashima, M., Shinoda, T., Suto, H., Unno, T., Tsuboi, R., et al., 2002:** New yeast species, *Malassezia dermatitis*, isolated from patients with atopic dermatitis. *J. Clin. Microbiol.*, 40, 1363—1367.
55. **Sugita, T., Kodama, M., Saito, M., Ito, T., Kato, Y., Tsuboi, R., 2003:** Sequence diversity of the intergenic spacer region of the rRNA gene of *Malassezia globosa* colonizing the skin of patients with atopic dermatitis and healthy individuals. *J. Clin. Microbiol.*, 41, 3022.
56. **Sugita, T., Takashima, M., Kodama, M., Tsuboi, R., Nishikawa, A., 2003:** Description of a new yeast species, *Malassezia japonica*, and its detection in patients with atopic dermatitis and heathly subjects. *J. Clin. Microbiol.*, 41, 4695—4699.
57. **Sugita, T., Tajima, M., Amaya, M., Tsuboi, R., Nishikawa, A., 2004:** Genotype analysis of *Malassezia restricta* as the major cutaneous flora in patients with atopic dermatitis and healthy subjects. *Microbiol. Immunol.*, 48,755—759.
58. **Sugita, T., Tajima, M., Tsubuku, H., Tsuboi, R., Nishikawa, A., 2006:** Quantitative analysis of cutaneous *Malassezia* in atopic dermatitis patients using real-time PCR. *Microbiol. Immunol.*, 50, 549—552.
59. **Summerbell, R., 2011:** *Identifying Fungi: A Clinical Laboratory Handbook*, 2nd edn., Belmont, US Star Publishing Co. Ltd., 168—169.
60. **Theelen, B., Silvestri, M., Gueho, E., van Belkum, A., Boekhout, T., 2001:** Identification and typing of *Malassezia* yeasts using amplified fragment length polymorphism (AFLP), random amplified polymorphic DNA (RAPD) and denaturing gradient gel electrophoresis (DGGE). *FEMS Yeast Res.*, 1, 79—86.
61. **Woodgyer, A., 2004:** *Malassezia* update. *The Official Newsletter of the Australian Federation of Medical Veterinary Mycology*, 9, 2—18.

Received January19, 2018
Accepted April 4, 2018

sciendo

DOI: 10.2478/fv-2018-0014

FOLIA VETERINARIA, 62, 2: 30—34, 2018

A SLAUGHTERHOUSE SURVEY FOR PORCINE CIRCOVIRUS TYPE 2 IN COMMERCIAL PIGS IN IBADAN, SOUTHWEST NIGERIA

Aiki-Raji, C. O., Adebiyi, A. I., Oluwayelu, D. O.

Department of Veterinary Microbiology, University of Ibadan, Ibadan Nigeria

ogloryus@yahoo.com

ABSTRACT

Porcine circovirus type 2 (PCV2) is recognized as one of the most important agents of reproductive disorders in gilts and sows worldwide. It is associated with considerable economic losses in the swine industry due to the unthriftiness, and variable morbidity and mortality it causes in pigs. In spite of the devastation caused by this virus to the global pig industry, there is little or no report of its occurrence in Nigeria. Hence, a slaughterhouse based survey was conducted to determine the prevalence of PCV2 infections in pigs in Ibadan, southwest Nigeria. Using a commercial ELISA kit, 364 pig sera collected from a major abattoir were screened for IgG antibodies against PCV2. The overall prevalence of anti-PCV2 antibodies in the pigs was 1.4 % (5/364), with more female pigs (4/237, 1.7 %) being seropositive than males (1/127, 0.8 %). Since there is no routine vaccination against this swine disease in Nigeria, thus the antibodies detected in the pig sera indicated a natural exposure to the virus. The absence of clinical disease in the pigs also suggests the possibility of a carrier status for these animals and shows that they could serve as hosts for the perpetuation of the disease. These findings underscore the need for continuous surveillance for PCV2 among pigs in Nigeria in order to determine its contribution to production losses incurred in the Nigerian swine industry and aid the development of prevention and control strategies against the disease.

Key words: antibodies; commercial pigs; Nigeria; porcine circovirus type 2; slaughterhouse

INTRODUCTION

Porcine circoviruses (PCV) are small non-enveloped DNA viruses containing a unique single-stranded circular genome (31). Two species of PCV have been identified; porcine circovirus type 1 (PCV1), and porcine circovirus type 2 (PCV2). According to different studies [6, 32, 33], PCV1 does not cause clinical disease and is non-pathogenic in pigs. However, PCV2 is the primary causative agent of several syndromes collectively known as porcine circo-

virus-associated disease (PCVAD) including: systemic or post-weaning multi-systemic wasting syndrome [17], respiratory (18), and enteric [19] diseases in pigs.

Porcine circovirus type 2 is recognized as one of the most important viruses causing severe economic impact in the swine industry worldwide and it has been described as causing different conditions depending on the virus, host immunity, co-infections and other environmental characteristics [22, 28]. PCV2 can be transmitted in several ways with the main route being by oro-nasal contact with infected faeces, urine or directly with infected pigs [9, 23, 28]. In addition, PCV2 is shed in respiratory, oral and urinary secretions, and faeces in both clinically affected, as well as in infected but apparently healthy pigs [28]. Generally, a clinical disease directly associated with PCV2 is not very common. However, in the subclinical infection, the presence of PCV2 can be responsible for production losses, mostly due to growth retardation and reduced average daily weight gain. Also, the infection of sows can lead to late-term abortions and stillbirths [22].

The Food and Agriculture Organization [13] estimated the per capita food availability of Nigerians as 2603 kcal/day of which meat contributed only 3 %. This low level contribution of meat to the daily food intake of Nigerians compared, for instance, with the United States of America where meat contributes 12 % of the total intake of 3825 kcal/day is further worsened by the scourge of infectious diseases such as African swine fever which negatively impact the country's swine population. With the growing demand for animal protein and the need to access regional and international markets for animals and animal products, continuous monitoring of animal diseases of economic importance in the country becomes imperative. Therefore, in Nigeria where pig production is becoming increasingly popular and with an estimated pig population of about seven million [14], there is a need to investigate the presence of infectious diseases that affect pig productivity. Previous studies [2, 4] based on slaughtered pigs at a major municipal abattoir in southwest Nigeria revealed serological evidence of viral diseases such as classical swine fever and porcine foot-and-mouth disease which hitherto had not been reported in Nigeria. However, although several studies have reported PCV2 in pigs elsewhere [10, 15, 34], there is a paucity of information on this disease in pigs in Nigeria. According to Segales [30], serum is the most commonly used sample to assess PCV2 antibodies and genome detection. Consequently, slaughterhouse surveys may provide an ease of sample collection during slaughter for the detection of antibodies against PCV2. Moreover, slaughterhouses are reported as critical points in the meat production scale, as well as key components of the disease control chain among animals and humans [1].

Thus, this study was carried out to determine the seroprevalence of PCV2 among apparently healthy, unvaccinated pigs slaughtered at the Bodija municipal abattoir, in Ibadan, southwest Nigeria.

MATERIALS AND METHODS

Study area and animals

A total of 364 apparently healthy pigs were randomly selected at the Bodija municipal abattoir located in Ibadan, the capital city of Oyo State in southwest Nigeria. They comprised Large White (n = 255), Duroc (n = 84) and Large Black (n = 25) breeds. Pigs slaughtered for human consumption at this abattoir were brought in from different parts of the region and may thus give a reasonable representation of the disease pattern in pigs in the region [4]. The ages of the pigs could not be determined but interaction with the pig suppliers (mainly smallholder farmers) revealed that they were adult pigs culled and sold off due to declining reproductive performance as a result of ageing. The pig slaughterhouse workers were interviewed on veterinary services and observed for any form of meat inspection in the pig slaughterhouse.

Sample collection and storage

Blood was aseptically collected into labelled plain sample bottles at slaughter from each of 364 pigs (127 males and 237 females). The blood samples were left at room temperature for about one hour to clot. Separated sera were stored at –20 °C until tested.

Detection of serum anti-PCV2 IgG antibodies

The sera were screened by an indirect enzyme-linked immunosorbent assay (ELISA) (Shenzhen Lvshiyuan Biotechnology, China) for the presence of IgG antibodies to PCV2 according to the manufacturer's instructions. The test kit, which was based on the solid-phase ELISA principle, utilized PCV2 antigen-coated microtitre plates. The test serum was first added to the antigen-coated plates.

This was followed by addition of the enzyme-labelled conjugate (anti-pig IgG antibody) which specifically bound with the complex of coated antigen and PCV2 antibody on the microtitre plate. The substrate (tetramethylbenzidine) was subsequently added and the reaction terminated with a stop solution. The optical density (OD) values were read at dual wavelengths of 450 and 630 nm. Valid results were obtained when the average OD value of the PCV2 positive control was ≥ 0.40 and that of the negative control was less than 0.20. Samples with OD value > 0.40 and < 0.40 were considered positive and negative, respectively.

Statistical analysis

The results from serology were analysed using Graph Pad prism version 5.0 (Graph Pad software, San Diego, CA, USA). The significance of differences in seroprevalence obtained based on the breed and sex of pigs was evaluated by the Chi-square test. A two-tailed P-value of 0.05 was considered statistically significant.

RESULTS AND DISCUSSION

The overall prevalence of anti-PCV2 antibodies in the pig sera was 1.4 % (5/364), with more female pigs (4/237, 1.7 %) being seropositive than males (1/127, 0.8 %). All of the seropositive pigs were of the Large White breed, while none of the samples from the Duroc or Large Black pigs were positive. Also, based on the interview conducted among the slaughterhouse workers and our observations, it was discovered that there was no form of veterinary service or meat inspection at the pig slaughterhouse.

Slaughterhouses are a source of helpful information on the incidence of animal diseases and conditions including diseases of zoonotic and economic importance. Hence, abattoir or slaughterhouse surveys are essential components of infectious disease control and eradication programmes worldwide [8]. In the present study which is part of ongoing surveillance for porcine viruses of economic importance in Nigeria [2, 3, 4], the detection of PCV2 IgG antibodies in asymptomatic pigs slaughtered at a major abattoir in southwest Nigeria indicates natural infection with the virus since vaccination against the disease is not practised in the country. It was observed in this study that there was no meat inspection in the pig slaughterhouse probably due to lack or inadequate veterinary personnel. This corroborates the findings of previous workers who reported that many abattoirs and slaughter slabs in developing countries have poor slaughter and meat inspection facilities [1, 2, 25].

The low (1.4 %) prevalence of PCV2 antibodies obtained in apparently healthy, unvaccinated adult pigs in this study suggests a low level exposure of the pigs to PCV2 as of the time of sample collection. Considering that PCV2 replicates first in the tonsils [6, 27], there may be the possibility of detecting higher level of antibodies in oral fluids [26]. However, this possibility could not be ascertained as oral fluids were not collected for this study. We therefore recommend the collection of both sera and oral fluids for future PCV2 surveillance studies in Nigeria.

Furthermore, this finding is consistent with earlier reports that PCV2 can be detected in the absence of clinical evidence of infection, suggesting the occurrence of subclinical infections or virulence variations [20] and is of veterinary importance because the infection of sows can lead to significant reproductive losses, mostly due to late-term abortions, stillbirths and birth of piglets too weak to survive [22]. More importantly, PCV2 is an endemic and very stable virus [26] that may persist in pens [12] and it has been demonstrated that pigs subclinically infected with PCV2 may excrete medium to high loads of the virus in faeces [21, 24]. In addition, Csank et al. [11] reported the shedding of the virus during subclinical infection in the presence of post-infection antibodies. Hence, these pigs could serve as reservoirs shedding the virus into the environment. This makes them potential sources for perpetuation of this viral disease that causes great economic losses as a result of the death of young animals, abortions, reduced fertility and decreased quality and quantity of the meat [26] as a result of prolonged time to slaughter weight, decreased nutritional use efficiency, and weight loss in more susceptible breeds and animals, especially when adequate contact prevention devices have not been implemented on commercial farms [12].

The diagnosis of PCV2 disease based on clinical signs is often difficult because symptoms may vary considerably depending on the virus, age of animals and production system [29]. This may account for the paucity of published information on PCV2 in Nigeria, and possibly explain the under-reporting or lack of reporting on PCV2 in the country.

To our knowledge, this study is the first report on PCV2 disease in Nigeria. The findings reveal that PCV2 presently

circulates among pigs in Ibadan, southwest Nigeria. Since this disease is considered of high economic importance due to its contribution to ill-thriftiness as well as the variable morbidity and mortality rates it causes in pigs [5, 16], there is a need for continuous surveillance for PCV2 among pigs in the country. Further studies aimed at identifying and characterizing PCV2 strains circulating in Nigeria are under consideration.

REFERENCES

1. **Adesokan, H. K., Oyedotun, A. A., Ishola, O. O., Cadmus, S. I. B., 2012:** Management and operations of selected slaughter houses in Oyo and Lagos states, south western Nigeria: public health implications. *Trop. Vet.*, 30, 161—169.
2. **Aiki-Raji, C. O., Adebiyi, A. I., Adeyemo, I. A., Fagbohun, O. A., Oluwayelu, D. O., 2014:** Seroprevalence of classical swine fever antibodies in slaughtered pigs at Bodija municipal abattoir, Ibadan, South West Nigeria. *Europ. J. Sci. Res.*, 126, 402—407.
3. **Aiki-Raji, C. O., Adebiyi, A. I., Abiola, J. O., Oluwayelu, D. O., 2017:** Prevalence of porcine reproductive and respiratory syndrome virus and porcine parvovirus antibodies in commercial pigs, southwest Nigeria. Beni-Suef Univ. *J. Basic Appl. Sci.*, http://dx.doi.org/10.1016/j.bjbas.2017.07.006.
4. **Aiki-Raji, C. O., Oluwayelu, D. O. Adeyemo, I. A. Adebiyi, A. I., 2016:** Seroprevalence of foot-and-mouth disease in slaughtered pigs in Ibadan, Southwest Nigeria, Alex. *J. Vet. Sci.*, 48, 18—22.
5. **Alarcon, P., Velasova, M., Werling, D., Stark, K. D., Chang, Y. M., Nevel, A., et al., 2011:** Assessment and quantification of post-weaning multi-systemic wasting syndrome severity at farm level. *Prev. Vet. Med.*, 98, 19—28.
6. **Allan, G. M., McNeilly, F., Cassidy, J. P., Greilly, A., Adair, B., Ellis, W. A., Mc Nulty, M. S., 1995:** Pathogenesis of porcine circovirus; experimental infections of colostrum deprived piglets and examination of pig foetal material. *Vet. Microbiol.*, 44, 49—64.
7. **Allan, G. M., McNeilly, F., Meehan, B. M., Ellis, J. A., Connor, T. J., McNair, I., et al., 2000:** A sequential study of experimental infection of pigs with porcine circovirus and porcine parvovirus: immunostaining of cryostat sections and virus isolation. *J. Vet. Med.*, 47, 81—94.
8. **Al-Qudah, K. M., Al-Majali, A. M., Obaidat, M. M., 2008:** A study on pathological and microbiological conditions in goats in slaughterhouses in Jordan. *Asian J. Anim. Vet. Adv.*, 3, 269—274.
9. **Bolin, S. R., Stoffregen, W. C., Nayar, G. P., Hamel, A. L., 2001:** Post-weaning multisystemic wasting syndrome induced after experimental inoculation of cesarean-derived, colostrum-deprived piglets with type 2 porcine circovirus. *J. Vet. Diagn. Invest.*, 13, 185—194.
10. **Chen, Q. X., Ye, J. X., Zhou, J. Y., Chen, T. F., Shen, H. G., Shang, S. B., 2007:** Serological survey of serum antibodies against porcine circovirus type 2 (PCV2) in swine, chicken, duck, goat and cattle from Zhejiang province, China. *Revue Méd. Vét.*, 158, 458—462.
11. **Csank, T., Pistl, T., Pollakova, T., Bhide, T., Herich, T., 2013:** Dynamics of antibody response and viraemia following natural infection of porcine circovirus 2 (PCV-2) in a conventional pig herd. *APMIS*, 121, 1207—1213.
12. **Dvorak, C. M., Lilla, M. P., Baker, S. R., Murtaugh, M. P., 2013:** Multiple routes of porcine circovirus type 2 transmission to piglets in the presence of maternal immunity. *Vet. Microbiol.*, 166, 365—374.
13. **Food and Agriculture Organization (FAO), 2009:** Food and Agriculture Organization of the United Nations. *The State of Food and Agriculture 2009: Livestock in the Balance,* 2010, 176 pp., www.fao.org.
14. **Food and Agriculture Organization (FAO), 2014:** *Animal Production and Health, 2014.* Cited April 11, 2017. Available at http://www.fao.org/faostat/en.
15. **Gillespie, J., Opriessnig, T., Meng, X. J., Pelzer, K., Buechner-Maxwell, V., 2009:** Porcine circovirus type 2 and porcine circovirus-associated disease. *J. Vet. Intern. Med.*, 23, 1151—1163.
16. **Grau-Roma, L., Stockmarr, A., Kristensen, C. S., Enoe, C., López-Soria, S., Nofrarías, M., et al., 2012:** Infectious risk factors for individual post weaning multisystemic wasting syndrome (PMWS) development in pigs from affected farms in Spain and Denmark. *Res. Vet. Sci.*, 93, 1231—1240.
17. **Harding, J., Clark, E., 1997:** Recognizing and diagnosing post-weaning multisystemic wasting syndrome (PMWS). *J. Swine Health Prod.*, 5, 201—203.
18. **Harms, P. A., Halbur, P. G., Sorden, S. D., 2002:** Three cases of porcine respiratory disease complex associated with porcine circovirus type 2 infection. *J. Swine Health Prod.*, 10, 27—30.
19. **Kim, J., Ha, Y., Jung, K., Choi, C., Chae, C., 2004:** Enteritis associated with porcine circovirus 2 in pigs. *Can. J. Vet. Res.*, 68, 218—221.

20. **Larochelle, R., Magar, R., D'allaire, S., 2003:** Comparative serologic and virologic study of commercial swine herds with and without post-weaning multisystemic wasting syndrome. Can. *J. Vet. Res.*, 67,114—120.

21. **Lopez-Rodriguez, A., Dewulf, J., Meyns, T., Del-Pozo-Sacristan, R., Andreoni, C., Goubier, A., et al., 2016:** Effect of sow vaccination against porcine circovirus type 2 (PCV2) on virological profiles in herds with or without PCV2 systemic disease. *Can. Vet. J.*, 57, 619—628.

22. **Madec, F., Rose, N. Grasland, B., Cariolet, R. Jestin, A., 2008:** Post-weaning multisystemic wasting syndrome and other PCV2-related problems in pigs: a12-year experience. *Transbound. Emerg. Dis.*, 55, 273—283.

23. **Magar, R., Larochelle, R., Thibault, S., Lamontagne, R., 2000:** Experimental transmission of porcine circovirus type 2 (PCV2) in weaned pigs: A sequential study. *J. Comp. Pathol.*, 123, 258—269.

24. **McIntosh, K. A., Tumber, A., Harding, J. C., Krakowka, S., Ellis, J. A., Hill, J. E., 2009:** Development and validation of a SYBR green real-time PCR for the quantification of porcine circovirus type 2 in serum, buffy coat, faeces and multiple tissues. *Vet. Microbiol.*, 133, 23—33.

25. **Mkupasi, E. M., Ngowi, H. A., Nonga, H., 2011:** Prevalence of extra-intestinal porcine helminth infections and assessment of sanitary conditions of pig slaughter slabs in Dar es Salaam city, Tanzania. *Trop. Anim. Hlth. Prod.*, 43, 417—423.

26. **Opriessnig, T., Meng, X. J., Halbur, P. G., 2007:** Porcine circovirus type 2 associated disease: update on current terminology, clinical manifestations, pathogenesis, diagnosis and intervention strategies. *J. Vet. Diagn. Invest.*, 19, 591—615.

27. **Rosell, C., Segales, J., Plana-Duran, J., Balasch, M., Rodriguez-Arrioja, G. M., Kennedy, S., et al., 1999:** Pathological, immunohistochemical and in situ hybridization studies of natural cases of post-weaning multisystemic wasting syndrome (PMWS) in pigs. *J. Comp. Pathol.*, 120, 59—78.

28. **Segales, J., Allan, G. M., Domingo, M., 2005:** Porcine circovirus diseases. Anim. *Hlth. Res. Rev.*, 6, 119—142.

29. **Segales, J., Kekarainen, T., Cortey, M., 2013:** The natural history of porcine circovirus type 2: from an inoffensive virus to a devastating swine disease? *Vet. Microbiol.*, 165, 13—20.

30. **Segales, J., 2012:** Porcine circovirus type 2 (PCV2) infections: clinical signs, pathology and laboratory diagnosis. *Virus Res.*, 164, 10—19.

31. **Tischer, I., Gelderblom, H., Vettermann, W., Koch, M. A., 1982:** A very small porcine virus with circular single-stranded DNA. *Nature*, 295, 64—66.

32. **Tischer, I., Mields, W., Wolff, D., Vagt, M., Griem, W., 1986:** Studies on epidemiology and pathogenicity of porcine circovirus. *Arch. Virol.*, 91, 271—276.

33. **Tischer, I., Rasch, R., Tochtermann, G. 1974:** Characterization of papovavirus-and picornavirus-like particles in permanent pig kidney cell lines. *Zentralbl. Bakteriol. (Orig A)*, 226, 153—167.

34. **Walker, I. W., Konoby, C. A., Jewhurst, V. A., McNair, I., McNeilly, F., Meehan, B. M., et al., 2000:** Development and application of a competitive enzyme-linked immunosorbent assay for the detection of serum antibodies to porcine circovirus type 2. *J. Vet. Diagn. Invest.*, 12, 400—405.

Received December 9, 2017
Accepted April 11, 2018

sciendo

DOI: 10.2478/fv-2018-0015

FOLIA VETERINARIA, 62, 2: 35—44, 2018

SPINAL CORD INJURIES IN DOGS PART I: A REVIEW OF BASIC KNOWLEDGE

Šulla, I.[1], Balik, V.[2], Horňák, S.[3], Ledecký, V.[3]

[1]Department of Anatomy, Histology and Physiology
[3]Small Animal Clinic, University of Veterinary Medicine and Pharmacy
Komenského 73, 041 81 Košice
Slovakia
[2]Institute of Molecular and Translational Medicine
University Hospital and Faculty of Medicine and Dentistry
Palacky University, I. P. Pavlova 6, 772 20 Olomouc
Czechia

igor.sulla@uvlf.sk

ABSTRACT

Spinal cord injuries (SCI) in dogs are not frequent, but they are serious pathological conditions accompanied with high morbidity and mortality. The pathophysiology of SCI involves a primary insult, disrupting axons, blood vessels, and cell membranes by mechanical force, or causes tissue necrosis by ischemia and reperfusion. The primary injury is followed by a cascade of secondary events, involving vascular dysfunction, edema formation, continuing ischemia, excitotoxicity, electrolyte shifts, free radical production, inflammation, and delayed apoptotic cell death. The most frequent cause of SCI in dogs is an acute intervertebral disc extrusion, exogenous trauma or ischemia. Neurological symptomatology depends on the location, size and the type of spinal cord lesions. It is characterized by transient or permanent, incomplete or complete loss of motor, sensory, autonomic, and reflex functions caudal to the site of the lesion. In a case of partial spinal cord (SC) damage, one of the typical syndromes develops (e. g. Brown-Séquard syndrome, central SC syndrome, ventral SC syndrome, dorsal SC syndrome, conus medullaris syndrome, or traumatic cauda equina syndrome). The severe transversal spinal cord lesion in the cervical region causes paresis or plegia of all four extremities (tetraparesis, tetraplegia); in thoracic or lumbosacral region, paresis or plegia of the pelvic extremities (paraparesis, paraplegia), i. e. sensory-motor deficit, urinary and foecal incontinence and sexual incompetence. The central nervous system in mammals does not regenerate, so the neurological deficit in dogs following severe SCI persists for the rest of their lives and animals display an image of permanent suffering. The research strategy presented here involved a PubMed, Medline (Ovid) and ISI Web of Science literature search from Januray 2001 to December 2017 using the term "canine spinal cord injury" in the English language; also references from selected papers were scanned and relevant articles included.

Key words: dog; pathophysiology; spinal cord injury; symptomatology

INTRODUCTION

A spinal cord injury (SCI) is defined as damage to the spinal medulla (a traumatic medullopathy, i. e. TM) inflicted by a mechanical insult or ischemia [10, 11, 21]. The annual incidence of SCIs is relatively low (3—5/100 000 in humans, much lower in animals), but they are devastating neurological disorders, remaining important causes of morbidity and mortality [14, 23, 30, 36, 39]. Survivors often have major sequelae, including tetra- or paraparesis, eventually tetra- or paraplegia, urinary and fecal incontinence, sexual incompetence and are partially or completely physically dependent for the rest of their lives [3, 14, 30, 42, 55]. The neurological deficit in SCI develops through two pathological events — the primary and secondary damage [4, 16, 41]. The primary injury encompasses the immediate lesion to the spinal cord tissue that occurs at the moment of insult, which is irreversible and not preventable [46, 56]. The secondary injury develops as a result of the pathological processes initiated at the time of the primary event, continues for several days and even months after trauma and is amenable by therapy [13, 24, 39, 40, 56]. The clinical outcome in individuals with SCIs is determined by the location and size of the neural tissue damage, age of a patient and associated complications [3, 27, 42, 50]. The most frequently observed causes of acute SCIs in humans are traffic accidents, falls and sport injuries. Spinal cord traumatic incidents are reported in domestic animals, especially in dogs, too [10, 11, 14, 48]. The irreversible loss of functions due to the damage of the spinal cord tissue has been recognised for centuries, but only limited therapeutic options are available until the present time [1, 2, 8, 31]. So the management of SCIs in humans as well as in other animals is basically targeted at preservation of remaining functions and prevention of complications; especially pulmonary and urinary tract infections, spasticity and pressure sores, i. e. decubitus [3, 14, 23, 27, 39, 50]. In spite of a specialised attendance and application of different therapeutic interventions, the neurological deficit in a dog following serious SCI does not improve and it displays an image of permanent suffering for the rest of the dog's life (Fig. 1).

The ambition to improve the unfavourable situation inspired the authors to review recently published studies related to SCIs in small laboratory animals, in dogs and pigs as well as in humans and translate the recent information to everyday clinical practices [4—7, 16—18, 36, 52].

Basic anatomical and physiological facts

The brain (*cerebrum*) and spinal cord (*medulla spinalis*) constitute the central nervous system (CNS). The brain is enclosed within the skull (*cranium*), the spinal medulla within the vertebral canal (*canalis vertebralis*). The spinal cord is a direct continuation of the brain stem (*medulla oblongata,* myelencephalon). It has two enlargements (*intumescentia cervicalis* giving origin to the nerves of *plexus*

Fig. 1. Dog with ischemic paraplegia due to 30-min. of thoracic aorta cross-clamping

brachialis and *intumescentia lumbalis* — the origin of *plexus lumbosacralis*). The spinal medulla in dogs has a total 36 segments (8 cervical, 13 thoracic, 7 lumbar, 3 sacral and 5 caudal) and it extends from the 1st cervical nerves to the caudal part of an elongated cone (*conus medullaris*) consisting of spinal cord segments S2, S3, Ca1 to Ca5 [19, 20]. The sacral and caudal segments appear successively smaller and they are surrounded by caudally directed spinal roots [19]. About 1 cm caudal to the last segment (spinal cord termination), the medulla is reduced to a strand of glial and ependymal cells called terminal filament (*filum terminale*). The development of the spinal cord (*medulla spinalis*) begins in the canine embryo soon after the post-somite phase, when the cord reaches into the coccygeal part of the vertebral canal. In later developmental stages, the bones and cartilages of the vertebral column grow more rapidly than the cord itself. The disproportional growth of these structures as well as the difference in length of the individual spinal cord segments cause cranial "shift" of the spinal cord termination [20]. The caudalmost pairs of lumbar (L6 and L7), all sacral (S1—S3) and caudal/coccygeal (Cd/Cco1-5) spinal roots continue within the vertebral canal to corresponding intervertebral foramina [19, 20]. The structure resembles the tail of a horse, so the anatomic nomenclature adresses it as the cauda equina (CE). Skeletotopic localisation of the medullary cone depends on the breed of the animal. In giant dogs it is located at the mid-body of the 6th lumbar vertebra, in big dogs at the L6/L7 intervertebral space, in intermediate sized dogs at the L7/S1 intervertebral space, in small dogs at the level of the S1 vertebra [19, 20]. The basis for dividing the spinal cord into segments are the attachments of the nerve roots. Each dorsal or ventral nerve root (*radix dorsalis, radix ventralis*) is composed of thousands of axons. The axons of every root are bound together laterally where dorsal and ventral roots join to form the spinal nerve, but as roots approach the spinal cord, their axons regroup into separate bundles called rootlets (*fila radicularia*) attaching serially along the spinal cord. At the level of the intervertebral foramen, the spinal roots join and become a spinal nerve. At the terminal parts of the dorsal nerve roots (just before their junctions with the ventral nerve roots) are located aggregations of pseudounipolar neurons named spinal ganglia (*ganglia spinalia*). The pseudounipolar cells deliver central and peripheral processes. The central processes form the dorsal root filaments (sensitive), the peripheral processes intermingle with the axons of the ventral root filaments (motoric) in forming the main trunk of the spinal nerve containing both, sensory and motor fibres. The spinal cord and spinal roots inside the vertebral canal are enveloped by three protective layers termed meninges. The superficial layer (*dura mater*) is fibrous and thick. It forms a cylinder surrounding the spinal medulla and through lateral extensions it (together with *arachnoidea* and *pia mater*) ensheathe spinal roots. The thin arachnoid membrane also lines the inner surface of the dura mater. A subarachnoid space containing the cerebrospinal fluid (CSF) is located

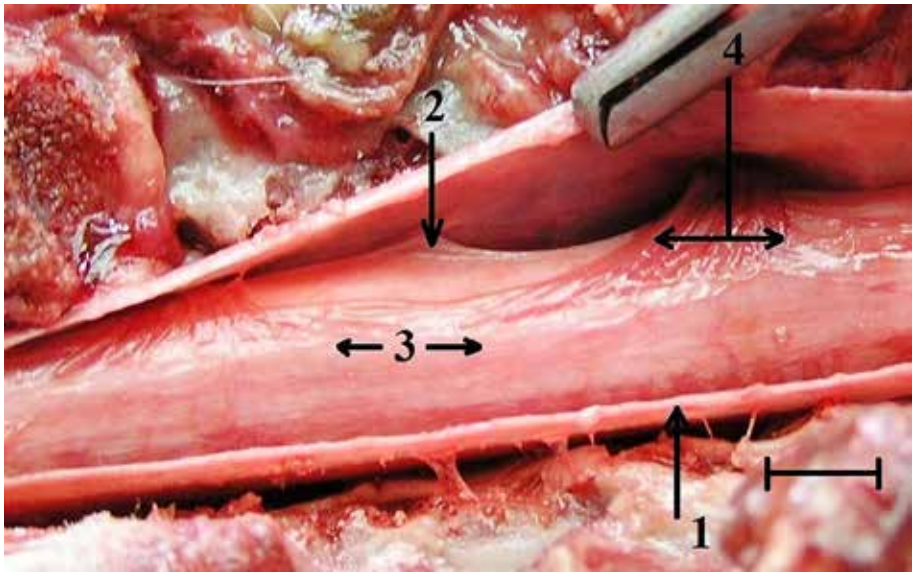

Fig. 2. An anatomical specimen of canine spinal cord after laminectomy and durotomy
1 — dura mater spinalis; 2 — dental ligament; 3 — spinal medulla covered by arachnoidal membrane and pia mater; 4 — spinal nerve roots. Bar = 5 mm

below the arachnoid membrane (Fig. 2). The *pia mater*, the deepest, most vascular meninx, is bound to glial cells at the spinal cord surface [20].

The spinal cord performs three main functions:

1. Via spinal nerve connections it processes afferent (centripetal) information from muscles, tendons, joints, ligaments, blood vessels, skin and viscera, and discharges efferent (centrifugal) commands controlling muscles and regulates glands.
2. The spinal cord is a reflex center producing subconscious responses of muscles and glands to specific stimuli.
3. The spinal cord conducts and modifies information to and from the brain through a system of axonal tracts by which the brain receives informations from peripheral organs and tissues while dispersing commands that control posture, movement and the visceral aspects of behaviour [14, 19, 20].

Etiology of SCI in dogs

The most common causes of acute spinal cord damage (myelopathy) in dogs is an extrusion of material from the central part of the disc (*nucleus pulposus*) into the spinal canal due to intervertebral disc degenerative changes (Hansen type I disc disease), exogenous traumatic events and infarction due to ischemia [9, 10, 11, 22, 23, 33].

Degenerative disc disease is a common problem in dogs, but relatively rare in cats [14, 33, 35, 39]. There are two basic types of intervertebral disc diseases, referred to as chondroid and fibroid degeneration. In chondroid degeneration, the normally gelatinous pulpous inner part of disc (*nucleus pulposus*) undergoes degradation of glycosaminoglycan components and loses its water-binding capacity. The abnormal contents of the nucleus pulposus herniate (extrude) through the thinner dorsal part of the external fibrous ring of the disc (*annulus fibrosus*) into the vertebral canal. This type of canine intervertebral disc disease (IVDD) is called Hansen type I IVDD and most frequently is seen in chondrodystrophic breeds of dogs (e. g. Basset Hounds, Beagle, Dachshund, Shi Tzu, Lhasa Apso). The Hansen I type of IVDD is characteristicly a sudden rupture of the dorsal part of the annulus fibrosus with an explosive release of the nucleus pulposus material. It causes concussion or compression of the spinal medulla and results in varying degrees of neurological dysfunctions [22, 33, 39]. The severity of the spinal cord damage caused by type I disc extrusion is related to the rate of herniation (force of impact), the duration of neural structure's compression and the volume of the extruded disc material. The incidence of dogs presenting with neurological symptoms due to intervertebral disc herniation is about 2 % of all cases admitted to veterinary facilities [9, 23, 39, 48].

The second most frequent cause of SCIs in dogs is trauma. It usually occurs in association with traffic accidents, vertical falls, animal-animal or human-animal interactions, gunshot or stab wounds and usually accompany vertebral fractures or luxations. At present, about 60 % of traumatic SCIs in dogs are the consequences of traffic accidents [10, 14, 39].

Fibrocartilaginous (FCE) embolism is a rare cause of an acute spinal cord dysfunction [11, 35, 43, 59]. It is induced by the occlusion of spinal vasculature (leptomeningeal and intramedullary vessels) by material from the nucleus pulposus producing ischemia of dependent region of the spinal cord parenchyma. The clinical presentation is of a peracute, non-progressive paralysis with a distribution and severity depending on the site of the infarction. Since the definitive diagnosis of FCE is not possible without histological examination, diagnostic procedures should exclude compressive myelopathy, particularly that caused by intervertebral disc herniation [9, 23, 32, 48]. The true incidence of FCEs is difficult to assess; the condition predominantly affects dogs of big and giant breeds [11, 21, 35, 43, 60].

Clinical presentation

The neurological deficit characteristics for spinal cord injury depends upon the location, size and the rate of development of the lesion [14, 23, 24, 55]. The signs of spinal cord trauma are typically acute and may further progress in instances of unstable fractures or luxations [14, 39]. A severe medullary damage may cause paraplegia with increased extensor tone in the thoracic limbs. The symptom is called Schiff-Sherrington phenomenon [45]. A small unilateral damage of the spinal medulla will likely cause symptoms predominantly on the side of the lesion. Large lesions or lesions associated with substantial cord swelling will result in the development of bilateral symptomatology [39, 54, 55].

A benign spinal cord injury, when the traumatic forces cause functional derangement of spinal cord circuits only, but no mechanical disruption of the medulla or its tracts, is called spinal cord concussion (*Commotio medullae spi-*

nalis). It belongs to the so called mild spinal traumas and in a majority of the cases it is inflicted by a blow to the vertebral column [49]. It leads to transient paresis, but the patient never reveals symptomatology of a complete (transversal) spinal cord lesion [14, 45].

In case a partial medullary damage develops, one of the syndromes results in an incomplete spinal cord lesion [14, 34, 56]. The clinical symptomatology of an incomplete medullary lesion is given by their anatomic relationships, i. e. by the course of motor and the sensitive tracts and the location of the spinal cord vessels. If the whole spinal medulla is mechanically or functionally damaged, the situation is termed a transversal spinal cord lesion. In this situation neurological examination reveals a complete loss of motor, sensitive and vegetative functions caudally from the epicentre (Fig. 2). It is important to stress, that immediately after spinal trauma even patients with incomplete medullary lesions reveal transient supression or loss of muscle tone and segmental spinal reflexes caudal to the SCI. This phenomenon is called spinal shock, which differs essentially from the neurogenic shock [15, 31, 47]. Compared with big apes and humans, where spinal shock resolves in a series of phases extending over days to weeks, the recovery from the spinal shock in non-primates is relatively rapid (e. g. the patellar reflex in rabbits reappears 10—15 minutes following SCI, between 30 minutes and 2 hours in cats and dogs); it does not attract the major attention of veterinarians, so far [47, 55]. In an acute phase of SCI, the gross reactions of the organism are characterised by tachycardia, later on it is replaced by bradycardia; blood pressure fluctuates, too — the initial hypertension is later on substituted by hypotension [55, 56]. The peripheral vascular resistance declines, the cardiac output is diminished, blood levels of cathecholamines increase, and then subsequently decrease. In the case of cervical SCIs, the respiration is endangered and dogs succumb or are euthanized at the place of the event [14, 24, 34, 39, 44].

Spinal cord hemisection syndrome (Brown-Séquard syndrome or BSS) occurs when just one side of the spinal medulla is damaged or it is injured much more severely than the other. It is rare to see the spinal cord truly hemisected, much more frequently it is called Brown-Séquard plus syndrome or partial lesions due to the penetrating injuries (e. g. gunshot or stab wounds) or vertebral fractures and luxations (Fig. 3).

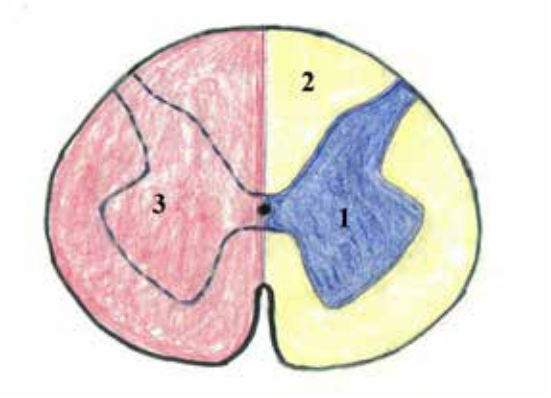

Fig. 3. Schematic representation of spinal cord hemisection syndrome, i. e. Brown-Séquard syndrome (BSS)
1 — gray matter; 2 — white matter; 3 — lesioned part of spinal cord (pink area)

On the ipsilateral side of the lesion, the body loses motor functions, proprioception, the sense of vibration and touch. On the contralateral side of the injury pain and temperature sensations are lost [14, 34].

Central spinal cord syndrome (central cord syndrome or CCS) usually results from the damage to the cervical part of the spinal medulla due to the neck hyperextension in patients with cervical spinal stenosis (Fig. 4).

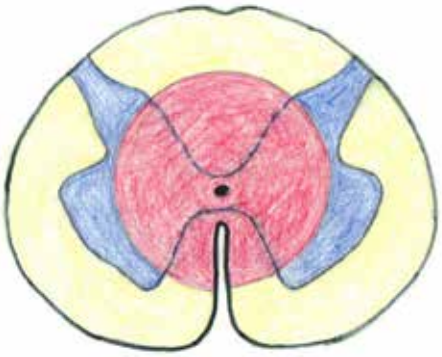

Fig. 4. Schematic representation of a central spinal cord syndrome (CCS) (pink area)

The CCS is characterized by weakness in the thoracic extremities with relative sparing of the pelvic extremities and loss of sensation of pain, temperature, light touch, and pressure caudal to the level of injury [14]. The spinal tracts that serve thoracic limbs are more affected due to their central location in the spinal cord, while the corticospinal fibers destined for the pelvic limbs are spared due to their more external location [14, 34].

Ventral spinal cord syndrome (ventral cord syndrome or VCS) is caused by damage to the ventral portion of the spinal medulla or the reduction in the blood supply from the ventral spinal artery (Fig. 5) compressed by fragments

of vertebral bodies or herniated intervertebral discs [10, 14, 34]. The VCS is characterized by urinary retention, loss of motor functions, pain and temperature sensation caudal to the level of injury, while the sense of touch and position in space remains intact [14, 34, 39].

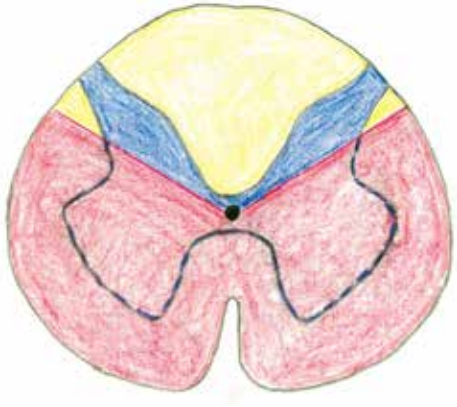

Fig. 5. Schematic representation of a ventral spinal cord syndrome (VCS) (pink area)

Dorsal spinal cord syndrome (dorsal cord syndrome or DCS), in which the dorsal columns of the spinal medulla are affected (Fig. 6), is usually seen in patients with vertebral canal degenerative stenosis or infarction of the posterior spinal arteries [14, 34, 39]. The DCS is characterized by the loss of proprioception and the sense of vibration caudal to the level of the lesion, while motor functions and the sensation of pain, temperature, and touch remain intact [14, 34].

Conus medullaris syndrome (CMS) is caused by an injury to the caudal end of the spinal medulla [14]. This region is responsible for bowel, urinary bladder and sexual functions; perianogenital and tail sensation. The Achilles tendon reflex can be affected also. The symptoms occur bilaterally [14, 34, 55].

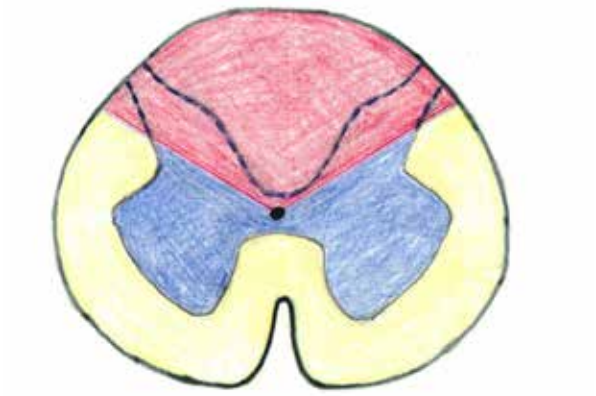

Fig. 6. Schematic representation of a dorsal spinal cord syndrome (DCS) (pink area).

Traumatic cauda equina syndrome (cauda equina syndrome or CES) results from a lesion to L7—Cd5 spinal nerve roots due to the fracture and dislocation of the sacral bone or L7/S1 intervertebral disc herniation [14, 34, 39]. It is not a true spinal cord syndrome, since the spinal cord nerve roots damaged in CES are actually peripheral nerves. The CES can occur by itself or alongside with the CMS. It is characterized by: low back pain, weakness in the pelvic extremities, nociceptive deficits in the medial areas of the pelvic limbs, perineum and tail, and bowel and urinary bladder dysfunctions [14, 34]. Unlike the conus medullaris syndrome, symptoms of CES often occur unilaterally (Fig. 7).

Pathophysiology of spinal cord injury

The damage in SCIs begins suddenly at the moment of a traumatic event when displaced vertebrae, their fragments, intervertebral disc material or ligaments compress or tear the spinal medulla and its blood vessels [4, 10, 14, 16]. External forces sever axons and blood vessels which causes hemorrhage (predominantly in the gray matter) and ischemia [16, 18, 26, 37, 41]. Within several minutes the spinal cord swells and fills the spinal canal [16, 37, 41, 44, 61]. The increased compression of vessels diminishes blood flow, decreases medullary tissue oxygen supply and enhances ischemia. The situation further deteriorates due to systemic blood pressure drop as the body loses the ability to autoregulate. The changes in blood flow start in the epicenter and spread to adjacent, undamaged tissue, which can last for as long as 24 hours and progressively worsens. Due to the differences in tissue composition, the impact of these events is greater on the interior gray matter of the spinal medulla than on the outlying white matter. Not only the blood vessels in the gray matter are damaged by the external mechanical forces, but also intact capillaries begin to leak due to the blood — spinal cord barrier (BSCB) disruption, sometimes as early as 5 minutes following the injury [16, 37, 44, 61]. Edema of the spinal cord appears. The combination of vessel leakage, tissue swelling and reduction of blood circulation aggravate the physiological delivery of oxygen and nutrients to neurons causing their destruction [16]. The loss of ionic homeostasis manifested by intracellular shift of Ca^{2+} together with Na^{+} and efflux of K^{+}, appears immediately following spinal trauma [13, 16, 41, 56—58]. It is exaggerated by excessive release of neurotransmitters, especially glutamate, the substance used by nerve cells to signal each other and stimulate their activity. The flooding

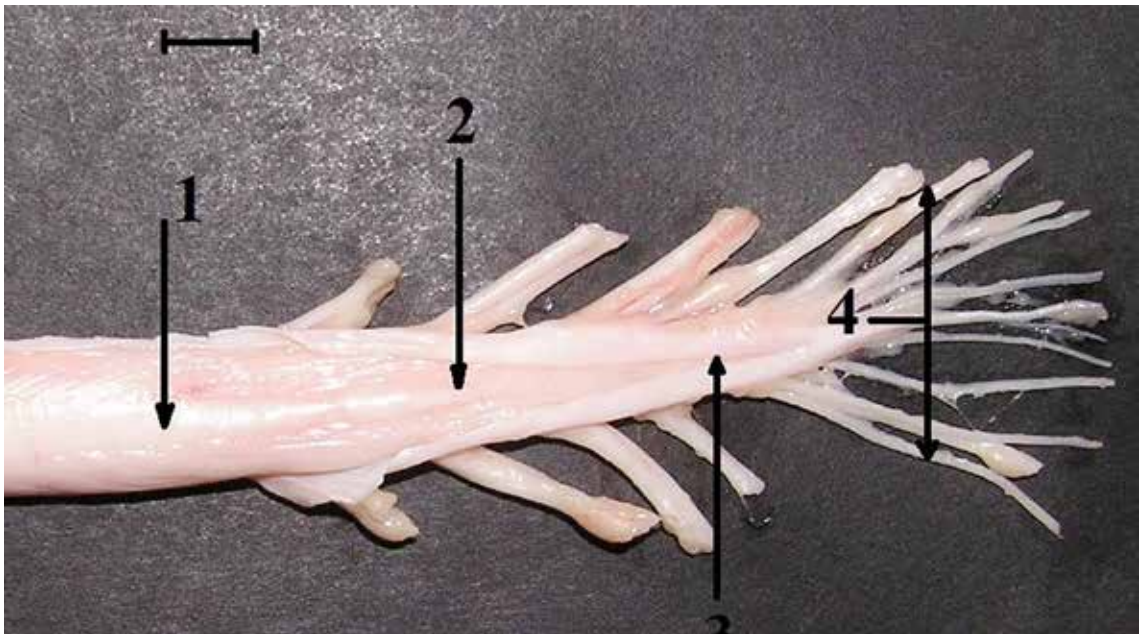

Fig. 7. An anatomical specimen of the caudal end of the spinal cord, medullary cone and cauda equina following removal from the vertebral canal and spinal dural sac
1 — spinal cord; 2 — medullary cone; 3 — terminal filament; 4 — cauda equina nerve roots. Bar = 5 mm. (An original picture)

of the area of SCI by neurotransmitters and the loss of ionic homeostasis are central features of necrotic and apoptotic cell death [16, 41, 57—59, 61]. Specifically, dysregulation of the Ca^{2+} ion concentration is not only a common element in cell death, but initiates a number of damaging processes including the activation of calpains, mitochondrial dysfunction and increasing free radical production [12, 13, 25]. Free radicals mediate lipid peroxidation contributing to axonal disruption and the death of both, neurons as well as glial cells. Lipid peroxidation is a self-perpetuating free radical reaction causing membrane damage leading to heart rate drop, cell lysis, the dysfunction of organelles, and further contributes to the calcium dyshomeostasis through the oxidation of membrane lipids [13, 25, 28]. When the BSCB is broken, large molecules and immune system cells enter the spinal cord tissue. This invasion triggers an inflammatory response, characterized by fluid accumulation and the influx of immune cells – neutrophils, T-cells, macrophages and monocytes [6, 53]. The physiological function of the immune system (IS) is fighting infection and cleaning debris. However, the above mentioned response of the IS to SCI also triggers the activation of microglia and the release of cytokines – a group of messenger molecules (e. g. IL-6, IL-13, TNF-α) with a distinct negative effect on the nerve cells [13, 38, 41, 44, 46, 51].

Another consequence of the immune system cells entry into the area of SCI is that inflammation accelerates the production of highly reactive forms of oxygene molecules called free radicals. They appear as by-products of normal cell metabolism. In the healthy spinal cord their numbers are too small to cause any harm. But the SCI and the subsequent wave of inflammation, signals particular cells to overproduce free radicals. Then they attack and damage molecules crucial for cell function, especially those in cell membranes, by modifying their chemical structure [5]. In the past it was supposed that the only way in which cells died in SCIs was a direct result of the traumatic event [16]. However, recent findings have revealed that cells in the damaged spinal medulla also die from a kind of programmed cell death called apoptosis [14, 25, 46, 57]. Apoptosis is a physiological cellular event that occurs in tissues and cell systems. It helps the body get rid of old or ill cells by causing them to shrink and implode. Nearby scavenger cells then engulf and remove debris. For reasons that are still unclear, SCI starts apoptosis, which kills oligodendrocytes, the cells that form myelin wrapping around axons. So apoptosis damages myelin sheets on intact axons in adjacent pathways, too [29, 44, 57].

All of above mentioned mechanisms of secondary injury increase the area of destruction in the damaged spi-

Table 1. Primary and secondary mechanisms involved in traumatic SCIs

Primary, i. e. injury phase	Secondary phase
Compresion Distraction Laceration Shearing mechanisms Ischemia	Vascular changes: failure of autoregulation, systemic hypotension, haemorrage, blood flow reduction, impaired microcirculation, vasospasms, thrombosis, BSCB disruption, edema
	Ionic dysregulation: intracellular shift of Ca^{++} and Na^{+}, extracellular drift of K^{+}
	Biochemical changes: excessive release of neurotransmitters, free radicals production, release of excitotoxic aminoacids (glutamate) and prostaglandins, lipid peroxidation
	Inflammation: fluid accumulation, influx of immune cells (neutrophils, T-cells, macrophages, monocytes), release of cytokines

nal medulla. Affected axons become dysfunctional either because they are stripped of their myelin or because they are disconnected from the cranial regulatory centers [17]. Glial cells accumulate to form a scar creating a barrier to axons that could potentially regenerate. A few intact axons may remain, but they are not enough to convey meaningful information from the periphery to the brain (41).

Over weeks to months following the SCI (chronic phase), the lesion site: continues Wallerian degeneration, axon fragmentation, progressive apoptosis of the oligodendrocytes, demyelination, maturation of glial scar, cavitation of medullary tissue (*syringomyelia*), and stabilisation of the lesion. At about the same time the start of the reparatory processes and neuronal and axonal sprouting (supported by brain derived neurotrophic factor, i. e. BDNF) begins, but concurrently the production of neuron growth inhibitors (especially three isophorms of neurite outgrowth inhibitors, i. e. NOGO A, B, and C, myelin-associated glycoprotein, i. e. MAG, or Rho-kinase, i. e. ROCK) impede the regeneration [7, 17, 29, 44].

CONCLUSION

This review provides an overview of the current information of the etiology, pathophysiology and neurological symptomatology of spinal cord injuries in dogs.

ACKNOWLEDGEMENT

The accumulation and study of literature dealing with different aspects of spinal cord injuries as well as the preparation of this paper was supported by a grant from the Agency of the Ministry of Education, Science, Research and Sport of the Slovak Republic for the Structural Funds of EU, ITMS 26220220202 and VEGA grant No. 1/0898/15.

REFERENCES

1. **Aciduman, A., Belen, D., Simsek, S., 2006:** Management of spinal disorders and trauma in Avicenna's Canon of medicine. *Neurosurgery*, 59, 397—403.
2. **Adams, F., 1886:** *The Genuine Works of Hippocrates Translated from the Greek with a Preliminary Discourse and Annotations*. Vol. 2, William Wood and Co, New York, 411 pp.
3. **Adams, M. M., Hicks, A. L., 2005:** Spasticity after spinal cord injury. *Spinal Cord*, 43, 577—586.
4. **Akhtar, A. Z., Pippin, J. J., Sandusky, C. B., 2008:** Animal models in spinal cord injury: a review. *Rev. Neurosci.*, 19, 47—60.
5. **Anderson, K. M., Welsh, C. J., Young, C., Levine, G. J., Kerwin, S. C., Boudreau, C. E., 2015:** Acute phase proteins in cerebrospinal fluid from dogs with naturally-occurring spinal cord injury. *J. Neurotrauma,* 32, 1658—1665.
6. **Anwar, M. A., Al Shehabi, T. S., Eid, A. I., 2016:** Inflammogenesis of secondary spinal cord injury. *Front. Cell. Neurosci.,* 10, 98. doi: 10.3389/fncel.2016.00098.
7. **Borrie, S. C., Baeumer, B. E., Badtlow, C. E., 2012:** The nogo-66 receptor family in the intact and diseased CNS. *Cell Tissue Res.*, 349, 105—117.
8. **Breasted, J. H., 1980:** T*he Edwin Smith Surgical Papyrus, Volume 1: Hieroglyphic Transliteration, and commentary*. Univ. Chicago press, Chicago, 596 pp.
9. **Brisson, B. A., 2010:** Intervertebral disc disease in dogs. *Vet. Clin. North Am. Small Anim. Pract.*, 40, 829—858.

10. **Bruce, C. W., Brisson, B. A., Gyselinck, K., 2008:** Spinal fracture and luxation in dogs and cats: a retrospective evaluation of 95 cases. *Vet. Comp. Orthop. Traumatol.*, 21, 280—284.
11. **Cauzimille, L., Kornegay, J. N., 1996:** Fibrocartilaginous embolism of the spinal cord in dogs: Review of 36 histologically confirmed cases and retrospective study of 26 suspected cases. *J. Vet. Intern. Med.*, 10, 241—245.
12. **David, S., Kroner, A., 2011:** Repertoire of microglial and macrophage responses after spinal cord injury. *Nat. Rev. Neurosci.*, 12, 388—399.
13. **Devaux, S., Cizkova, D., Quamico, J., Franck, J., Nataf, S., Pays, L., et al., 2016:** Proteomic analysis of the spatio-temporal based molecular kinetics of acute spinal cord injury identifies a time- and segment-specific window for effective tissue repair. *Moll. Cell. Proteomics*, 15, 2641—2670.
14. **Dewey, C. W., 2008:** *A Practical Guide to Canine and Feline Neurology*. 2nd edn., Iowa State University Press, Ames, Iowa, USA, 706 pp.
15. **Ditunno, J. F., Little, J. W., Tessler, A., Burns, A. S., 2004:** Spinal shock revisited: a four-phase model. *Spinal Cord*, 42, 383—395.
16. **Dumont, R. J., Okonkwo, D. O., Verma, S., Hurlbert, R. J., Boulos, P. T., Ellegala, D. B., et al., 2001:** Acute spinal cord injury, Part. I: Pathophysiologic mechanisms. *Clin. Neuropharm.*, 24, 254—264.
17. **Filbin, M. T., 2003:** Myelin-associated inhibitors of axonal regeneration in the adult mammalian CNS. *Nat. Rev. Neurosci.*, 4, 703—713.
18. **Fleming, J. C., Noremberg, M. D., Ramsay, D. A., Dekalan, G. A., Marcillo, A. E., Saenz, A. D., et al., 2006:** The cellular inflammatory response in human spinal cords after injury. *Brain*, 169, 3249—3269.
19. **Fletcher, T. F., Kitchell, R. L., 1966:** Anatomical studies on the spinal cord segments of the dog. *Am. J. Vet. Res.*, 27, 1759—1767.
20. **Fletcher, T. F., 2013:** Spinal cord and meninges. In **Evans, H. P., de Lahunta, A., (Eds.):** *Miller's Anatomy of the Dog.* 4th edn., Elsevier, Saunders, St. Louis, USA, 589—610.
21. **Gandini, G., Cizinauskas, S., Lang, J., Fatzer, R., Jaggy, A., 2003:** Fibrocartilaginous embolism in 75 dogs: clinical findings and factors influencing the recovery rate. *J. Small Anim. Pract.*, 44, 76—80.
22. **Hansen, H. J., 1951:** A pathologic-anatomical interpretation of disc degeneration in dogs. *Acta Orthop. Scand.*, 20, 280—293.
23. **Henke, D., Vandevelde, M., Doher, M. G., Stockli, M., Forterre, F., 2013:** Correlations between severity of clinical signs and histopathological changes in 60 dogs with spinal cord injury associated with acute thoracolumbar intervertebral disc disease. *Vet. J.*, 198, 70—75.
24. **Jeffery, N. D., Hamilton, L., Granger, N., 2011:** Designing clinical trials in canine spinal cord injury as a model to translate successful laboratory interventions into clinical practice. *Vet. Rec.*, 168, 102—107.
25. **Jeong, S. Y., Seol, D. W., Li, F. C., Chen, Q. X., 2008:** The role of mitochondria in apoptosis. *BMB Reports*, 41, 11—22.
26. **Kato, S., Kawakaza, N., Tomita, K., Murakami, H., Demura, S., Fujimaki, Y., 2008:** Effects on spinal cord blood flow and neurologic function secondary to interruption of bilateral segmental arteries which supply the artery of Adamkiwicz. *Spine*, 33, 1533—1541.
27. **Kruger, E. A., Pires, M., Ngann, Y., Sterling, M., Rubay, S., 2013:** Comprehensive management of pressure ulcers in spinal cord injury. *Biomaterials*, 30, 2582—2590.
28. **Lacroix, S., Chang, L., Rose-John, S., Tuszynski, M. H., 2002:** Delivery of hyper-interleukin-6 to the injured spinal cord increases neutrophil and macrophage infiltration and inhibits axonal growth. *J. Comp. Neurol.*, 454, 213—228.
29. **Lee, J. Y., Choi, S. Y., Oh, T. H., Yune, T. Y., 2012:** 17β-estradiol inhibits apoptotic cell death of oligodendrocytes by inhibiting Rhoa-JNK3 activation after spinal cord injury. *Endocrinology*, 153, 3815—3827.
30. **Levine, G. J., Levine, J. M., Budke, C. M., Kerwin, S. C., Au, J., Vinayak, A., et al., 2009:** Description and repeatability of a newly developed spinal cord injury scale for dogs. *Prev. Vet. Med.*, 89, 121—127.
31. **Mack, E. H., 2013:** Neurogenic shock. *Open Ped. Med. J.*, 7 (Suppl. 1: M4), 16—18.
32. **Marketos, S. G., Skiadas, P. K., 1999:** Galen. A pioneer of spine research. *Spine*, 24, 2358—2362.
33. **McKee, W. M., Downes, C. J., Pink, J. J., Gemmill, T. J., 2010:** Presumptive exercise-associated peracute thoracolumbar disc extrusion in 48 dogs. *Vet. Rec.*, 166, 523—528.
34. **McKinley, W., Santos, K., Meade, M., Brooke, K., 2007:** Incidence and outcomes of spinal cord injury clinical syndromes. *J. Spinal Cord Med.*, 30, 215—224.
35. **Nakamoto, Y., Ozawa, T., Katanabe, K., Nishiya, K., Yasuda, N., Mashita, T., et al., 2009:** Fibrocartilaginous embolism of the spinal cord diagnosed by characteristic clinical findings and magnetic resonance imaging in 26 dogs. *J. Vet. Med. Sci.*, 71, 171—176.
36. **Navarro, R., Juhas, S., Keshavarzi, S., Juhasova, J., Motlik, J., Johe, K., et al., 2012:** Chronic spinal compression model in minipigs: a systematic behavioral, qualitative, and quantita-

tive neuropathological study. *J. Neurotrauma*, 29, 499—513.

37. **Noble, L. J., Donovan, F., Igarashi, T., Goussev, S., Werb, Z., 2002:** Matrix metalloproteinases limit functional recovery after spinal cord injury by modulation of early vascular events. *J. Neurosci.*, 22, 7526—7535.
38. **Okon, E. B., Streijger, F., Lee, J. H., Anderson, L. M., Russel, A. K., Kwon, B. K., 2013:** Intraparenchymal microdialysis after acute spinal cord injury reveals differential metabolic responses to contusive spinal cord injury. *J. Neurotrauma*, 30, 1564—1576.
39. **Olby, N., 2010:** The pathogenesis and treatment of acute spinal cord injuries in dogs. *Vet. Clin. N. Am. Small Anim. Pract.*, 40, 791—807.
40. **Orr, M. B., Gensel, J. C., 2017:** Interactions of primary insult biomechanics and secondary cascades in spinal cord injury: implications for therapy. *Neural Regen. Res.*, 12, 1618—1619.
41. **Oyinbo, C. A., 2011:** Secondary injury mechanisms in traumatic spinal cord injury: a nugget of this multiply cascade. *Acta Neurobiol. Exp.*, 71, 281—299.
42. **Quin, W., Bauman, W. A., Cardozo, C., 2010:** Bone and muscle loss after spinal cord injury: organ interactions. *Ann. N. Y. Acad. Sci.*, 1211, 66—84.
43. **Risio, L. D., Platt, S. R., 2010:** Fibrocartilaginous embolic myelopathy in small animals. *Vet. Clin. North Am. Small Anim. Pract.*, 40, 859—869.
44. **Rowland, J. W., Hawryluk, G. W. J., Kwon, B., Fehlings, M. G., 2008:** Current status of acute spinal cord injury pathophysiology and emerging therapies: promise on the horizon. Neurosurg. *Focus,* 25, E2. doi:10.317/FOC.2008.25.11.E2.
45. **Sherrington, C. S., 1947:** *Action of the Nervous System*. 2nd edn., Cambridge University Press, Cambridge, UK, 241—250.
46. **Silva, N. A., Sousa, N., Reis, R. L., Salgado, A. J., 2014:** From basics to clinical: a comprehensive review on spinal cord injury. *Progr. Neurobiol.*, 114, 25—57.
47. **Smith, P. M., Jeffery, N. D., 2005:** Spinal shock — comparative aspects and clinical relevance. *J. Vet. Intern. Med.*, 19, 788—793.
48. **Srugo, I., Aroch, I., Christopher, M. M., Chai, O., Goralnik, I., Bdolah-Abram, I., et al., 2011:** Signs and outcome in acute nonambulatory thoracolumbar disc disease in dogs. J. *Vet. Intern., Med.*, 25, 846—855.
49. **Staffeldt, K., 1963:** Zur Morphogenese der pathologisch-anatomischen Befunde bei der "Commotio medullae spinalis". *Arch. Psych. Nervenkrankheiten*, 204, 328—341.
50. **Stiffer, K. S., Stevenson, M. A., Sanchez, S., Barsanti, J. A., Hofmeister, E., Budsberg, S. C., 2006:** Prevalence and characterization of urinary tract infections in dogs with surgically treated type I thoracolumbar intervertebral disc extrusion. *Vet. Surg.*, 35, 330—336.
51. **Sullivan, P. G., Krishnamurthy, S., Patel, S. P., Pandya, J. D., Rabchevsky, A. G., 2007:** Temporal characterization of mitochondrial bioenergetics after spinal cord injury. *J. Neurotrauma*, 24, 991—999.
52. **Šulla, I., Balik, V., Petrovičová, J., Almášiová, V., Holovská, K., Oroszová, Z., 2016:** A rat spinal cord injury experimental model. *Folia Veterinaria*, 60, 41—46.
53. **Taylor, A. R., Welsh, C. J., Young, C., Spoor, E., Kerwin, S. C., Griffin, J. F., et al., 2014:** Cerebrospinal fluid inflammatory cytokines and chemokines in naturally occuring canine spinal cord injury. *J. Neurotrauma,* 31, 1561—1569.
54. **Tomko, P., Farkaš, D., Čížková, D., Vanický, I., 2017:** Longitudinal enlargement of the lesion after spinal cord injury in the rat: a consequence of malignant oedema ? *Spinal Cord*, 55, 255—263.
55. **Waters, R. L., Adkins, R. H., Yakura, J. S., 1991:** Definition of complete spinal cord injury. *Spinal Cord*, 29, 573—581.
56. **Webb, A. A., Ngan, S., Fowler, D. J., 2010:** Spinal cord injury I: a synopsis of the basic science. *Can. Vet. J.*, 51, 485—492.
57. **Wu, K. L. H., Hsu, C., Chan, J. Y. J., 2009:** Nitric oxide and superoxide anion differentially activate poly(ADP-ribose) polymerase-1 and Bax to induce nuclear translocation of apoptosis inducing factor and mitochondrial release of cytochrome C after spinal cord injury. *J. Neurotrauma*, 26, 965—977.
58. **Xu, J., Fan, G., Chen, S., Wu, Y., Xu, M., Hsu, C. Y., 1998:** Methylprednisolone inhibition of TNF-KB activation after spinal cord injury in rats. *Brain Res. Mol. Brain Res.*, 59, 135—142.
59. **Yang, L., Blumberg, P. C., Jones, N. R., Manavis, J., Sarvestami, G., Ghabriel, M. N., 2004:** Early expression and cellular localization of proinflammatory cytokines Interleukin-1β, Interleukin-6, and Tumor necrosis factor-α in human traumatic spinal cord injury. *Spine*, 29, 966—971.
60. **Zaki, F. A., Prata, R. G., 1976:** Necrotizing myelopathy secondary to embolization of herniated intervertebral disk material in the dog. *J. Am. Vet. Med. Assoc.*, 169, 222—228.
61. **Zhou, X., He, X., Ren, Y., 2014:** Function of microglia and macrophages in secondary damage after spinal cord injury. *Neural Reg. Res.*, 9, 1787—1795.

Received February 14, 2018
Accepted April 12, 2018

sciendo

DOI: 10.2478/fv-2018-0016

FOLIA VETERINARIA, 62, 2: 45—58, 2018

SPINAL CORD INJURIES IN DOGS PART II: STANDARDS OF CARE, PROGNOSIS AND NEW PERSPECTIVES

Šulla, I.[1], Balik, V.[2], Horňák, S.[3], Ledecký, V.[3]

[1]Department of Anatomy, Histology and Physiology
[3]Small Animal Clinic, University of Veterinary Medicine and Pharmacy, Komenského 73, 041 81 Košice
Slovakia
[2]Institute of Molecular Medicine and Translational Medicine
University Hospital and Faculty of Medicine and Dentistry, Palacky University, I. P. Pavlova 6, 772 20 Olomouc
Czechia

igor.sulla@uvlf.sk

ABSTRACT

Severe spinal cord injuries (SCI), causing physical handicaps and accompanied by many serious complications, remains one of the most challenging problems in both, human and veterinary health care practices. The central nervous system in mammals does not regenerate, so the neurological deficits in a dog following SCI persists for the rest of its life and the affected animals display an image of permanent suffering. Diagnostics are based on: neurological examination, plain x-rays of vertebral column, x-rays of the vertebral column following intrathecal administration of a water-soluble contrast medium (myelography), x-rays of the vertebral column following epidural administration of a contrast medium (epidurography), computed tomography (CT) and/or magnetic resonance imaging (MRI). Currently, only limited therapeutic measures are available for the dogs with SCIs. They include: the administration of methylprednisolone sodium succinate (MPSS) during the acute stage; early spinal cord decompression; stabilisation of vertebral fractures or luxations; prevention and treatment of complications, and expert rehabilitation. Together with the progress in the understanding of pathophysiologic events occurring after SCI, different therapeutic strategies have been instituted, including the local delivery of MPSS, the utilisation of novel pharmacological agents, hypothermia, and stem/precursor cell transplantation have all been tested in the experimental models and preclinical trials with promising results. The aim of this review is the presentation of the generally accepted methods of diagnostics and management of dogs with SCIs, as well as to discuss new therapeutic modalities. The research strategy involved a PubMed, Medline (Ovid), Embase (Ovid) and ISI Web of Science literature search from January 2001 to December 2017 using the term "spinal cord injury", in the English language literature; also references from selected papers were scanned and relevant articles included.

Key words: dog; diagnostics; new perspectives; spinal trauma; therapy

INTRODUCTION

The principal composition and function of the central nervous system (CNS) in dogs, cats, pigs and primates are similar [7, 8, 14, 16, 22, 31]. The spinal cord injuries (SCIs) naturally occur ing these species, but the regeneration of neurons within their brain and spinal cord is limited [68]. The neurological symptomatology, complication rate and their character may be also similar, and the treatment options and the prognosis resemble the situation in people [2, 14, 22, 31, 47, 58, 77]. The same diagnostic and therapeutic measures are utilised in both, human and veterinary medicine [6, 19, 29, 53, 64, 69]. That is why the authors decided to review recently published papers relating to canine spinal trauma and inform the health care professionals about the generally accepted methods and new achievements, ready to be tested in preclinical and clinical trials.

DIAGNOSTICS

The trauma patients may suffer significant damage not only to the vertebral column, but also to other body systems. These accompanying injuries may pose more immediate threats to their lives than the damage to the spinal cord. So when evaluating an animal with a neurologic deficit due to a suspected trauma, it is necessary to assess the overall stability of the organism, i. e. function of pulmonary and cardiovascular systems in the first place, then proceed with careful examination of the entire nervous system [9, 12, 14, 45]. The clinical experience has shown that traumatic brain lesions, especially in their mild forms, accompany different traumatic events quite often, and multilevel cord damage is also possible [53, 67]. A theoretical progression of clinical symptomatology is as follows: pain—ataxia—paresis—plegia — and the loss of deep pain sensations [67]. The simple scales recommended for primary, informative assessment of spinal cord functions applicable in dogs are the Tarlov grading system and the American Spinal Injury Association impairment scale, i. e. ASIA scale [12, 31, 40, 53, 64]. More details are in Table 1. The plegia and loss of deep pain sensations are very important indicators of severe spinal cord lesions. They are usually associated with the damage to the significant parts of the white matter, while dogs that are only painful and ataxic, likely have only restricted spinal cord involvement [12, 69, 75].

Table 1. Tarlov grading system modified for dogs [40]

Grade 0	—	Complete paralysis (tetra- or paraplegia) with no extremity function
Grade 1	—	Minor joint movements
Grade 2	—	Major joint movements
Grade 3	—	Animal can stand
Grade 4	—	Animal can walk
Grade 5	—	Animal can climb a 20° inclined plane

However, there are symptoms, which help to localise the spinal cord lesion in a dog more precisely (Table. 2).

Table 2. Neurological symptoms related to localisation of a spinal cord lesion [14, 48, 77]

Lesion localization	Clinical findings
C1 – C5	Crossed extensor reflex in all 4 extremities, neck pain, Horner syndrome, proprioceptive deficits 4x, increased myotatic reflexes 4x, increased tone 4x, tetraparesis/tetra-plegia, increased tone, upper motor neuron urinary bladder
C6 – Th2	Absent cutaneous trunci reflex, neck pain, decreased thoracic limb tone/withdrawal reflexes, pelvic limb crossed extensor reflexes, back pain, proprioceptive deficits 4x, Horner syndrome, tetraparesis/tetraplegia, increased pelvic limb myotatic reflexes, upper motor neuron urinary bladder, increased pelvic limb tone
Th3 – L3	Absent cutaneous trunci reflexes near level of lesion, paraparesis/paraplegia, pelvic limb crossed extensor reflexes, back pain, proprioceptive deficits in pelvic limbs, increased pelvic limb myotatic reflexes, upper motor neuron urinary bladder, increased pelvic limb tone
L4 – S3	Lumbosacral pain, decreased anal tone/reflex, lower motor neuron urinary bladder, decreased pelvic limb myotatic reflexes, decreased pelvic limb tone/withdrawal reflexes, paraparesis/paraplegia, pelvic limb proprioceptive deficits, limp tail
L4 – S3	Lumbosacral pain, decreased anal tone/reflex, lower motor neuron urinary bladder, decreased pelvic limb myotatic reflexes, decreased pelvic limb tone/withdrawal reflexes, paraparesis/paraplegia, pelvic limb proprioceptive deficits, limp tail

Legend: 4x — in all four extremities; C — cervical
Th — thoracic; L — lumbar; S — sacral

Imaging diagnostic techniques

Röntgenological investigations are still crucial in determining an accurate diagnosis of spinal pathology [9, 30]. Plain radiographs, sometimes in different projections (ventro-dorsal, lateral, oblique) are especially helpful in identifying bone abnormalities, such as luxations and/or

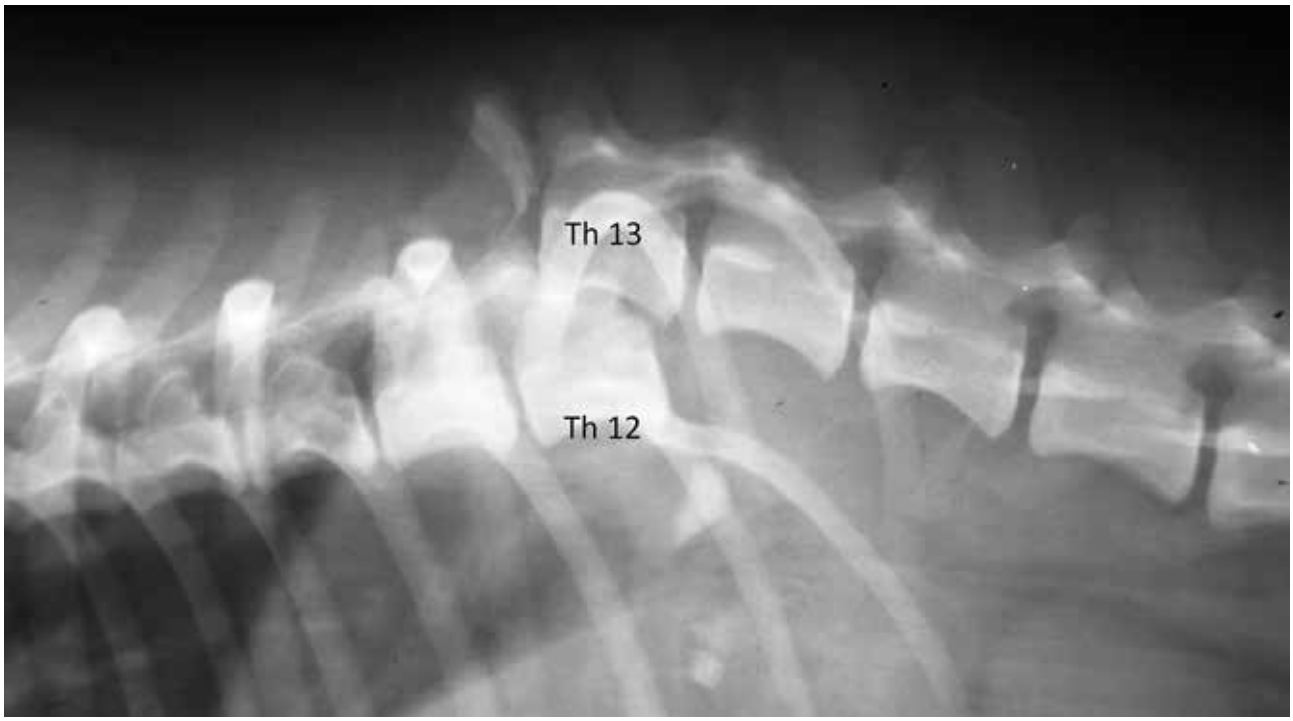

Fig. 1. Plain röntgenogram of a dog with fracture-luxation Th12/Th13 vertebrae; lateral projection

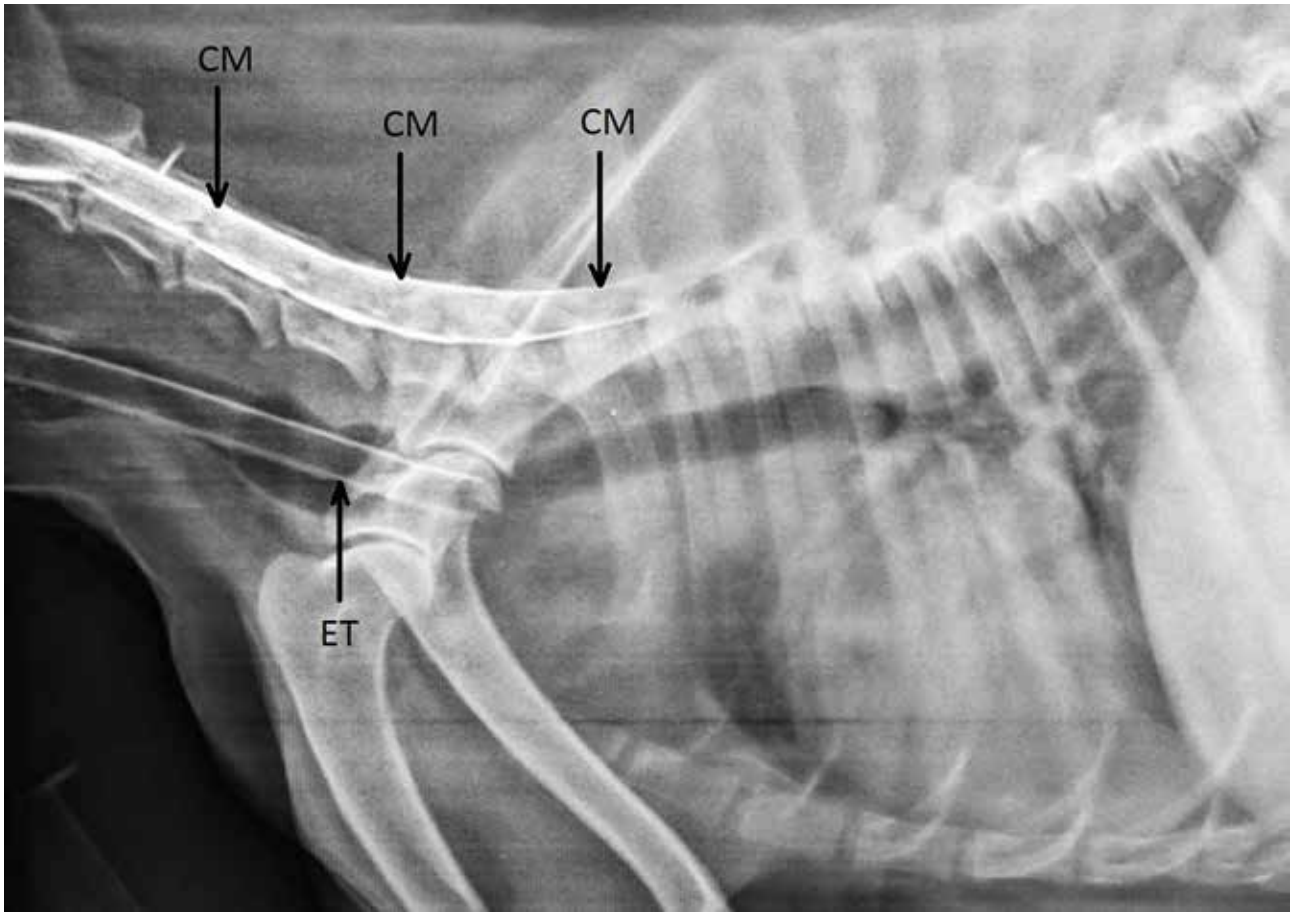

Fig. 2. An example of contrast x-ray examination (myelography) of cervical and cranial part of thoracic spinal canal in a dog; lateral projection. The procedure was performed under general endotracheal anaesthesia
CM —contrast medium; ET — endotracheal tube

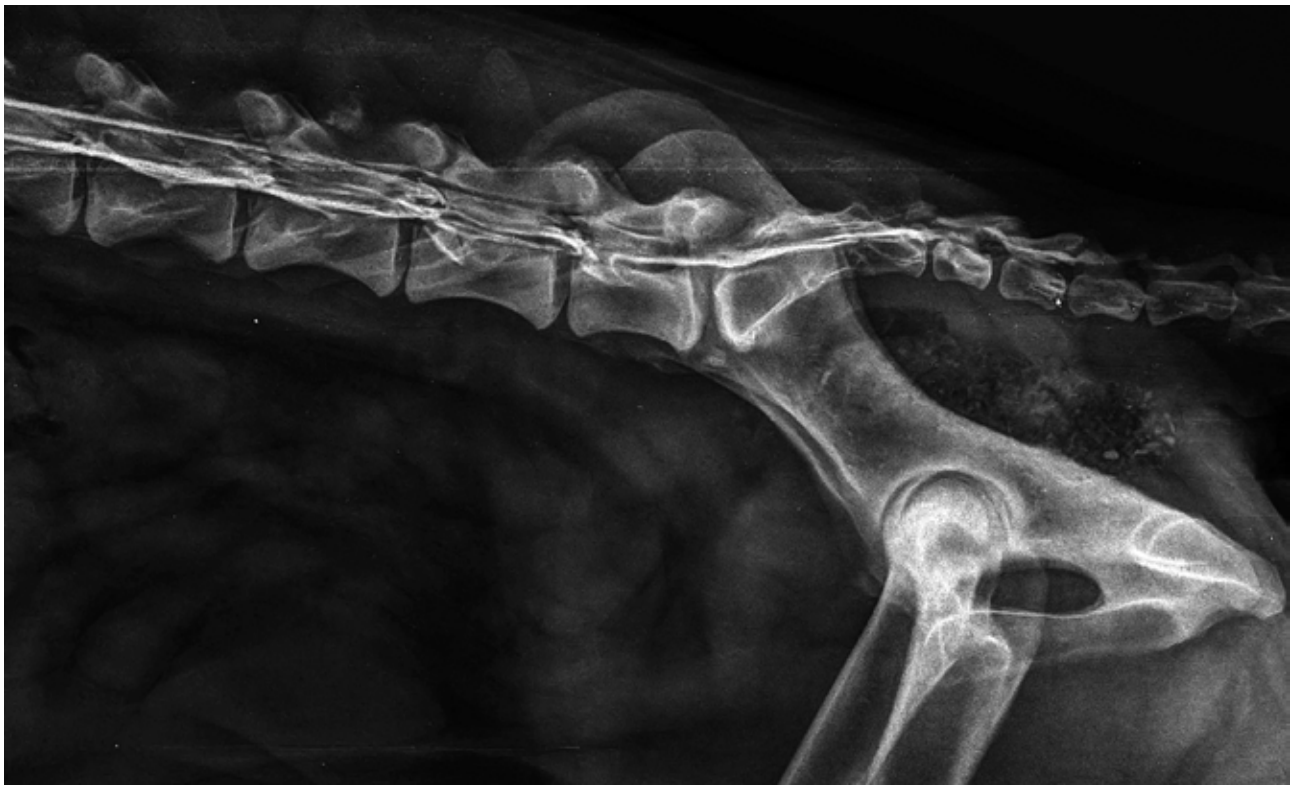

Fig. 3. An example of a contrast x-ray examination of the lumbosacral region of the vertebral canal (epidurography) in a dog; lateral projection

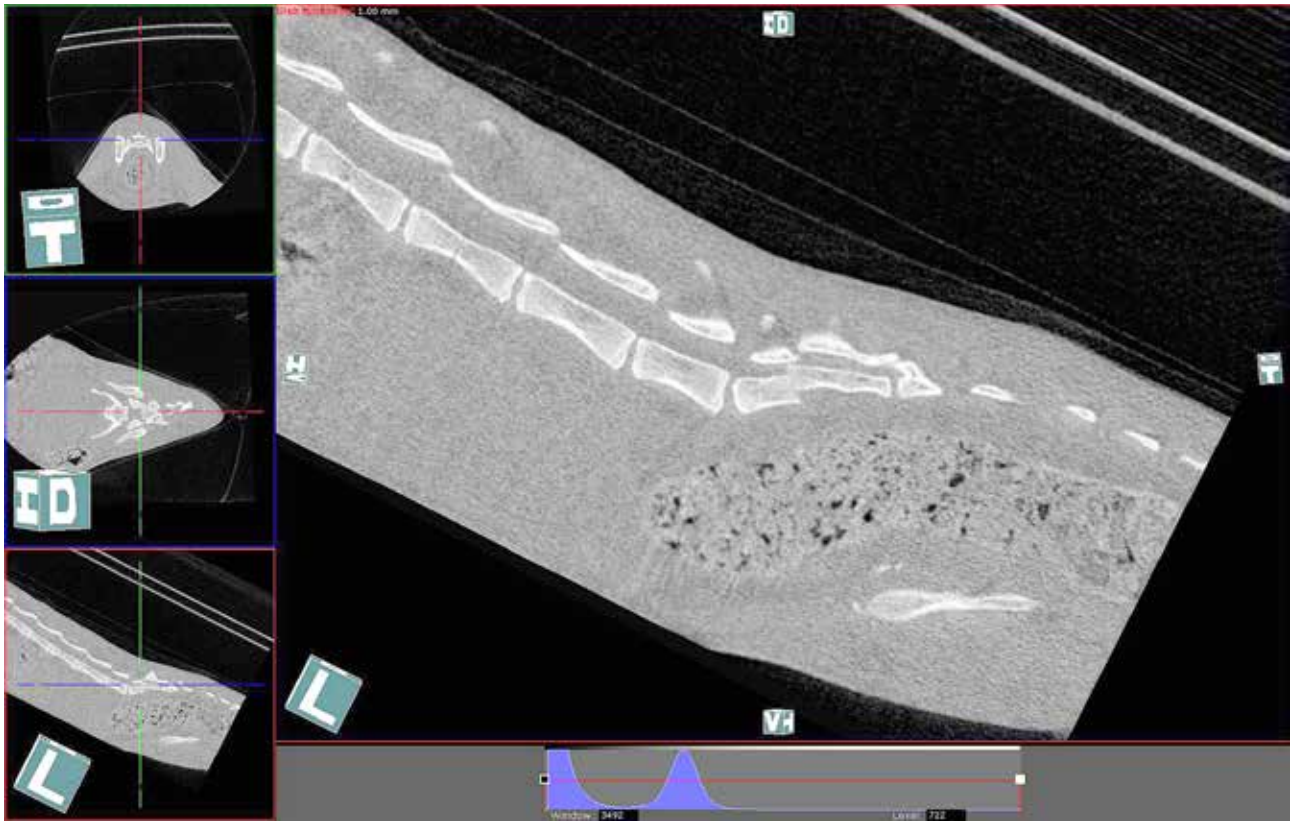

Fig. 4. A CT examination of a dog with a sacral bone fracture causing the traumatic *cauda equina* syndrome. Obstipation developed due to anal sphincter hypertone
T — transversal plane; D — dorsal plane; L — lateral plane

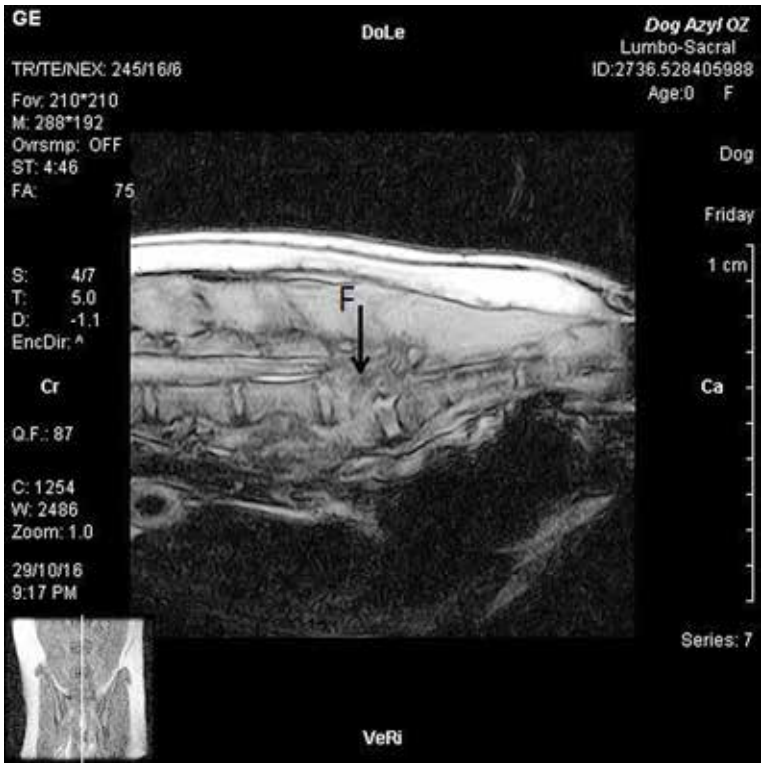

Fig. 5. A MRI examination (T2-weighted image) of a dog with a fracture of L7 vertebra, traumatic *conus medullaris* syndrome, intra- as well as a paraspinal haematoma of the soft tissues. F — fracture

fractures of vertebrae; sometimes they are able to show narrowing of the intervertebral space, which is an indirect sign of intervertebral disc disease (IVDD) [7, 63].

It is necessary to stress, that negative plain x-rays do not exclude vertebral column or spinal cord injury. That is why advanced diagnostic techniques, e. g. myelography (x-rays following administration of water-soluble contrast medium into the spinal dural sack), epidurography (x-rays following the administration of water-soluble contrast medium into the spinal epidural space), comput ed tomography (CT scan) and magnetic resonance imaging (MRI), are more frequently used nowadays [49, 55]. The CT scans provide much greater details of the bony structures and are able to show the extent of any encroachment on the spinal canal by vertebral displacements or bone fragments. MRI gives information about the spinal cord and soft tissues. This imaging technique is able to reveal the cause of the cord compression, whether from bone, prolapsed discs, ligamentous damage, or instraspinal haematomas [75]. CT and MRI are the best available diagnostic tools currently.

Differential diagnosis

Several non-traumatic spinal cord lesions can cause the symptomatology of tetra- or paraplegia/tetra- or paraparesis [28]. The most important of them are:

1. Fibrocartilaginous embolism (FCE) is encountered in dogs quite frequently [10, 21]. It occurs when material from the nucleus pulposus of the intervertebral disc forms an embolus that obstructs vessels within the spinal medulla. FCE commonly affects dogs of large or giant breeds [75]. Dogs typically present with a peracute neurologic deficits that progress for about 24 hours. The neurological symptomatology can be asymmetric and dogs are usually painless [21, 75]. To establish a definitive diagnosis of FCE it is possible only by the help of histopathologic examination, which shows fibrocartilaginous emboli within the spinal cord vasculature identical to the nucleus pulposus [10, 21, 75]. Perimyelography or CT scans can be used to make a presumptive diagnosis, but the best antemortem diagnostic tool is MRI currently [75]. Different treatment modalities (e. g. administration of steroids) for FCE have been

attempted, but no significant positive effects have been found. So the treatment of FCE is conservative, usually it includes rest, followed by physical therapy [10, 20, 21, 57].

2. Spinal epidural or subdural bleeding — are rare pathological events in dogs. Clinical presentation is characterised by a sudden pain in a specific region of the spine (depending on the affected part of the body axis) accompanied by neurological deficits progressing to tetra- or paraplegia [12, 53]. This clinical entity can occur after light falls, jumps, or excessive training, but sometimes may even occur spontaneously. For the localisation and extent of the suspected haematoma, it helps to assess perimyelography; however, to establish the exact diagnosis it is possible only by the help of CT scans. This menacing situation may be solved by an urgent surgical revision and removal of the blood clot [53, 77].

3. Spinal epidural abscess or subdural empyema. They occur rarely, in the majority of the cases accompany meningitis or different purulent processes. The patient has fever and symptoms of meningeal irritation. Perimyelography helps the diagnostics, but CT or MRI are preferable. In the treatment of an urgent surgical revision, evacuation of pus, bacteriological identification of the microorganisms and prolonged administration of antibiotics are recommended [28].

4. Viral (*Herpes simplex* virus, *Varicella-zoster* virus, *Cytomegalovirus*, Tick *encephalo-myelitis* virus), fungal (*Cryptococcus* spp.) or parasitic (*Toxoplasma gondii, Schistosoma mansoni*) transverse myelitis can develop in dogs. Infectious agents mostly enter the spinal medulla by haematogenous transit (from a distant focus) or directly in the time of penetrating injuries or surgical interventions. The perimyelography helps to exclude spinal cord compression, and MRI is able to verify myelitis. The exact diagnosis is dependent on bacteriological and serological tests [28, 30].

5. Many **pathological conditions** occurring in dogs may produce clinical symptoms that mimic SCI. The diagnostic problems may appear in neurological diseases such as: the Wobbler syndrome, the canine distemper, degenerative myelopathy, tick paralysis, toxoplasmosis and polyradiculoneuropathy [12].

6. Wobbler syndrome is a common cervical problem. It occurs especially in Great Danes and Doberman Pinschers. The clinical symptomatology is caused by compression of the cervical spinal cord by the vertebral malformation-malarticulation of C5, C6, and C7. The onset is usually insidious with signs which are normally progressive, but sometimes acute. Owners generally recognise ataxia of the pelvic limbs. Dogs often cross, abduct or collapse on walking and turning. The animal gives an impression that it does not know where its limbs are because of a proprioceptive deficit. The thoracic limb signs (if present) are similar, but less marked [12].

7. Canine distemper (hardpad disease) is caused by a single-stranded RNA virus of the family Paramixoviridae. The disease impacts several body systems, including gastrointestinal and respiratory tracts, but acts predominantly on the spinal cord. Canine distemper is highly contagious and fatal in about 50 % of the cases [12]. Dogs younger than 1 year are especially suspect of having the disease. The affected animal reveals signs of segmental myelopathy with progressive neurological deficits. An example is mild thoracic limb deficit in a paraplegic dog. Quite often additional symptoms (e. g. head tilt, nystagmus, head tremor, nasal and ocular discharge, harsh lung sounds, hyperkeratosis of the nose and foot pads, chorioretinopathy and myoclonus) may be seen. There is no specific treatment for the disease. The prevention is vaccination [12].

8. Degenerative myelopathy (DM) is a progressive disease with no specific cure. Currently it is suspected that DM is an immune-mediated illness resembling Multiple sclerosis (MS) in humans. It occurs predominantly in aging German Shepherds and is characterised by a slowly progressive paraparesis and ataxia of the pelvic limbs. The onset is insidious and may continue for five to six months. Proprioception is the first affected function, along with crossed limbs and hyperreflexia of the pelvic extremities. Symptomatology may be asymmetrical. The neurological deficit is caused by diffuse degeneration of the myelin sheaths and neural axons in both ascending and descending tracts of the spinal cord. The peripheral nerves may be involved too, resulting in the lower motor neuron signs. The diagnosis is based on: the breed of the dog, its age, typical history, clinical symptomatology and exclusion of other intraspinal lesions. The myelography, CT and MRI negate compression of neural structures, and the CSF examinations are normal [12].

9. Tick paralysis is caused by a neurotoxin produced in the tick's salivary gland. Clinical presentation begins with paresis, hyporeflexia and ataxia five to seven days after the attachment of the tick and the symptomatology can progress to paralysis with areflexia. Finding ticks on the

dog helps to establish the diagnosis. The CSF examination is normal, however the neurotoxin reduces nerve conduction velocity, the amplitude of muscle action potentials and causes a total blockade of transmission at the myoneural junctions [30]. Following the removal of the tick, the neurological deficit subsides [12, 30].

10. Toxoplasmosis can cause various clinical signs. They include seizures, blindness, tremor, hemi- or paraparesis, and hindquarter paralysis. Spinal reflexes may be absent and extensor rigidity present in one or both pelvic extremities. The history is usually of a young dog showing gradual progressive paralysis. A positive diagnosis is difficult, but serology may be of some help [12].

1**1. Polyradiculoneuropathy** (coonhound paralysis). The etiology of this disease is unknown. The functional lesion is on the ventral nerve roots and peripheral nerves. The disease is initiated by raccoon bites one to two weeks before the onset of any clinical signs. The majority of the affected dogs show paresis and hyporeflexia of the pelvic limbs and dysphonia. The neurological deficits progresses to tetraplegia with areflexia, while the animal demonstrates alertness and has a normal temperature. Adult hunting dogs are most commonly affected [12].

SPINAL TRAUMA MANAGEMENT

It is very important to have an initial assessment aimed at identifying all of the imminently life-threatening injuries. The basic ABC examination (the patency of the airways, the ability of the dog to breathe, and the effectiveness of circulation) is recommended [9, 14, 31, 67]. Most animals with significant traumatic events will present a state of hypovolemic shock due to inappropriate vasodilation, blood loss, or both. Hypovolemia and hypoxemia can contribute to secondary spinal cord damage, so rapid correction of perfusion deficit is of paramount importance. In dogs with a systolic blood pressure less than 90 mmHg require aggressive fluid resuscitation [9, 53]. The administration of synthetic colloids (e. g. "Dextran-70" 10—20 ml.kg^{-1} over 15—20 min, or hypertonic saline 4—5 ml.kg^{-1} over 15—20 min) are indicated for hypovolemic shock. Dehydrated trauma victims should receive isotonic crystalloids (e. g. lactated "Ringer's solution" or 0.9 % saline). In animals unresponsive to fluid therapy, vasopressor agents (e. g. dopamine 5—12 μg.kg^{-1}min^{-1} or epinephrine infusion 1—10 μg.kg^{-1}min^{-1}) should be used to maintain adequate systemic blood pressure [9, 13, 29, 53]. Hyperoxygenation is recommended for most trauma patients. Dogs who are conscious should be administered supplemental oxygen via nasal cannulae or nasal oxygen catheters. The face masks tend to stress dogs, so they should only be used temporarily. Animals with airway obstruction or SCIs causing hypoventilation should be intubated and ventilated [29, 53, 69].

Specific therapy for spinal trauma

While there are significant differences between humans and non-primate animals in terms of supraspinal motor control of extremities, the basic brainstem-spinal control systems for walking are similar [2, 65, 70, 76]. More importantly, cellular mechanisms (activation of microglia, apoptosis, axonal sprouting, and inhibition effects within adult CNS) do not differ [3, 13, 22, 32, 38, 42, 58, 62, 68, 72, 73, 76].

Once the diagnosis of a traumatic SCI has been made and the location of the lesion and the cause of medullary damage has been established, a decision must be made concerning what type of treatment will be pursued. Basically, it is determined by the personal opinion of the veterinary surgeon and the choice of the owner [9, 53, 55, 63]. Vertebral fractures and luxations may be treated conservatively (e. g. by a strict rest for 2—6 weeks and/or immobilization using external braces, supplemented by administration of analgesics, anti-inflammatory drugs and physical therapy). However, the surgical methods, i. e. decompression, reposition of fragments and internal fixation are more and more frequently preferred nowadays, since the literature provides strong evidence, that the early surgical decompression is associated with better recovery at 6 months after the event as defined by a 2-grade improvement in the grading system (impairment scale) modified for dogs [9, 31, 40, 52, 63]. Surgical management is generally recommended when: the dog has preserved only minimal voluntary motor function or is completely paraplegic; there is a clinical or radiographic evidence of unstable vertebral fracture/luxation; or the neurologic deficit is progressing despite an appropriate conservative management [9, 52, 77].

The first proven pharmacological treatment for SCI in humans was introduced in the 1990s [6, 29]. In a multicentre clinical study, a high dose of the synthetic corticosteroid methylprednisolone (MPSS) was reported to reduce disability when administered within 8 h of trauma. MPSS

reduces swelling, glutamate release, free-radical accumulation, upregulates anti-inflammatory factors, and decreases oxidative stress [35, 73]. According to the Cochrane review, the MPSS treatment should be started by a 30 $mg.kg^{-1}$ bolus within the first 3 hours after injury and continued by 5.4 $mg.kg^{-1}.h^{-1}$ for 24 hours. [6]. On the other hand, the treatment with a high-dose of MPSS is associated with serious complications (e. g. gastric bleeding, wound infections, myopathy) outweighing potential benefit for neurological improvement [20, 56, 66]. That is why a local delivery of MPSS to the epicentre of the injury is currently being tested [32, 34, 35]. The majority of patients following SCIs are in the chronic phase of their disease. With an aim to help them, different neuroregenerative proceedings are being experimentally tested [31, 33, 35, 70].

A critical part of any treatment for SCI is an effective rehabilitation strategy. It is aimed to reduce chronic complications (e. g. pressure ulcers, spasticity, and development of deformities) and enhance residual functions [1, 19, 40, 74]. The physical rehabilitation improves muscle tone and mobility, activates preserved intramedullary circuits, maintains existing neural cell connections, promotes synaptogenesis, myelination and neurite sprouting, i. e. it is able to raise the physical as well as emotional condition of the patient [9, 19, 26]. That is why the more advanced rehabilitation procedures are recommended in the treatment of dogs with SCIs [31, 53, 63].

Complications

The most frequent complications connected with SCIs in dogs are: neuropathic pain, problems with the evacuation of the urinary bladder, spasticity, pressure ulcers and sexual incompetence.

Two thirds of humans with SCI report pain and about a third of them rate their pain as severe. It is reasonable to assume about the same occurrence of post-injury chronic pain syndromes in animals also. Pain can be at the level of the injury, or it can be experienced in other areas, where sensation is usually limited or absent. Neuroscientists suppose that at-level pain results from damage to spinal cord one or more segments cranial to the lesion, whereas pain caudally from the lesion can result from the interruption of axon pathways, the formation of abnormal connections within the spinal cord and/or functional changes in neurons, which make them hyperexcitable. Consequently, a more aggressive treatment in the first few hours after injury could limit the secondary damages and reduce the development of chronic pain syndromes following SCIs [10, 14, 20, 54].

The majority of patients with post traumatic tetra- or paraplegia are not able to control voiding and suffer with recurrent urinary tract infections due to bladder over distension and urine stagnation [12, 48]. The treatment consists of regular urinary bladder evacuation and administration of antibiotics. There are two types of problems with bladder evacuation — the upper motor neuron (UMN) dysfunction and the lower motor neuron (LMN) dysfunction [12, 48]:

a) The UMN bladder dysfunction is caused by spinal cord lesions between the pons and the L7 segment. The hallmark of this lesion is interference with the detrusor reflex and hyperactivity of the urethral musculature. The bladder fills with urine, but the dog is not able to urinate. Upon palpation, the bladder is turgid and it is difficult to express the urine manually. The intermittent catheterization can solve the problem [12, 48].

b) The LMN bladder dysfunction occurs with lesions of the sacral spinal cord or nerves of the lumbosacral plexus. The hallmark of the LMN bladder dysfunction is decreased tone of both, detrusor as well as urethral musculature. This lesion attenuates or abolishes the detrusor reflex and the dog constantly dribbles urine; decreased or absent perineal reflexes and sensation accompany the condition. The application of light abdominal pressure easily evacuate urine [12, 48].

About 60 % of animals following SCIs suffer with spasticity. Recent studies indicate that the loss of descending tracts results in the decreased activity of inhibitory interneurons. It causes the over reaction of moto neurons to excitatory stimuli [1, 12, 53]. If spasticity appears in paraplegic dogs, medical therapy (administration of drugs acting within the CNS – baclofen, diazepam or directly on skeletal muscles – dandrolene) is recommended. In spasticity resistant to pharmacological interventions, there is severing of the reflex pathways (surgical rhizotomy or myelotomy) [1].

Dogs with paraplegia due to SCI, its chronic comorbidities, impaired autonomic innervation as well as protective sensory perception are particularly vulnerable to developing pressure sores – pressure ulcers (decubitus). They also are at high risk for the occurrence of recurrent ulcers which can be life-threatening as a potential source of infections and sepsis. The pressure ulcer is defined as a soft tissue damage resulting from prolonged pressure over bony prominences

resulting in ischemia and necrosis [36]. The pathological sequelae of pressure can be reversed at the ischemic stage if pressure and supportive factors (e. g. shear, friction and/or moisture) are excluded. So changing the position of paraplegic animal (every 2 hours) and the removal of supportive factors are effective preventive measures [37, 53]. There are four clinical stages of pressure ulcers. The sores of stage 1 and 2 positively react to the relief of pressure, debridement of necrotic skin and subcutaneous fat, control of bacterial colonization, and nutrition supplementation; the ulcers of stage 3 demand surgical excision and tissue reconstruction. The best solution for dogs with deep necrosis involving bones, joints and tendons (stage 4) is euthanasia. The decision of therapeutic interventions depends on the attitude and financial situation of the owner [9, 14, 24, 37, 63].

Dogs afflicted with SCI reveal two types of sexual problems. The tetra-, or paraparesis/tetra- or paraplegia hinders or excluded copulatory activities, i. e. mounts and intromission in males, lordosis in females [48]. The severe SCI disrupts the reflex mediated increase in genital blood flow (required for engorgement of erectile tissues in males and vasocongestion of clitoris, vaginal wall, and lubrication of the vaginal surface in females). Even if the sympathetically mediated arousal is intact, the males have problems to maintain erection and suffer a retrograde (intravesical) ejaculation, due to incompetence of the internal urethral sphincter [48]. As a result, male reproductive function is significantly affected. On the contrary, the female dogs with SCI are able to become pregnant, as well as undergo normal pregnancy and delivery [48].

PROGNOSIS

Dogs with tetraplegia due to the lesion of the cervical spinal cord have a poor prognosis. Many of them perish before any therapeutic intervention is available or they are euthanized immediately after the incident. The financial burdens of tetraparetic animal's treatment also are rather high, so the majority of owners prefer an early euthanasia.

1. In paraparetic/paraplegic dogs with intervertebral disc herniation (Hansen type 1 disc disease) but intact perception, a decompressive operation (hemilaminectomy or laminectomy and removal of the disc fragments from the vertebral canal) is indicated as soon as possible. Following an active therapy, they can recover completely, their prognosis is considered favourable with surgery [7, 27, 40, 46, 53]. Hansen type 1 disc herniation accompanied by loss of deep pain sensation (lack of nociception), the prognosis is less favourable. Decompressive surgery can help to regain nociception and the ability to ambulate without assistance in about 60 % of the deep pain negative dogs [55, 63]. Dogs with paraparesis due to the intervertebral disc protrusion but intact nociception have a favourable prognosis with conservative management. The decompressive operation is not indicated; animals make significant improvements and are ambulatory with medical treatment only [7, 53].

2. Dogs with vertebral instability due to fracture and/or luxation, paraplegia and lack of nociception have a poor prognosis. The surgical revision, decompression of neural structures and stabilisation of vertebral column is recommended (it helps to start an early rehabilitation programme), however results are dubious, so many owners prefer euthanasia [9, 31, 53]. A much better prognosis is in animals with vertebral fractures and/or luxations accompanied with intact sensations. Early surgical decompression and stabilisation are indicated [9, 31].

3. Clinical observations show that the prognosis in patients with spinal cord syndromes are significantly more favourable than in patients with tetra- or paraplegia [26]. As far as recovery of motor function is concerned, the best outcome was observed in patients with Brown-Séquard syndrome — 75—90 % of them were able to ambulate independently following long-term rehabilitation [26]. On the other hand, the anterior spinal cord syndrome has a poor prognosis with only a 10—20 % chance of functional recovery, and even in those with some improvement, the muscle power is significantly impaired and coordination of movements is insufficient [26, 47]. Patients with posterior spinal cord syndrome have preserved muscle strength, temperature and pain sensation, but lost proprioceptive and vibration sense caudally to the level of the spinal cord lesion. They generally show the least favourable recovery from impaired perception. They are able to ambulate, but with a tendency to falls [26, 47]. The cauda equina syndrome has a better prognosis for neurological recovery than SCIs because nerve roots are able to regenerate. The most important predictors for a favourable outcome are early diagnosis and surgical decompression [26, 47].

4. Prognosis for dogs with fibrocartilaginous embolism is generally favourable; the majority of patients will show recovery of some functions within 2 weeks of me-

dicament treatment, but maximal improvement may take several months [21, 29]. The surgical intervention is not indicated. The negative prognostic factor is lack of nociception [53, 57, 75].

NEW TRENDS IN SCI MANAGEMENT

It is well known, that brain and spinal cord tissue does not regenerate. That is why the management of SCI in humans and domestic animals is currently targeted at preservation of remaining functions and prevention of complications. However, multiple experimental studies performed on different laboratory animals brought at least partially positive results, when therapeutic measures concentrated on:

1. The suppression of a secondary injury cascade by: the administration of a sodium-channel blocker "riluzole"; central nervous system stromal cells, antibiotic with anti-inflammatory properties (including inhibition of tumour necrosis factor-α, i.e. TNF-α, interleukin 1β, i.e. IL-1β, cyclooxygenase-2, nitric oxide synthase, i. e. NOS) and microglial activation "minocyclin"; systemic or local mild hypothermia (33—34 °C); more accurate delivery of intravenously injected MPSS bond to ferromagnetic nanoparticles to the epicentre of the lesion by help of a magnet placed on exposed dura mater through laminectomy, which reduces the risk of serious side effects of the methylprednisolone [3, 22, 23, 25, 29, 35, 37, 41, 43, 58, 59, 71], so all of these things may prove to be helpful. Clinical utilisation of hypothermia is still controversial, since the systemic hypothermia is often accompanied by serious complications and its results are not unequivocally positive. Obviously, the systemic hypothermia is too complex of a procedure for veterinary practice. So local hypothermia by cold saline applied through laminectomy during the operation together with potential administration of methylprednisolone seem to be the most promising method for dogs and cats with acute SCIs [6, 14, 23]. The clinical utilisation of different strategies and pharmacological agents mentioned in previous texts are considered experimental therapy, so far.

2. The suppression of spinal cord cell necrosis by the application of "fibroblast growth factor" i.e. FGF or "curcumine" (protect against excitotoxic cell death and mitigate oxygen free radical production); or antiapoptotic molecules i.e. "valproic acid", "vitamin E", "17β-estradiol", "melatonine" [27, 37—39, 41, 53, 60, 72].

3. Restraining of axon demyelination or supporting their remyelination by cellular therapy [5, 18, 33, 44, 51, 61, 70].

4. Suppression of axon growth and regeneration inhibiting proteins expression [15, 44, 69, 71]. Significant therapeutic opportunities offer the utilisation of endogenous and exogenous repair mechanisms, as well as drugs suppressing the activation of axonal sprouting inhibitors, e. g. chondroitin sulfate proteoglycans, CSPGs, myelin-associated glycoproteins, MAGs, oligodendrocyte-myelin glycoprotein, OMGP, and neurite outgrowth inhibitor-A, NOGO-A, acting on receptors associated with the Rho-ROCK pathway, directly able to inhibit neurite growth. In rat experimental models monoclonal antibodies against CSPGs, MAGs, OMGP and Nogo-A significantly improved regeneration of damaged spinal cords [5, 15, 33, 44, 71]. Alongside of a direct inhibition of Rho-ROCK pathway, another therapeutic modality was discovered. The enzyme chondroitinase ABC (Ch-ABC) degrades CSPGs in the glial scar and effectively removes initiators of the Rho-ROCK cascade. In rodent models of SCI, intrathecal or intraparenchymal administration of Ch-ABC reduced the expression of CSPGs as well as scar and cavity volume [11, 37, 71].

5. Support of physiologic production or administration of guiding molecules directing axonal growth to the target structures [4, 8, 17, 29, 33, 50, 61, 70].

6. Generation of bridges in post traumatic intramedullary cysts and syringomyelic cavities providing support and protection for regenerating axons by chitozan microtubules and/or transplanted progenitor/stem cells [4, 51, 58, 71].

7. **Production of regenerative molecules** by transplanted precursor/stem cells obtained from autologous bone marrow, fat tissue, olfactory bulbs, olfactory fibres or ensheathing (Schwann) cells [8, 51, 61, 69, 70].

8. Autotransplantation of modified mesenchymal precursor/stem cells harvested from adult bone marrow or fat tissue and expanded in cell cultures to neural, oligodendritic or astrocytic lines, which are potentially able to replace damaged spinal cord tissues [3, 18, 33, 50, 51, 61, 70].

CONCLUSION

This review provides an overview of the current information on canine spinal cord injuries, their treatment, imply new therapeutic options, and discusses new trends in SCI research.

ACKNOWLEDGEMENTS

The accumulation and study of literature dealing with different aspects of the spinal cord injuries as well as the preparation of our paper was supported by the grant for the Agency of the Ministry of Education, Science, Research and Sport of the Slovak Republic for the Structural Funds of EU, ITMS 26220220127 and VEGA grant No. 1/0898/15. The authors are grateful to Silvia Ficova, DVM from SIBRA, Centre for Veterinary Medicine, Bratislava, Slovakia for providing the CT and MRI scans.

REFERENCES

1. **Adams, M. M., Hicks, A. L., 2005:** Spasticity after spinal cord injury. *Spinal Cord*, 43, 577—586.
2. **Akhtar, A. Z., Pippin, J. J., Sandusky, C. B., 2008:** Animal models in spinal cord injury: a review. *Rev. Neurosci.*, 19, 47—60.
3. **Badner, A., Vawda, R., Laliberte, A., Hong, J., Mikhail, M., Jose, A., et al., 2016:** Early intravenous delivery of human brain stromal cells modulates systemic inflammation and leads to vasoprotection in traumatic spinal cord injury. *Stem Cells Transl. Med.*, 5, 991—1003.
4. **Bockurt, G., Mothe, A. J., Zahir, T., Kim, H., Shoichet, M. L., Tator, C. H., 2010:** Chitosan channels containing spinal cord-derived stem/progenitor cells for repair of subacute spinal cord injury in the rat. *Neurosurgery*, 67, 1733—1744.
5. **Borrie, S. C., Baeumer, B. E., Badtlow, C. E., 2012:** The nogo-66 receptor family in the intact and diseased CNS. *Cell Tissue Res.*, 349, 105—117.
6. **Bracken, M. B., 2012:** Steroids for acute spinal cord injury. Review. *Cochrane Database Syst. Rev.*, 1, Art. No.: CD001046.
7. **Brisson, B. A., 2010:** Intervertebral disc disease in dogs. *Vet. Clin. North Am. Small Anim. Pract.*, 40, 829—858.
8. **Brock, J., Rosenzweig, W. E., Blesch, A., Moseanko, R., Havton, L., Edgerton, V., et al., 2012:** Local and remote growth factor effects after primate spinal cord injury. *J. Neurosci.*, 30, 9728—9737.
9. **Bruce, C. W., Brisson, B. A., Gyselinck, K., 2008:** Spinal fracture and luxation in dogs and cats: a retrospective evaluation of 95 cases. *Vet. Comp. Orthop. Traumatol.*, 21, 280—284.
10. **Cauzimille, L., Kornegay, J. N., 1996:** Fibrocartilaginous embolism of the spinal cord in dogs: Review of 36 histologically confirmed cases and retrospective study of 26 suspected cases. *J. Vet. Intern. Med.*, 10, 241—245.
11. **Devaux, S., Cizkova, D., Quamico, J., Franck, J., Nataf, S., Pays, L., et al., 2016:** Proteomic analysis of the spatio-temporal based molecular kinetics of acute spinal cord injury identifies a time- and segment-specific window for effective tissue repair. *Moll. Cell. Proteomics*, 15, 2641—2670.
12. **Dewey, C. W., 2008:** *A Practical Guide to Canine and Feline Neurology*. 2nd edn., Iowa State University Press, Ames, Iowa, USA, 706 pp.
13. **Dumont, R. J., Okonkwo, D. O., Verma, S., Hurlbert, R. J., Boulos, P. T., Ellegala, D. B., et al., 2001:** Acute spinal cord injury, Part I: Pathophysiologic mechanisms. *Clin. Neuropharm.*, 24, 254—264.
14. **Eminaga, S., Palus, V., Cherubini, G. B., 2011:** Acute spinal cord injury in the cats: causes, treatment and prognosis. *J. Feline Med. Surg.*, 13, 850—862.
15. **Filbin, M. T., 2003:** Myelin-associated inhibitors of axonal regeneration in the adult mammalian CNS. *Nat. Rev. Neurosci.*, 4, 703—713.
16. **Fletcher, T. F., 2013:** Spinal cord and meninges. In **Evans, H. P., de Lahunta, A., (Eds.):** *Miller's Anatomy of the Dog*. 4th edn., Elsevier, Saunders, St. Louis, USA, 589—610.
17. **Fouad, K., Ghosh, M., Vavrek, R., Tse, A. D., Pearse, D. D., 2009:** Dose and chemical modification considerations for continuous cyclic AMP analog delivery to the injured CNS. *J. Neurotrauma*, 26, 733—740.
18. **Fraga, J. S., Silva, N. A., Lourenco, A. S., Gincalves, V., Neves, N. M., Reis, R. L., et al., 2013:** Unveiling the effects of the secretome of mesenchymal progenitors from the umbilical cord in different neuronal cell populations. *Biochimie*, 95, 2297—2303.
19. **Frood, R. T., 2011:** The use of treadmill training to recover locomotor ability in patients with spinal cord injury. *Biosci. Hor.*, 4, 108—117.
20. **Galandiuk, S., Raque, C., Appel, S., Polk, jr., H. C., 1993:** The two-edged sword of large-dose steroids for spinal cord trauma. *Ann. Surg.*, 218, 419—427.
21. **Gandini, G., Cizinauskas, S., Lang, J., Fatzer, R., Jaggy, A., 2003:** Fibrocartilaginous embolism in 75 dogs: clinical findings and factors influencing the recovery rate. *J. Small Anim. Pract.*, 44, 76—80.
22. **Gedrova, S., Galik, J., Marsala, M., Zavodska, M., Pavel, J., Sulla, I., 2018:** Neuroprotective effect of local hypothermia in a computer-controlled compression model in minipig: correlation of tissue sparing along the rostro-caudal axis with neurological outcome. *Exp. Therap. Med.*, 15, 254—270.
23. **Grulova, I., Slovinska, L., Nagyova, M., Cizek, M., Cizkova, D., 2013:** The effect of hypothermia on sensory-motor func-

tion and tissue sparing after spinal cord injury. *Spine J.*, 13, 1881—1891.

24. **Haisma, J. A., van der Woude, L. H., Stam, H. J., Bergen, M. P., Sluis, T. A., Post, M. W., et al., 2007:** Complications following spinal cord injury: occurrence and risk factors in a longitudinal study during and after in patient's rehabilitation. *J. Rehab. Med.*, 39, 393—398.
25. **Hanseobout, R. R., Hansebout, C. R., 2014:** Local cooling for traumatic spinal cord injury: outcomes in 20 patients and review of literature. *J. Neurosurg. Spine*, 20, 550—561.
26. **Harkema, S. J., Schmidt-Read, M., Lorenz, D. J., Edgerton, V. R., Behrman, A. L., 2012:** Balance and ambulation improvements in individuals with chronic incomplete spinal cord injury using locomotor training-based rehabilitation. *Arch. Phys. Med. Rehabilit.*, 93, 1508—1511.
27. **Henke, D., Vandevelde, M., Doher, M. G., Stockli, M., Forterre, F., 2013:** Correlations between severity of clinical signs and histopathological changes in 60 dogs with spinal cord injury associated with acute thoracolumbar intervertebral disc disease. *Vet. J.*, 198, 70—75.
28. **Hess, C. W., 2005:** Nicht-traumatische akute Querschnittsyndrome. *Praxis* (Basel), 94, 1151—1159.
29. **Hulbert, R. J., Hadley, M. N., Walters, B. C., Aarabi, B., Dhall, S. S., Gelb, D. E., et al., 2013:** Pharmacological therapy for acute spinal cord injury. *Neurosurgery*, 72, 93—105.
30. **Ilkiv, J. E., Turner, D. M., Howlett, C. R., 1987:** Infestations in the dog by the paralysis tick Ixodes holocyclus. 1. Clinical and histological findings. *Aust. Vet. J.*, 64, 137—139.
31. **Jeffery, N. D., Hamilton, L., Granger, N., 2011:** Designing clinical trials in canine spinal cord injury as a model to translate successful laboratory interventions into clinical practice. *Vet. Rec.*, 168, 102—107.
32. **Jeong, S. Y., Seol, D. W., Li, F. C., Chen, Q. X., 2008:** The role of mitochondria in apoptosis. *BMB Reports*, 41, 11—22.
33. **Kabu, S., Gao, Y., Kwon, B. K., 2015:** Drug delivery, cell based therapies, and tissue engineering approaches for spinal cord injury. *J. Control. Rel.*, 219, 141—154.
34. **Kakulas, B. A., 2004:** Neuropathology: the foundation for new treatments in spinal cord injury. *Spinal Cord*, 42, 549—563.
35. **Kim, Y. T., Caldwell, J. M., Bellamkonda, R. V., 2009:** Nanoparticle-mediated local delivery of methylprednisolone after spinal cord injury. *Biomaterials*, 30, 2582—2590.
36. **Kruger, E. A., Pires, M., Ngann, Y., Sterling, M., Rubay, S., 2013:** Comprehensive management of pressure ulcers in spinal cord injury: current concepts and future trends. *J. Spin. Cord Med.*, 36, 572—585.
37. **Kwon, B. K., Okon, E., Hillyer, J., Mann, C., Baptiste, D., Weaver, L. C., et al., 2011:** A systematic review of non-invasive pharmacologic neuroprotective treatments for acute spinal cord injury. *J. Neurotrauma*, 28, 1545—1588.
38. **Lee, J. Y., Kim, H. S., Choi, S. Y., Oh, T. H., Ju, B. G., Yune, T. Y., 2012:** Valproic acid attenuates blood-spinal cord barrier disruption by inhibiting matrix metalloproteinase-9 activity and improves functional recovery after spinal cord injury. *J. Neurochem.*, 121, 818—829.
39. **Lee, J. Y., Choi, S. Y., Oh, T. H., Yune, T. Y., 2012:** 17β-estradiol inhibits apoptotic cell death of oligodendrocytes by inhibiting Rhoa-JNK3 activation after spinal cord injury. *Endocrinology*, 153, 3815—3827.
40. **Levine, G. J., Levine, J. M., Budke, C. M., Kerwin, S. C., Au, J., Vinayak, A., et al., 2009:** Description and repeatability of a newly developed spinal cord injury scale for dogs. *Prev. Vet. Med.*, 89, 121—127.
41. **Lin, M. S., Lee, Y. H., Chiu, W. T., Hung, K. S., 2011:** Curcumin provides neuroprotection after spinal cord injury. *J. Surg. Res.*, 166, 280—289.
42. **Liu, W. M., Wu, J. Y., Li, F. C., Vhen, Q. X., 2011:** Ion channel blockers and spinal cord injury. *J. Neurosci. Res.*, 89, 791—801.
43. **Lo, T. P., Cho, K. S., Garg, M. S., Lynch, M. P., Marcillo, A. E., Koivisto, D. L., et al., 2009:** Systemic hypothermia improves histological and functional outcome after cervical spinal cord contusion in rats. *J. Comp. Neurol.*, 514, 433—448.
44. **Low, K., Culbertson, M., Bradke, F., Tessier-Lavigne, M., Tuszynski, M. H., 2008:** Netrin-1 is a novel myelin-associated inhibitor to axon growth. *J. Neurosci.*, 28, 1099—1108.
45. **Mack, E. H., 2013:** Neurogenic shock. *Open Ped. Med. J.*, 7 (Suppl. 1: M4), 16—18.
46. **McKee, W. M., Downes, C. J., Pink, J. J., Gemmill, T. J., 2010:** Presumptive exercise-associated peracute thoracolumbar disc extrusion in 48 dogs. *Vet. Rec.*, 166, 523—528.
47. **McKinley, W., Santos, K., Meade, M., Brooke, K., 2007:** Incidence and outcomes of spinal cord injury clinical syndromes. *J. Spinal Cord Med.*, 30, 215—224.
48. **McMurray, G., Casey, J. H., Naylor, A. M., 2006:** Animal models in urologic disease and sexual dysfunction. *Br. J. Pharm.*, 147, S52—S79.
49. **Nakamoto, Y., Ozawa, T., Katanabe, K., Nishiya, K., Yasuda, N., Mashita, T., et al., 2009:** Fibrocartilaginous embolism of the spinal cord diagnosed by characteristic clinical findings and magnetic resonance imaging in 26 dogs. *J. Vet. Med. Sci.*, 71, 171—176.
50. **Nakano, R., Edamura, K., Sugiya, H., Narita, T., Oka-**

bayashi, K., Moritomo, T., et al., 2013: Evaluation of mRNA expression levels and electrophysiological function of neuron-like cells derived from canine bone marrow stromal cells. *Am. J. Vet. Res.*, 74, 1311—1320.

51. **Nishida, H., Nakayama, M., Tanaka, H., Kitamura, M., Hatoya, S., Sugiura, K., et al., 2011:** Evaluation of transplantation of autologous bone marrow stromal cells into the cerebrospinal fluid for treatment of chronic spinal cord injury in dogs. *Am. J. Vet. Res.*, 72, 1118—1123.
52. **Noble, L. J., Donovan, F., Igarashi, T., Goussev, S., Werb, Z., 2002:** Matrix metalloproteinases limit functional recovery after spinal cord injury by modulation of early vascular events. *J. Neurosci.*, 22, 7526—7535.
53. **Olby, N., 2010:** The pathogenesis and treatment of acute spinal cord injuries in dogs. *Vet. Clin. N. Am. Small Anim. Pract.*, 40, 791—807.
54. **Ormond, D. R., Peng, H., Zeman, R., Das, K., Murali, R., Jhanwar-Uniyal, M., 2012:** Recovery from spinal cord injury using naturally occurring anti-inflammatory compound curcumin: laboratory investigation. *J. Neurosurg. Spine*, 16, 497—503.
55. **Penning, V., Platt, S. R., Dennis, R., Capello, R., Adams, V., 2006:** Association of spinal cord compression seen on magnetic resonance imaging with clinical outcome in 67 dogs with thoracolumbar intervertebral disc extrusion. *J. Small Anim. Pract.*, 47, 644—655.
56. **Quian, T., Guo, X., Levi, A. D., Vanni, S., Shebert, R. T., Sipski, M. L., 2005:** High-dose methylprednisolone may cause myopathy in acute spinal cord injury patients. *Spinal Cord*, 43, 199—203.
57. **Risio, L. D., Platt, S. R., 2010:** Fibrocartilaginous embolic myelopathy in small animals. *Vet. Clin. North Am. Small Anim. Pract.*, 40, 859—869.
58. **Rowland, J. W., Hawryluk, G. W. J., Kwon, B., Fehlings, M. G., 2008:** Current status of acute spinal cord injury pathophysiology and emerging therapies: promise on the horizon. *Neurosurg. Focus*, 25, E2.
59. **Saganova, K., Orendacova, J., Cizkova, D., Vanicky, I., 2008:** Limited minocycline neuroprotection after balloon-compression spinal cord injury in the rat. *Neurosci. Letters*, 433, 246—249.
60. **Samantaray, S., Das, A., Thakore, N. P., Matzelle, D. D., Reiter, R. J., Ray, L. K., et al., 2009:** Therapeutic potencial of melatonin in traumatic central nervous system injury. *J. Pineal Res.*, 47, 134—142.
61. **Sarmento, C. A. P., Rodrigues, M. N., Bocabello, R. Z., Mess, A. M., Miglino, M. A., 2014:** Pilot study: bone marrow stem cells as a treatment for dogs with chronic spinal cord injury. *Reg. Med. Res.*, 2, 9.
62. **Silva, N. A., Sousa, N., Reis, R. L., Salgado, A. J., 2014:** From basics to clinical: a comprehensive review on spinal cord injury. *Progr. Neurobiol.*, 114, 25—57.
63. **Srugo, I., Aroch, I., Christopher, M. M., Chai, O., Goralnik, I., Bdolah-Abram, I., et al., 2011:** Signs and outcome in acute nonambulatory thoracolumbar disc disease in dogs. *J. Vet. Intern., Med.*, 25, 846—855.
64. **Steward, O., Popovich, P. G., Dietrich, W. D., Kleitman, N., 2012:** Replication and reproducibility in spinal cord injury research. *Exp. Neurol.*, 233, 597—605.
65. **Šulla, I., Balik, V., Petrovičová, J., Almášiová, V., Holovská, K, Oroszová, Z., 2016:** A rat spinal cord injury experimental model. *Folia Veterinaria*, 60, 41—46.
66. **Tsao, T. Y., Chen, E. L., Tsai, W. C., 2009:** Steroids for acute spinal cord injury: revealing silent pathology. *Lancet*, 374 (9688), 500.
67. **Waters, R. L., Adkins, R. H., Yakura, J. S., 1991:** Definition of complete spinal cord injury. *Spinal Cord*, 29, 573—581.
68. **Webb, A. A., Ngan, S., Fowler, D. J., 2010:** Spinal cord injury I: a synopsis of the basic science. *Can. Vet. J.*, 51, 485—492.
69. **Webb, A. A., Ngan, S., Fowler, D. J., 2010:** Spinal cord injury II: prognostic indicators, standards of care, and clinical trials. *Can. Vet. J.*, 51, 598—604.
70. **Wewetzer, K., Radtke, C., Kocsis, J., Baumgärtner, W., 2011:** Species-specific control of cellular proliferation and the impact of large animal models for the use of olfactory ensheathing cells and Schwann cells in spinal cord repair. *Exp. Neurol.*, 229, 80—87.
71. **Wilson, J. R., Foergione, N., Fehlings, M. G., 2013:** Emerging therapies for acute traumatic spinal cord injury. *Canad. Med. Assoc. J.*, 71, 281—299.
72. **Wu, K. L. H., Hsu, C., Chan, J. Y. J., 2009:** Nitric oxide and superoxide anion differentially activate poly(ADP-ribose) polymerase-1 and Bax to induce nuclear translocation of apoptosis inducing factor and mitochondrial release of cytochrome C after spinal cord injury. *J. Neurotrauma*, 26, 965—977.
73. **Xu, J., Fan, G., Chen, S., Wu, Y., Xu, M., Hsu, C. Y., 1998:** Methylprednisolone inhibition of TNF-alpha expression and NF-KB activation after spinal cord injury in rats. *Brain Res. Mol. Brain Res.*, 59, 135—142.
74. **Ying, Z., Roy, R. R., Edgerton, V. R., Gómez-Pinilla, F., 2005:** Exercise restores levels of neurotrophins and synaptic plasticity following spinal cord injury. *Exp. Neurol.*, 193, 411—419.

75. Zaki, F. A., Prata, R. G., 1976: Necrotizing myelopathy secondary to embolization of herniated intervertebral disk material in the dog. *J. Am. Vet. Med. Assoc.*, 169, 222—228.

76. Zhou, X., He, X., Ren, Y., 2014: Function of microglia and macrophages in secondary damage after spinal cord injury. *Neural Reg. Res.*, 9, 1787—1795.

77. Zhu, H., Feng, Y. P., Wise, Y., Yon, S. W., Shen, X. F., Liu, Y. S., et al., 2008: Early neurosurgical intervention of spinal cord contusion: an analysis of 30 cases. *Chin. Med. J.*, 121, 2473—2478.

Received February 14, 2018
Accepted April, 15, 2018

sciendo

DOI: 10.2478/fv-2018-0017

FOLIA VETERINARIA, 62, 2: 59—66, 2018

ANALYSIS OF NICKEL-BINDING PROTEINS FROM VARIOUS ANIMAL SERA

Šimková, J.[1], Milkovičová, M.[1], Valko-Rokytovská, M.[1], Kostecká, Z.[1] Bencúrová, E.[2, 3], Pulzová, L.[2], Čomor, Ľ.[2], Bhide, M. R.[2, 4]

[1]Department of Chemistry, Biochemistry and Biophysics
University of Veterinary Medicine and Pharmacy in Košice, Komenského 73, 041 81 Košice
[2]Laboratory of Biomedical Microbiology and Immunology
University of Veterinary Medicine and Pharmacy in Košice, Komenského 73, 041 81 Košice
Slovakia
[3]Department of Bioinformatics, Julius-Maximilian University of Wuerzburg, Am Hubland, 970 74 Wuerzburg
Germany
[4]Instituteof Neuroimmunology, Slovak Academy of Sciences, Dúbravská cesta 9, 845 10 Bratislava 45,
Slovakia

jana.simkova@uvlf.sk

ABSTRACT

Nickel-binding proteins play an important role in the biological processes and can also be utilized in several fields of biotechnology. This study was focused on analysing the nickel-binding proteins from the blood sera of humans (*Homo sapiens*), cattle (*Bos taurus*), sheep (*Ovis aries*), red deer (*Cervus elaphus*), mouflon (*Ovis orientalis*), fallow deer (*Dama dama*), horses (*Equus ferus caballus*), pigs (*Sus scrofa domesticus*), wildboars (*Sus scrofa*), brown bears (*Ursus arctos*) and pheasants (*Phasianus colchicus*). The presence of higher abundance proteins in the blood serum, such as albumins, may mask the detection of lower abundance proteins. The samples were depleted from these higher abundance proteins to facilitate the detection of those with lower abundance. For the characterization of these proteins, nickel cations bound to tetradentate ligand nitrilotriacetic acid(Ni-NTA)immobilized on agarose beads were incubated with animal sera to capture nickel-binding proteins and subsequently the proteins were eluted and fractionated on sodium dodecyl sulphate-polyacrylamide gel electrophoresis (SDS-PAGE). The results showed a set of nickel-binding proteins with various molecular weights within different animal species. A unique ~42 kDa nickel-binding protein in the brown bear serum, which was not present in any of the other species, was further characterized and identified by matrix-assisted laser desorption/ionization-time-of-flight/mass spectrometry (MALDI-TOF/MS). This protein was identified as ahaptoglobin-like protein. This result may provide some valuable clue for the physiological difference in the metal binding proteins in the serum of Ursus arctos and other animals.

Key words: animal sera; mass spectrometry; nickel-binding proteins; proteomics

INTRODUCTION

Metalloproteomics is a rapidly developing field of science that involves the comprehensive analysis of all metal-containing or metal-binding proteins in a biological sample [13].

Metals play pivotal roles in a broad range of biological processes in all living organisms. Most of these metal ions are bound to specific proteins or enzymes, and exert their effects as active or structural centers of proteins [12]. It is estimated that approximately one-third of all proteins and enzymes require a metal cofactor for functionality; thus named "metalloproteins" [2, 37]. Among the metal-containing proteins, Mg and Zn belong to the most abundant elements; however, Ca, Mn, Fe, and Ni are also frequently observed [35].

Metal-binding proteins and metalloproteins are responsible for many metabolic processes, such as biological energy conversion in photosynthesis and respiration; they are also involved in signalling processes, gene expression and regulation. Metal sites in protein structures also control other processes such as catalysis, substrate binding and enzyme activation. Moreover, they can serve as the reservoir of metal ions and their storage for the cell maintenance [3]. The ability of proteins to bind essential and toxic metals plays an important physiological role in both normal and diseased states [4–7]. Therefore, the characterization of metalloproteins is important for understanding the structure and biological functions of such proteins, thus leading to a clear understanding of metal-associated diseases [1].

Nickel is an essential trace element for each animal species [8]. Nickel is involved in the key processes in the animal body — it interacts with haeme iron and helps in oxygen transport, stimulates the metabolism and is regarded as a key metal element in many plants and animal enzyme systems. As it was shown before, Ni^{2+} ions are necessary for the metabolism of sugars [18] as well as in the transmission of the genetic code (DNA, RNA) [29].

The essential role of nickel ions consists of the action or formation of cGMP, a signalling agent that regulates various physiological processes including blood pressure control, sperm physiology, sodium metabolism and cardiovascular health. Nickel is consistently present in RNA and is bound to several biological substances such as proteins (keratin, insulin), amino acids and serum albumin [39]. In animals, nickel deficiency inhibits growth, reduces reproductive rates, and alters glucose and lipid metabolism that are associated with anemia, hemoglobin reduction, alternations of metal ion contents, and reduced activity of several enzymes [31].

It has been shown by many studies that aminoacids such as histidine, aspartate, glutamate, tyrosine, methionine, trypthophan and cysteine mediate strong interactions with the metal ions [14, 16, 21, 23, 27]. This property was used in the immobilized metal ion affinity chromatography (IMAC) [30] as well as in the other affinity chromatography techniques providing separation and purification of various metal-binding proteins.

Wang et al. [38] used metal affinity chromatography to enrich a fraction of human serum proteins on immobilized columns loaded with cadmium, nickel, zinc, copper or lead in Bis-Tris saline and these proteins were identified using liquid chromatography-tandem mass spectrometry (LC-MS/MS). They identified tens of nickel-binding proteins, e.g. complement C3, α_2-macroglobulin, serum albumin, apolipoprotein B-100, complement component 4B preproprotein and histidine-rich glycoprotein. A similar approach was used in the work of She et al. [33] where they examined the Cu- and Zn-binding proteins from the human hepatoma using the IMAC and mass spectrometry. Nickel-binding proteins are relatively well-known in microorganisms [22, 32, 36].

In this study, we analysed the nickel-binding proteins in the sera of omnivores (humans, pigs, wild-boars), carnivores (brown bears), polygastric (cattle, sheep, red deer, mouflon, fallow deer) and monogastric (horses) herbivores and a bird (pheasants).

MATERIALS AND METHODS

Animals and blood sampling

Samples of venous blood from four to twenty individual animals (humans, cattle, sheep, red deer, mouflon, fallow deer, horses, pigs, wildboars, brown bears and a pheasant) were collected into sterile glass tubes.

Serum preparation

After blood coagulation (12 h, 18 °C) and centrifugation (25 min, 2500 r. p. m., 4 °C) serum samples were filtered through 0.22 μm syringe filters (Minisoft), pooled, aliquoted and stored at –80 °C until use.

Albumin depletion

The sera were then incubated in 0.1 M NaCl (Sigma-Aldrich, USA) and cold ethanol (Sigma-Aldrich, USA) with gentle rotation at 4 °C for 60 min. The samples were centrifuged at 16,000 × g for 45 min at 4 °C. The supernatants were transferred into fresh tubes and the pellet (No. 1) was retained for further processing. The pH of the supernatants was lowered to 5.7 with cold Na-acetate (pH 4) (Sigma-Aldrich, USA) and mixed with gentle rotation at 4 °C for 60 min. After centrifugation, supernatants containing albumins were removed and the pellet (No. 2) was resuspended in RNA free water (Invitrogen, USA) and mixed with the first pellet. This pellet contained the albumin depleted fraction of proteins.

Metal affinity binding chromatography and protein fractionation

The albumin depleted proteins (approx. 200 µg) were incubated with metal affinity Ni-NTA beads (Nickel-Nitrilotriacetic acid) under the native conditions as per the manufacturer's instructions (Jena Bioscience, Germany). The metal affinity beads were washed in spin-column with native wash buffer (0.05 M NaH_2PO_4, 0.3 M NaCl, 10 % glycerol, 0.1 % Tween) (Sigma-Aldrich, USA).

Proteins were then loaded onto the column with the beads, and mixed gently at 4 °C overnight. Beads were then washed with native wash buffer at least five times and the bound proteins were eluted in NuPAGE® Lithium dodecyl sulfate Sample Buffer (NuPAGE®LDS Sample Buffer) (Invitrogen, USA). The detailed protocol of this pull-down assay is described in the publication by Mlynarcik et al. [24]. Proteins were separated by SDS-PAGE on 10 % polyacrylamide gel and visualised using Coomassie Brilliant Blue staining.

Western-blot analysis of nickel-binding proteins

The eluted proteins from the metal affinity binding chromatography were fractionated by SDS-PAGE (Invitrogen, USA) and electrotransferred onto a nitrocellulose membrane. The membrane was blocked for 45 min in 0.05 % TTBS (Tris Buffered Saline TBS) (25 mM Tris, 150 mM NaCl, pH 7.2) with 0.05 % Tween 20 (Sigma-Aldrich, USA) containing 2 % bovine serum albumin (BSA) (Sigma-Aldrich, USA). After two washings with TTBS, the membrane was incubated with horseradish peroxidase-conjugated Ni-NTA(Ni-HRP conjugate) (Pierce, USA) (1 : 5000 diluted in 0.05 % TTBS) (Pierce, USA) for 1 h. After five washings with TTBS, the membrane was incubated in enhanced chemiluminescence substrate (Pierce, USA) for 5 min and the signal was documented by an imaging system (Li-Core, USA).

Mass spectrometry and database searching

A protein band with an approximate molecular weight of 42 kDa from the brown bear was excised from gel under keratin-free conditions, washed in RNA-free water and digested by trypsin [34]. The digested aliquots were mixed with α-cyano-4-hydroxycinnamic acid (Bruker, Germany) in 33 % aqueous acetonitrile and 0.25 % trifluoroacetic acid (Sigma-Aldrich, USA). This mixture was deposited onto a 600 µm AnchorChip prestructured matrix-assisted laser desorption/ionization (MALDI) probe (Bruker-Daltonics) and allowed to dry. Matrix-assisted laser desorption/ionization mass spectrometry (MALDI-MS) data were obtained in an automated analysis loop (Ultraflex, Bruker-Daltonics) equipped with a LIFT-MS/MS device. Spectra were acquired in the positive-ion mode at 50 Hz laser frequency, and 100 to 1000 individual spectra were averaged. The automated analysis of the peptide mass data were performed (FlexAnalysis software; Bruker-Daltonics). MALDI-MS and MALDI-MS/MS data were combined (BioTools, Bruker-Daltonics) to search a non-redundant protein database (NCBInr) using Mascot software (Matrix Science) and the results were subjected to the BLAST analysis (http://blast.ncbi.nlm.nih.gov/) compared by NCBI (https://www.ncbi.nlm.nih.gov/) and UniProt (http://www.uniprot.org/) databases.

Functional category analysis

The EggNOG 4.5.1 (Evolutionary Genealogy of Genes: Non-supervised Orthology Groups) was carried out to determinate the orthologous genes and the functional category analysis (http://eggnogdb.embl.de) [11].

RESULTS

Nickel-binding proteins

SDS-PAGErevealed the presence of a few nickel-binding proteins in the serum of each animal species (Fig. 1). These proteins can be classified into several groups: the protein with molecular weight approximately 100 kDa, observed in

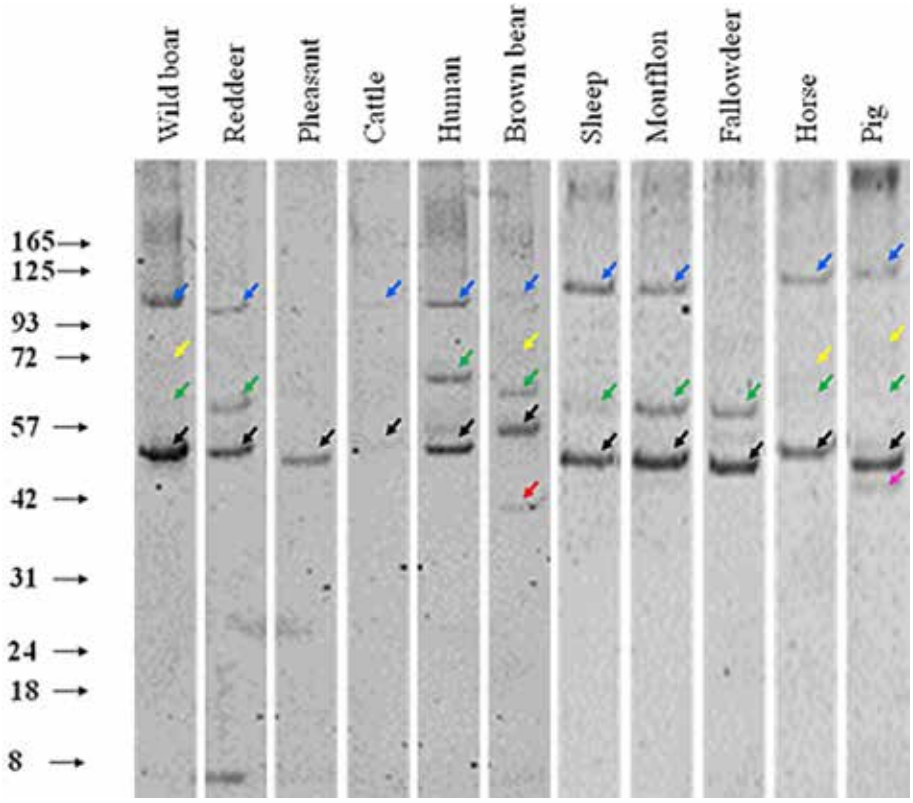

Fig. 1. Assessment of nickel-binding proteins by metal affinity binding chromatography. The nickel-binding proteins from the sera of various animals and humans were bound to metal affinity beads and fractionized by SDS-PAGE

blue arrow — Ni-binding protein with molecular weight of approx. 100 kDa; **yellow arrow** — Ni-binding protein with a molecular weight of between 68—72 kDa; **green arrow** — Ni-binding protein with a molecular weight of approximately 60 kDa; **black arrow** — Ni-binding protein with a molecular weight of approximately 54 kDa; **red arrow** — 42 kDa Ni-binding protein of the bear chosen for identification; **magenta arrow** — 50 kDa Ni-binding protein of a pig

all animal sera (Fig. 1, blue arrows) except the pheasant and fallow deer; the second with a molecular weight of around 60 kDa which were found in the sera of wild boar, red deer, human, brown bear, sheep, mouflon, fallow deer, horse and pig (Fig. 1, green arrows); the third with a molecular weight of approximately 54 kDa, detected in all sera (Fig. 1, black arrow). In the sera of the wild boar, bear, horse and pig, proteins with molecular weight between 68–72 kDa were found (Fig. 1, yellow arrow) and in the case of the pig, the low abundant 50-kDa protein was observed (Fig. 1, arrow with magenta colour). The unique 42-kDa protein was observed only in the serum of the bear (Fig. 1, red arrow). This protein was subjected to further identification by mass spectrometry.

Identification of 42-kDa nickel-binding protein in the bear

To confirm that the 42-kDa protein from the bear serum was a nickel-binding protein, a western blot was performed with a Ni-HRP conjugate (Fig. 2). This protein was further excised from polyacrylamide gel and analysed by MALDI/TOF/MS. The Mascot search revealed that this protein was a haptoglobin-like protein (Accession number–gi|301776456, score 597.6, 7 matched peptides) (Table 1).

EggNOG functional category analysis

In order to find the orthologous genes of the haptoglobin-like protein, the EggNOG analysis was used. Fifteen categories were identified with the score more than 500 (Table 2). The clusters with the highest score were identified as ENOG410CHIE, with the functional annotation amino acid transport and metabolism — haptoglobin, having the orthologs in 3 other species: Felis catus, Canis lupus familiaris and Mustela putorius furo (Fig. 3) [11].

Table 1. Results from the identification of 42 kDa protein of the brown bear from the Mascot server

Rank	Protein	Accession	Mw [kDa]	Score	No. Peptides	SC [%]	RMS90 [ppm]
1	Haptoglobin-like (*Ailuropoda melanoleuca*)	gi|301776456	38.2	597.6 (M: 597.6)	7	25.6	19.56

Mw — molecular weight; SC — sequence coverage

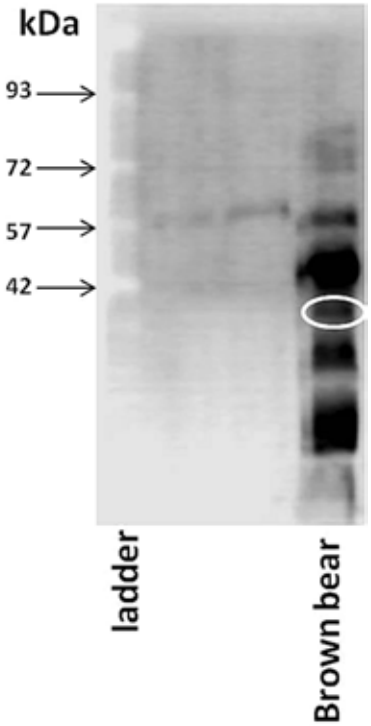

Fig. 2. Validation of nickel binding abilities of 42 kDa serum protein in the bear by the western blot. Albumin-depleted sera of the brown bear were electrotransferred onto a nitrocellulose membrane and the interaction of Ni-HRP conjugate with Ni-binding proteins was visualized. The 42 kDa serum protein in the bear is highlighted in the white ellipse

Table 2. The EggNOG automatic classification and functional analysis of the haptoglobin-like protein orthologs

EggNOG	Score	Function	Nr. of species/ proteins
ENOG410CHIE	807.5	Amino acid transport and metabolism	4/4
ENOG410UTJ0	707.0	Amino acid transport and metabolism	34/34
ENOG410RPEA	683.0	Amino acid transport and metabolism	4/4
ENOG4118TY1	681.4	Extracellular structures	5/5
ENOG411B3ZT	680.2	Amino acid transport and metabolism	17/17
ENOG4116793	652.1	Amino acid transport and metabolism	10/10
ENOG410A494	651.1	Amino acid transport and metabolism	40/42
ENOG410DRTE	651.1	Amino acid transport and metabolism	40/42
ENOG410VF3W	651.1	Amino acid transport and metabolism	40/42
ENOG4113N0R	651.1	Amino acid transport and metabolism	40/42
ENOG411CU98	651.1	Amino acid transport and metabolism	40/42
ENOG410S11U	642.8	Amino acid transport and metabolism	2/2
ENOG410V09D	642.8	Amino acid transport and metabolism	2/2
ENOG4116M9C	642.8	Amino acid transport and metabolism	2/2
ENOG411B98W	642.8	Amino acid transport and metabolism	2/2

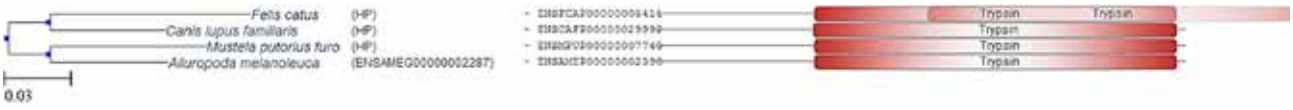

Fig. 3. Phylogenetic tree of the orthologs of haptoglobin-like protein (Ailuropoda melanoleuca) with the highest score (EggNOG ENOG410CHIE). The functional annotation from the Pfam database is depicted on the right [28]. The phylogenetic tree was generated by the EggNOG database

DISCUSSION

The results of our study demonstrated that various species, including birds, humans, and other mammals contained a repertoire of the nickel-binding proteins in their blood sera.

Some proteins of this repertoire have approximately similar molecular weights (e. g. 100 kDa, 60 kDa, and 54 kDa), so probably they were the ortholog of the same proteins, thus we focused on the unique, 42-kDa protein that was found in the bear serum only.

This unique protein was identified as a haptoglobin-like protein. This group of proteins is not well-known in mammals, although haptoglobins play a role in the acute phase response and their expression is stimulated by a broad range of the inflammatory stimuli. The haptoglobin-like proteins with the molecular weight around 40 kDa and pI in the range 7.7—8.6 have been observed also in human sera [38], while most studies of haptoglobin-like proteins are associated with the pathology of the female reproductive system [15, 19].

There is also very strong evidence for an essential role of haptoglobin in brown and black bears [9, 25]. Mominoki et al. [25] tested the concentration of haptoglobins in hibernating and non-hibernating bears. They determined a higher concentration of haptoglobins in the hibernating bears during winter than in spring, and they suggested that its concentration in plasma is more associated with the hibernation [25].

The group of nickel-binding proteins is very well-studied with regard to the important bacterial pathogens: Helicobacter pylori, *Escherichia coli, Klebsiella aerogenes* and others [10, 20, 22]. However, the function and utilization of nickel-binding proteins in mammals are poorly understood. Nickel is an essential component of several enzymes and it is involved in several metabolic pathways in both, prokaryotes and eukaryotes [40]. Nickel-binding proteins are usually histidine-rich plasma proteins, which are able to bind metals and other metal-containing proteins, e. g. zinc, copper, cadmium, heparin and haeme [17], but there are only 3 % of histidine residues in the amino acid sequence of the haptoglobin-like proteins of the giant panda (7 peptide match of 42 kDa with haptoglobin-like proteins of the giant panda). Furthermore, in the amino acid sequence there are no His-Pro rich domains or motifs usually responsible for the interaction with divalent cations [26]. On the other hand, the principle of immobilized metal ion affinity chromatography is an interaction of histidine residues of protein with transition metal ions (e. g. nickel or zinc) immobilized on the agarose or metal beads. However, as our identification in the case of the brown bear failed, we can only speculate that the 42-kDa protein found by SDS-PAGE has similar, but not identical sequence as the haptoglobin-like protein of the giant panda identified by the peptide mass fingerprinting analysis. The sequence analysis of the whole coding region of haptoglobin-like protein of brown bear will reveal the nickel binding pockets.

The affinity of serum proteins to Ni^{2+} has not been described in animal species and this study can be the first step toward a deeper characterization of the metabolism and unique features of nickel-binding proteins.

CONCLUSIONS

In the current study we found that several animal sera contained the specific nickel-binding proteins with varied molecular weights. The unique 42-kDa protein of the brown bear was chosen, which showed very strong binding to nickel in the western blot experiments. This protein was not present in any other animals tested or human sera and the identification showed the match with the haptoglobin-like protein of the giant panda. The function of this protein is unknown for us at present. The combination of metal affinity binding chromatography, protein fractionation and MALDI-TOF/MS represents a powerful tool for studying metal-binding proteins in biological tissues.

ACKNOWLEDGEMENT

This study was supported by APVV-14-0218, VEGA 1/0261/15, VEGA 1/0258/15. KB and LP were funded by the SF project Medipark (ITMS 26220220185). E.B. and L.P. were funded by ITMS 26220220185.

REFERENCES

1. **Andreini, C., Bertini, I., Rosato, A., 2009:** Metalloproteomes: a bioinformatic approach. *Acc. Chem. Res.*, 42, 1471—1479.
2. **Barnett, J. P., Scanlan, D. J., Blindauer, C. A., 2012:** Protein

fractionation and detection for metalloproteomics: challenges and approaches. *Anal. Bioanal. Chem.*, 402, 3311—3322.

3. **Cameron, K. S., Buchner, V., Tchounwou, P. B., 2011:** Exploring the molecular mechanisms of nickel-induced genotoxicity and carcinogenicity: a literature review. *Rev. Environ. Health.*, 26, 81—92.
4. **CDC, 2004:** Toxicological profile for copper [Accessed April 15, 2015l ;http://www.atsdr.cdc.gov/toxprofiles/tp132.pdf.
5. **CDC, 2005:** Toxicological profile for zinc [Accessed April 15, 2015]; http://www.atsdr.cdc.gov/toxprofiles/tp60.pdf.
6. **CDC, 2007:** Toxicological profile of lead. [Accessed April 15, 2015]; http://www.atsdr.cdc.gov/toxprofiles/tp13.pdf.
7. **CDC, 2012:** Toxicological profile for cadmium. [Accessed April 15, 2015]; http://www.atsdr.cdc.gov/toxprofiles/tp5.pdf.
8. **Cempel, M., Nikel, G., 2006:** Nickel: a review of its sources and environmental toxicology. *Pol. J. Environ. Stud.*, 15, 375—382.
9. **Chow, B. A., Donahue, S. W., Vaughan, M. R., McConkey, B., Vijayan, M. M., 2013:** Serum immune-related proteins are differentially expressed during hibernation in the American black bear. *PLoS One*, 8, e66119.
10. **de Reuse, H., Vinella, D., Cavazza, C., 2013:** Common themes and unique proteins for the uptake and trafficking of nickel, a metal essential for the virulence of *Helicobacter pylori*. *Front. Cell. Infect. Microbiol.*, 3, 94.
11. **EggNOG database.** Carnivora. Amino acid transport and metabolism, Haptoglobin. [online], http://eggnogdb.embl.de/#/app/results#ENOG410CHIE datamenu.
12. **Gao, Y., Chen, C., Zhao, J., Zhang, P., Chai, Z., He, W., Huang, Y., 2003:** An improved method for analysis of distribution of metalloproteins in human liver cytosol by synchrotron radiation X-ray fluorescence. *Anal. Chim. Acta*, 485, 131—137.
13. **Hagedoorn, P. L., 2015:** Microbial Metalloproteomics. *Proteomes*, 3, 424.
14. **Hara, M., Fujinaga, M., Kuboi, T., 2005:** Metal binding by citrus dehydrin with histidine-rich domains. *J. Exp. Bot.*, 56, 2695—2703.
15. **Honda, R., Katabuchi, H., 2014:** Pathological aspect and pathogenesis of endometriosis. In **Harada, T. (Ed.):** *Endometriosis: Pathogenesis and Treatment*. Springer Japan, 9—18.
16. **Hu, C., Chan, S. I., Sawyer, E. B., Yu, Y., Wang, J., 2014:** Metalloprotein design using genetic code expansion. *Chem. Soc. Rev.*, 43, 6498—6510.
17. **Jones, A. L., Hulett, M. D., Parish, C. R., 2005:** Histidine-rich glycoprotein: A novel adaptor protein in plasma that modulates the immune, vascular and coagulation systems. *Immunol. Cell. Biol.*, 83, 106—118.
18. **Khan, S., Moheman, A., 2006:** Effect of heavy metals (cadmium and nickel) on the seed germination, growth and metals uptake by Chilli (*Capsicum frutescens*) and sunflower plants (*Helianthus annuus)*. *Pollution Research*, 25, 99—104.
19. **Lavery, K., Way, A., Killian, G., 2003:** Identification and immunohistochemical localization of a haptoglobin-like protein in the tissues and fluids of the bovine (*Bos taurus*) ovary and oviduct. *Reproduction*, 125, 837—846.
20. **Lee, M. H., Pankratz, H. S., Wang, S., Scott, R. A., Finnegan, M. G., Johnson, M. K., et al., 1993:** Purification and characterization of Klebsiella aerogenes UreE protein: a nickel-binding protein that functions in urease metallocenter assembly. *Protein Sci.,* 2, 1042—1052.
21. **Loftin, I. R., Blackburn, N. J., McEvoy, M. M., 2009:** Tryptophan Cu (I)–π interaction fine-tunes the metal binding properties of the bacterial metallochaperone CusF. *J. Biol. Inorg. Chem.*, 14, 905—912.
22. **Martino, L., He, Y., Hands-Taylor, K. L., Valentine, E. R., Kelly, G., Giancola, C., Conte, M. R., 2009:** The interaction of the *Escherichia coli* protein SlyD with nickel ions illuminates the mechanism of regulation of its peptidyl-prolyl isomerase activity. *FEBS J.*, 276, 4529—4544.
23. **Mejáre, M., Bülow, L., 2001:** Metal-binding proteins and peptides in bioremediation and phytoremediation of heavy metals. *Trends Biotechnol.*, 19, 67—73.
24. **Mlynarcik, P., Bencurova, E., Madar, M., Mucha, R., Pulzova, L., Hresko, S., Bhide, M., 2012:** Development of simple and rapid elution methods for proteins from various affinity beads for their direct MALDI-TOF downstream application. *J. Proteomics*, 75, 4529—4535.
25. **Mominoki, K., Morimatsu, M., Karjalainen, M., Hohtola, E., Hissa, R., Saito, M., 2005:** Elevated plasma concentrations of haptoglobin in European brown bears during hibernation. *Comp. Biochem. Physiol. A Mol. Integr. Physiol.*, 142, 472—477.
26. **Mori, S., Takahashi, H. K., Yamaoka, K., Okamoto, M., Nishibori, M., 2003:** High affinity binding of serum histidine-rich glycoprotein to nickel-nitrilotriacetic acid: the application to microquantification. *Life Sci.*, 73, 93—102.
27. **Nair, N. G., Perry, G., Smith, M. A., Reddy, V. P., 2010:** NMR studies of zinc, copper, and iron binding to histidine, the principal metal ion complexing site of amyloid-β peptide. *J. Alzheimer's Dis.*, 20, 57—66.
28. **Pfam database.** trypsin Ailuropoda melanoleuca. [online],

https://pfam.xfam.org/search/keyword?query=trypsin+Ailuropoda+melanoleuca.

29. **Poonkothai, M., Vijayavathi, B. S., 2012:** Nickel as an essential element and a toxicant. *Int. J. Environ. Sci.*, 1, 285—288.
30. **Porath, J., 1988:** IMAC-Immobilized metal ion affinity based chromatography. *Trends in Analytical Chemistry*, 7, 254—259.
31. **Samal, L., Mishra, C., 2011:** Significance of nickel in livestock health and production. *International Journal for Agro Veterinary and Medical Sciences*, 5, 349—361.
32. **Sevcenco, A. M., Hagen, W. R., Hagedoorn, P. L., 2012:** Microbial metalloproteomes explored using MIRAGE. *Chem. Biodivers.*, 9, 1967—1980.
33. **She, Y. M., Narindrasorasak, S., Yang, S., Spitale, N., Roberts, E. A., Sarkar. B., 2003:** Identification of metal-binding proteins in human hepatoma lines by immobilized metal affinity chromatography and mass spectrometry. *Mol. Cell. Proteomics*, 2, 1306—1318.
34. **Shevchenko, A., Tomas, H., Havlis, J., Olsen, J. V., Mann, M., 2006:** In-gel digestion for mass spectrometric characterization of proteins and proteomes. *Nat. Protoc.*, 1, 2856—2860.
35. **Shi, W., Zhan, C., Ignatov, A., Manjasetty, B. A., Marinkovic, N., Sullivan, M., Huang, R., Chance, M. R., 2005:** Metalloproteomics: high-throughput structural and functional annotation of proteins in structural genomics. *Structure*, 13, 1473—1486.
36. **Tristao, G. B., Assuncao, L. do P., Dos Santos, L. P., Borges, C. L., Silva-Bailao, M. G., Soares, C. M., et al., 2014:** Predicting copper-, iron-, and zinc-binding proteins in pathogenic species of the *Paracoccidioides* genus. *Front. Microbiol.*, 5, 761.
37. **Waldron, K. J., Rutherford, J. C., Ford, D., Robinson, N. J., 2009:** Metalloproteins and metal sensing. *Nature*, 460, 823–830.
38. **Wang, F., Chmil, C., Pierce, F., Ganapathy, K., Gump, B. B., MacKenzie, J. A., et al., 2013:** Immobilized metal affinity chromatography and human serum proteomics. *J. Chromatogr. B Analyt. Technol. Biomed. Life Sci.*, 934, 26—33.
39. **Yokoi, K., Uthus, E. O., Nielsen, F. H., 2002:** The essential use of nickel affects physiological functions regulated by the cyclic-GMP signal transduction system. In *Proceedings of the 7th International Symposium on Metal Ions in Biology and Medicine*, May 5—9, St. Petersburg, Russia.
40. **Zhang, Y., Rodionov, D. A., Gelfand, M. S., Gladyshev, V. N., 2009:** Comparative genomic analyses of nickel, cobalt and vitamin B12 utilization. *BMC Genomics,* 10, 78.

Reeceived February 26, 2018

Accepted, May 10, 2018

sciendo

DOI: 10.2478/fv-2018-0018

FOLIA VETERINARIA, 62, 2: 67—72, 2018

ANTIFUNGAL EFFECT OF SELECTED ESSENTIAL OILS ON *MALASSEZIA PACHYDERMATIS* GROWTH

Váczi, P., Čonková, E., Marcinčáková, D., Sihelská, Z.

Institute of Pharmacology, Department of Pharmacology and Toxicology
University of Veterinary Medicine and Pharmacy, Komenského 73, 041 81 Košice
Slovakia

peter.vaczi@uvlf.sk

ABSTRACT

The antifungal activities of 14 selected essential oils (at the concentrations of 0.5 %, 5 %, and 30 %) against the yeast *Malassezia pachydermatis* (18 isolates and one reference strain) were investigated. The isolates of *M. pachydermatis* were obtained from swabs of external ear canals of healthy dogs using sterile swabs. The determination of the efficacy was based on a modified disc diffusion method (CLSI M44-A2). The best antifungal efficacy (100 %) was shown by clove, cinnamon and oregano at the concentration of 30 %; less significant efficacy was shown at the concentration of 5 % (38 %, 33 % and 5 %, respectively). Satureja inhibited the growth of *Malassezia* (efficacy of 16 %) only at the concentration of 30 %. Bergamot, lavender, juniper, cedar, sage, tea-tree, grapefruit, pine, chamomile and yarrow essential oils were not able to form inhibition zones as defined in the methodology used (greater or equal to 15 mm) in all concentrations used. Therefore, according to the interpretation criterion, they were considered ineffective. In all cases, the concentration of 0.5 % was not effective against the growth of *Malassezia* yeasts.

Key words: dog; essential oil; disc diffusion method; *Malassezia*; sensitivity

INTRODUCTION

Malassezia yeasts are eukaryotic microorganisms placed in the phylum Basidiomycota [12]. Currently, the genus *Malassezia* includes sixteen species, fifteen of which are lipid-dependent and are most frequently recovered from humans, ruminants, horses or parrots (*Malassezia furfur, M. globosa, M. obtusa, M. restricta, M. slooffiae, M. sympodialis, M. dermatis, M. nana, M. japonica, M. yamatoensis, M. equina, M. caprae, M. cuniculi, M. brasiliensis and M. psittaci*). The only one non-lipid-dependent species, *M. pachydermatis*, is commonly recovered from dogs and cats [1, 2, 3, 4, 27].

M. pachydermatis is a saprophytic and lipophilic yeast, which is part of the normal cutaneous microflora of several warm-blooded animals [20]. It is often found in the ear canals and skin of dogs, cats and other species of domestic and wild animals [14, 15]. *M. pachydermatis* is frequently

involved as a secondary factor in canine otitis externa and skin infections, which are manifested by irregularly superficial to interstitial dermatitis wherein hyperkeratosis and lymphocytic exocytosis are prominent [7, 19].

At the present, the therapy of malassezia-dermatitis is usually based on topical or systemic administration of antifungals (mainly those of azoles) and direct topical application of antiseptic substances. An alternative and attractive possibility of supportive therapy is the use of essential oils.

Essential oils (EOs) are concentrated, hydrophobic substances containing volatile aroma compounds from different parts of plants extracted by steam distillation and by various solvents [21, 22]. The main constituents of essential oils — mono- and sesquiterpenes including carbohydrates, alcohols, ethers, aldehydes and ketones — are responsible for the fragrant and biological properties of aromatic and medicinal plants. Various EOs produce pharmacological effects, demonstrating anti-inflammatory, antioxidant and anti-carcinogenic properties [16].

On the basis of the results obtained in the preliminary study [25], the main objective of this study was to determine the effectiveness of the selected EOs in three different concentrations (0.5 %, 5 % and 30 %) against *M. pachydermatis* isolated from the external ear canals of healthy dogs.

MATERIALS AND METHODS

Phenotypic and genotypic identification of *Malassezia pachydermatis*.

Isolates (n = 18) of *M. pachydermatis* were obtained from swabs of external ear canals of healthy dogs. The identification of yeasts was performed on the basis of detailed phenotypic features according to Kaneko et al. [17] and confirmed by genotypic PCR methods according to Gaitanis and Velegraki [13].

Selection and composition of essential oils

Essential oils of the following medicinal plants were tested: bergamot, cedar, chamomile, cinnamon, clove, grapefruit, juniper, lavender, oregano, pine, sage, satureja — winter savory, tea tree and common yarrow. The EOs were obtained from the Calendula company (Nová Ľubovňa, Slovakia) as pure substances (concentration of 100 %) and their composition is listed in Table 1. Three concentrations were used: 0.5 %, 5 % and 30 %. Mineral oil — liquid paraffin (Merck KGaA, Darmstadt, Germany) was chosen to dilute the pure essential oils to the required concentrations. It was selected for its inertness so as to prevent the false positivity (antifungal activity of the diluent itself). Pure and

Table 1. Composition of the essential oils according to the producer (Calendula company, Nová Ľubovňa, Slovakia)

Essential oil	Plant of origin	Content substances
Bergamot	*Citrus bergamia*	limonene 36 %, linalool 15 %, linalyl acetate 23 %
Cedar	*Cedrus* spp.	cineol 30 %, thujone 3 %, borneol 3 %
Chamomile	*Matricaria recucita*	bisabolol oxides 5 %, bisabolol 29 %, chamazulene 2.7 %
Cinnamon	*Cinnamonum aromaticum*	eugenol 77 %
Clove	*Syzygium aromaticum*	eugenol 85 %
Grapefruit	*Citrus paradisi*	limonene 87 %
Juniper	*Juniperus communis*	α-pinene 45 %, sabinene 2 %, β-pinene 4 %, β-myrcene 3.5 %, α-phellandrene < 1 %, limonene 13 %, terpinen-4-ol 0.5 %, bornyl acetate < 1 %, β-karyophylene 2 %
Lavender	*Lavandula angustifolia*	linalool 43 %
Oregano	*Origanum vulgare*	carvacrol 57 %
Pine	*Pinus sylvestris*	α-pinene 43 %, camphene 1.5 %, β-pinene 19 %, car-3-ene 17 %, β-myrcene 2.2 %, limonene 8 %, β-phellandrene < 2.5 %, p-cymene < 2 %, terpinolene < 4 %, bornyl acetate 2.3 %, β-karyophylene 2.5 %
Sage	*Salvia officinalis*	cineol 15 %, thujone 24 %, borneol 18 %
Satureja	*Satureja montana*	not established
Tea-tree	*Melaleuca alternifolia*	terpinen-4-ol 33 %
Yarrow	*Achillea millefolium*	chamazulene 6 %

also diluted EOs were stored under standard laboratory conditions (18 °C) and without access of light (wrapped in aluminium foil).

Testing of sensitivity

The sensitivity of 18 isolates and one reference strain of *M. pachydermatis* (CBS 1879, CBS-KNAW Fungal Biodiversity Centre, Utrecht, Netherlands) was evaluated by a modified disc diffusion method M44-A2 [9]. The method is based on pathogen growth inhibition, manifested by the development of diffusion zone due to the release of the antifungal substances from impregnated paper discs. A reference strain of *M. pachydermatis* was used as a control.

In the experiment, 7-day old cultures of *M. pachydermatis* passaged on Sabouraud dextrose agar with chloramphenicol — SCA (Himedia Laboratories Pvt. Ltd., India) were used. The yeast suspension was prepared in physiologic saline solution supplemented with 0.1 % of Tween 80 (Merck KGaA, Darmstadt, Germany) at the final concentration of 10^6 CFU.ml^{-1} corresponding to the standard 1 on a McFarland scale. The suspension was inoculated by using a sterile swab onto agar plates containing nutrient medium — SCA, twice in three directions, 15 minutes apart. Paper discs (Oxoid Ltd., United Kingdom) were applied to the surface of the agar. Each disc (6 mm in diameter) was impregnated with 15 µl of the respective essential oil (concentration of 30 %, 5 % and 0.5 % in liquid paraffin). The cultivation took place at a constant temperature of 32 °C for 96 hours. Subsequently, the size of the inhibitory zone was measured by using an Antibiotic zone scale (Himedia Laboratories Pvt. Ltd., India). Since the method M44-A2 is intended for *Candida* species [9] and does not include interpretation criteria for *Malassezia* strains, isolates that showed an inhibition zone greater or equal to 15 mm (2.5-fold larger than the disc diameter) were considered to be sensitive.

The validity of testing was confirmed on the basis of the sensitivity of *Candida albicans* reference strain CCM 8261 (Czech Collection of Microorganisms, Brno, Czech Republic) to itraconazole (10 mg per disc; Himedia Laboratories Pvt. Ltd., India). The inhibition zone of 20 mm was detected, which is in agreement with interpretation criteria specified in the methodology (18—20 mm).

The antifungal efficiency was expressed as a ratio of the number of sensitive isolates and the number of the isolates tested.

RESULTS

We evaluated the antifungal activity of the EOs at concentrations 0.5 %, 5 % and 30 %. The lowest tested concentration (0.5 %) was not sufficient to inhibit the growth of *Malassezia*; all the inhibition zones were 0 mm (data not shown).

Table 2 illustrates the antifungal activity of the EOs at a concentration of 5 % against isolates and reference strain of *M. pachydermatis*. Table 3 shows the effect of EOs at a concentration of 30 %. Essential oils obtained from clove, cinnamon and oregano exhibited an excellent effectiveness against *M. pachydermatis* growth at 30 % concentration. Clove and cinnamon EOs at a concentration of 5 % had an antifungal effect on less than half of the isolates tested (38 % and 33 %, respectively). The EOs of satureja, tea tree, bergamot, lavender, juniper, sage, grapefruit, cedar, pine, chamomile and yarrow showed insufficient antifungal properties against *M. pachydermatis* in all concentrations.

All essential oils at a concentration of 0.5 % were not sufficient to inhibit the growth of both the isolates and the reference strain (all the inhibition zones were 0 mm), therefore these are not included in the table.

DISCUSSION

The essential oils can act as antibacterial agents against a wide spectrum of pathogenic bacterial strains including *Listeria monocytogenes, L. innocua, Salmonella typhimurium, Escherichia coli, Shigella dysenteria, Bacillus cereus and Staphylococcus aureus*. Plant extracts, especially EOs, may afford a potential alternative to synthetic antiviral drugs: they have virocidal properties against *Herpes simplex* I [10]. Several EOs can act also on various microscopic fungi, e. g. *Aspergillus niger, Geotrichum candidum* [26], *Trichophyton rubrum, T. mentagrophytes, Microsporum canis, Epidermophyton floccosum* [8], *Candida albicans* and *Malassezia furfur* [11].

According to the results of our study, the essential oils of clove, cinnamon and oregano in concentration of 30 % showed excellent activity against *M. pachydermatis*. The formation of inhibition zones of cedar, chamomile, sage, grapefruit and tea-tree oil indicated their partial efficacy, however, based on the methodology they cannot be assessed as effective.

Table 2. Effectiveness of essential oils at a concentration of 5 % against *Malassezia pachydermatis*

Essential oil	Isolates (n = 18)		Reference strain
	Inhibition zones [ø ± SD]	E (ss/n) [%]	Inhibition zones [mm]
Clove	16.94 ± 5.97	38 % (7/18)	18
Cinnamon	15.44 ± 5.73	33 % (6/18)	15
Oregano	13 ± 2.86	5 % (1/18)	14
Satureja	7.49 ± 1.87	0 %	0
Cedar	3.22 ± 3.02	0 %	8
Chamomile	3.61 ± 3.44	0 %	6
Bergamot	0	0 %	0
Lavender	0	0 %	0
Grapefruit	0	0 %	0
Sage	0	0 %	0
Tea tree	0	0 %	0
Juniper	0	0 %	0
Pine	0	0 %	0
Yarrow	0	0 %	0

ø — average size of the inhibition zone in mm; SD — standard deviation; E — Percentage of efficacy (number of sensitive strains/ number of samples tested); ss — sensitive strains; n — number of samples tested

Table 3. Effectiveness of the essential oils at a concentration of 30 % against *Malassezia pachydermatis*

Essential oil	Isolates (n=18)		Reference strain
	Inhibition zones [ø ± SD]	E (ss/n) [%]	Inhibition zones [mm]
Clove	41.67 ± 4.81	100 % (18/18)	44
Cinnamon	40.14 ± 5.01	100 % (18/18)	50
Oregano	38.8 ± 4.45	100 % (18/18)	52
Satureja	23.26 ± 2.18	16 % (3/18)	12
Cedar	11.94 ± 1.89	0 %	12
Chamomile	11.17 ± 1.38	0 %	12
Bergamot	8.44 ± 1.67	0 %	10
Lavender	6.55 ± 4.32	0 %	8
Grapefruit	10.78 ± 2.39	0 %	10
Sage	10.06 ± 2.73	0 %	14
Tea tree	8.44 ± 4.87	0 %	10
Juniper	5.55 ± 3.26	0 %	8
Pine	4.44 ± 3.79	0 %	6
Yarrow	0	0%	0

ø — average size of the inhibition zone in mm; SD — standard deviation; E — percentage of efficacy (number of sensitive strains/ number of samples tested); ss — sensitive strains; n — number of samples tested

The antifungal effect of tea tree oil has also been reported by Carson et al. [5]. Studies investigating the mechanism of antifungal action have focused almost exclusively on *Candida albicans* as a model micro-organism. Similar to results found for bacteria, tea tree oil also alters the permeability of *C. albicans* cells.

Antifungal activity against *M. pachydermatis* was performed by Kim et al. [18] using disc-diffusion assays and well diffusion tests. The essential oils inhibited the growth of *M. pachydermatis* in a range from 0.5 % to 1.0 % concentrations. Thyme oil was found to be highly effective in inhibiting the growth of *M. pachydermatis* in a range from 0.125 % to 0.0625 %, while marjoram and then tea tree oil exhibited lower inhibitory capacities [18]. Compared to our results, tea tree oil inhibited the growth of *M. pachydermatis* only at higher concentration (30 %), while the lower one was not sufficient.

In another study, the possible synergistic anti-*Candida* effect between tea tree, oregano and *Pelargonium graveolens* EOs and Amphotericin B was investigated. The antifungal activity was assessed using the agar dilution method in eleven strains of *C. albicans, C. glabrata, C. guillermondi, C. krusei, C. parapsilosis* and *C. tropicalis*. The results obtained indicated the occurrence of a synergistic interaction between the essential oils under study and Amphotericin B. *P. graveolens* essential oil appeared to be the most effective, inhibiting all the *Candida* species evaluated in their study [23]. Also, the results of our study demonstrated, that the efficiency of oregano EO was excellent (100 %) at higher concentration,

In our results, 100 % efficiency was recorded by clove, cinnamon and these are comparable to the study of Rusenova and Parvanov [24]. In their study, twelve essential oils (thyme, clove, cinnamon, marjoram, tea tree, clary sage, peppermint, lemon, grapefruit, lemongrass, mandarin and oregano) were tested for inhibitory activity against some microorganisms of veterinary interest including *Candida* spp. and *M. pachydermatis* using the disc diffusion procedure. According to their results, the most potent essential oils were cinnamon, oregano, lemongrass and thyme.

Essential oils of various Juniperus species were tested by Cavaleiro et al. [6] against selected yeasts — *Candida albicans, C. krusei and C. parapsilosis*, molds — *Aspergillus fumigatus* and *A. flavus* and against dermatophytes — *Microsporum canis, M. gypseum, Trichophyton rubrum, T. mentagrophytes* and *Epidermophyton floccosum*. All essential oils inhibited dermatophyte strains, *C. krusei, C. glabrata* and *C. albicans*.

The antifungal action of various EOs against *Aspergillus niger* and *Geotrichum candidum* was also tested by Verma et al. [26]. By using different concentrations of EOs (5, 10, 20, 30, 40 and 50 ppm), it was concluded that clove, lemon, orange and peppermint oil, already at the lowest concentration, had activity comparable to ketoconazole in the same concentration, whereas the effect of castor, olive and cedar oil was inadequate.

CONCLUSIONS

The enormous development of chemical drugs is currently associated with the increasing emergence of serious adverse effects including drug-resistance. Traditional medicinal plants represent a reservoir of pharmacologically active substances, which can also be used in the treatment of infectious diseases due to their antimicrobial effects. The results of our study have revealed that essential oils of clove, cinnamon and oregano at concentrations of 30 % inhibited the growth of *Malassezia pachydermatis* isolates (100 % efficiency), implying their potential use in the treatment of *Malassezia* infections in dogs. The confirmation of their potential antimicrobial effect indicates that these plants may be useful in combined therapy or creation of natural antifungal medications.

ACKNOWLEDGEMENTS

This study was supported by the Slovak Research and Development Agency under the contract APVV-15-0377.

REFERENCES

1. **Batra, R., Boekhout, T., Guého, E., Cabañes, F. J., Dawson, T. L., Jr., Gupta, A. K., 2005:** *Malassezia* Baillon, emerging clinical yeasts. *FEMS Yeast Res.*, 5, 1101—1113.
2. **Cabañes, F. J., Theelen, B., Castellá, G., Boekhout, T., 2007:** Two new lipid-dependent *Malassezia* species from domestic animals. *FEMS Yeast Res.*, 7, 1064—1076.
3. **Cabañes, F. J., Veja, S., Castellá, G., 2011:** *Malassezia cunicu-*

li sp. nov., a novel yeast species isolated from rabbit skin. *Med. Mycol.*, 49, 40—48.

4. **Cabañes, F. J., Coutinho, S. D., Puig, L., Bragulat, M. R., Castellá, G., 2016:** New lipid-dependent *Malassezia* species from parrots. *Rev. Iberoam. Micol.*, 33, 92—99.
5. **Carson, C. F., Hammer, K. A, Riley, T. V., 2006:** *Melaleuca alternifolia* (Tea Tree) Oil: a Review of antimicrobial and other medicinal properties. *Clin. Microbiol. Rev.*, 19, 50—62.
6. **Cavaleiro, C., Pinto, E., Goncalves, M. J., Salgueiro, L., 2006:** Antifungal activity of *Juniperus* essential oils against dermatophyte, *Aspergillus* and *Candida* strains. *J. Appl. Microbiol.*, 100, 1333—1338.
7. **Chiavassa, E., Tizzani, P., Peano, A., 2014:** *In vitro* antifungal susceptibility of *Malassezia pachydermatis* strains isolated from dogs with chronic and acute otitis externa. *Mycopathologia*, 178, 315—319.
8. **Chuang, P. H., Lee, C. W., Chou, J. Y., Murugan, M., Shieh, B. J., Chen, H. M., 2007:** Anti-fungal activity of crude extracts and essential oil of *Moringa oleifera* Lam. *Biores. Technol.*, 98, 232—236.
9. **Clinical and Laboratory Standards Institute, 2009:** M44-A2. Method for antifungal disc diffusion susceptibility testing of yeast. *Approved Guideline*, 2nd edn., 1—23.
10. **Edris, A. E., 2007:** Pharmaceutical and therapeutic potentials of essential oils and their individual volatile constituents: A review. *Phytotherapy Res.,* 21, 308—323.
11. **Ferhout, H., Bohatier, J., Guillot, J., Chalchat, J. C., 1999:** Antifungal activity of selected essential oils, cinnamaldehyde and carvacrol against *Malassezia furfur* and *Candida albicans*. *J. Essent. Oil Res.*, 11, 119—129.
12. **Gaitanis, G., Magiatis, P., Hantschke, M., Bassukas, I. D., Velegraki, A., 2012:** The *Malassezia* genus in skin and systemic diseases. *Clin. Microbiol. Rev.*, 25, 106—141.
13. **Gaitanis, G., Velegraki, A., 2006:** Verifiable single nucleotide polymorphisms of the internal transcribed spacer 2 region for the identification of 11 *Malassezia* species. *J. Dermatol. Sci.*, 43, 214—217.
14. **Guillot, J., Bond, R., 1999:** *Malassezia pachydermatis*: A review. *Med. Mycol.*, 37, 295—306.
15. **Hammer, K. A., Carson, C. F., Riley, T. V., 2000:** *In vitro* activities of ketoconazole, econazole, miconazole and *Melaleuca alternifolia* (Tea Tree) oil against *Malassezia* species. Antimicrob. *Agents Chemother*., 44, 467—469.
16. **Kalemba, D., Kunicka, A., 2003:** Antibacterial and antifungal properties of essential oils. *Cur. Med. Chem.*, 10, 813—829.
17. **Kaneko, T., Makimura K., Abe, M., Shiota, R., Nakamura, Y., Kano, R., et al., 2007:** Revised culture-based system for identification of *Malassezia* species. *J. Clin. Microbiol.*, 45, 3737—3742.
18. **Kim, J. Y., Olivry, T., Son, W. G, 2012:** Characteristics of *Malassezia pachydermatis* isolated from dogs and antifungal effect of essential oils. J. *Vet. Clin.*, 29, 141—147.
19. **Mauldin, E. A., Scott, D. W., Miller, W. H., Jr., Smith, C. A., 1997:** *Malassezia* dermatitis in the dog — A retrospective histopathological and immunopathological study of 86 cases (1990—1995). *Vet. Dermatol.*, 7, 191—202.
20. **Nardoni, S., Mugnaini, L., Pistelli, L., Leonardi, M., Sanna, V., Perrucci, S., et al., 2014:** Clinical and mycological evaluation of an herbal antifungal formulation in canine *Malassezia* dermatitis. *J. Mycol. Med.*, 24, 234—240.
21. **Pistelli, L., Mancianti, F., Bertoli, A., Cioni, P. L., Leonardi, M., Pisseri, F., et al., 2012:** Antimycotic activity of some aromatic plants essential oils against canine isolates of *Malassezia pachydermatis*: An *in vitro* assay. *The Open Mycol. J.,* 6, 17—21.
22. **Raut, J. S., Karuppayil, S. M., 2014:** A status review on the medicinal properties of essential oils. *Ind. Crops. Prod.*, 62, 250—264.
23. **Rosato, A., Vitali, C., Gallo, D., Balenzano, L., Mallamaci, R., 2008:** The inhibition of *Candida* species by selected essential oils and their synergism with amphotericin B. *Phytomed.,* 15, 635—638.
24. **Rusenova, N., Parvanov, P., 2009:** Antimicrobial activities of twelve essential oils against microorganisms of veterinary importance. *Trakia J. Sci.*, 7, 37—43.
25. **Váczi, P., Čonková, E., Marcinčáková, D., Sihelská, Z., 2016:** Effectiveness of essential oils on *Malassezia pachydermatis*. *Folia veterinaria*, 59, 12—17.
26. **Verma, R. K., Chaurasia, L., Kumar, M., 2011:** Antifungal activity of essential oils against selected building fungi. *Indian J. Nat. Prod. Resour.*, 2, 448—451.
27. **Weiler, C. B., Kunz de Jesus, F. P., Nardi, G. H., Loreto, E. S., Santurio, J. M., Coutinho S. D. A., et al., 2013:** Susceptibility variation of *Malassezia pachydermatis* to antifungal agents according to isolate source. *Braz. J. Microbiol.*, 44, 174—178.

Received February 27, 2018
Accepted May 15, 2018

sciendo

DOI: 10.2478/fv-2018-0019

FOLIA VETERINARIA, 62, 2: 73—84, 2018

THE LEVEL OF ARSENIC IN WATER FROM MINERAL WATER SPRING GAJDOVKA IN KOŠICE AND THE ASSOCIATED HEALTH RISKS

Hudák, A.[1], Dudová, M.[2], Hudáková, T.[3], Holub, M.[4], Takáč, L.[5]

[1]Department of Chemistry, Biochemistry and Biophysics
[5]Department of the Environment, Veterinary Legislation and Economy
University of Veterinary Medicine and Pharmacy, Komenského 73, 041 81 Košice
[2]Institute of Recycling Technologies, Faculty of Materials, Metallurgy and Recycling
Technical University of Košice, Letná 9, 042 00 Košice
[3]Department of Medical Biology, Faculty of Medicine
Pavol Jozef Šafárik University in Košice, Tr. SNP č.1, 040 11 Košice
[4]Department of Environmental Engineering, Faculty of Civil Engineering
Technical University of Košice, Vysokoškolská 39/4, 042 00 Košice
Slovakia

alexander.hudak@uvlf.sk

ABSTRACT

In the recreation area Anička in Košice, there is a mineral spring that inhabitants call Gajdovka. It has been used with several breaks since the 19th century. Mineral water from this spring is specific by the presence of arsenic the concentration of which often exceeds the permitted limit level. This study focused on the analysis of the mineral composition of the spring water. Chemical and microbiological analysis was made in the years 2013—2015. In 2014, the mineral water Gajdovka was regularly monitored throughout the year with respect to the concentrations of arsenic, iron and hydrogen sulphide levels and water levels in the nearby river. The following mean concentrations were determined: total arsenic 0.063 mg.dm^{-3}; iron 0.275 mg.dm^{-3}; hydrogen sulfide 4.608 mg.dm^{-3}. The concentration of iron was below the limit, while the limit for As(III) was exceeded in 2014 for 7 months. The statistical analysis showed that the season affects significantly the level of H2S and Fe and the water levels in the nearby river.

Key words: arsenic; atomic absorption spectrometry; hydrogen sulphide; iron; mineral water

INTRODUCTION

Water in nature is subjected to constant circulation resulting in changes in its physical and chemical properties. It is enriched by various mineral substances and saturated by gases that change its microbiological properties,

pH and temperature. Of natural waters the mineral water with healing powers is important for humans. Water from many mineral springs have physiological and therapeutic effects and, therefore, they are used for treatments. Slovakia is a country that ranks among the most significant world countries in terms of quantity, capacity and chemical composition of mineral waters. Nowadays, there are more than 1600 sources of mineral and thermal waters of various chemical composition, capacity and temperature in the Slovak territory. In particular regions there are also less known springs used by local residents [2].

One of these lesser known springs is a mineral spring located in the area of Košice in a suburban park named Anička, nearby the river Hornad, which inhabitants call "Gajdovka". It has been known since 1881 when a spa was established at this location. During the First World War it started to become dilapidated. It was restored again later in 1923 and named Gajdove kúpele (Gajda spa) in honour of general Gajda [8, 24]. In the 1960s, the spa and the source of mineral water were closed for hygienic reasons.

In 1995 a new 30-m-deep mineral water well was drilled in this location. This well is used to this day and the spring is very popular with the residents of Košice concerning its availability. Some of them drink the mineral water sporadically during walks in the park. Others, mostly older people, take larger amounts of water home and use it for cooking. The spring is now managed by the Administration of urban green areas in Košice. The monitoring of the quality of this mineral water is executed four times a year by the Regional Public Health Authority based in Košice. This institution monitors the indicators of quality defined by the decree of the Ministry of Agriculture and Rural Development of the Slovak Republic No. 51, of 15 March 2004, as issued in the 25th chapter of the Food Code of the Slovak Republic. The Annex No. 1 of this material defines the microbiological, biological, physical and chemical indicators and demands on mineral water quality [29]. The spring water is also known for the fact that the level of arsenic in this mineral water often exceeds the limit value of arsenic determined by the relevant regulation [4, 5].

Arsenic belongs among the most significant contaminants of the environment with a high potential to harm human health. Arsenic is present in nature in many oxidation states (V, III, 0, -III). In natural waters it is mostly in the As(III) form, as an arsenite anion typical for ground waters with shortage of oxygen. As(V) dominates in surface water in the form of arsenate anions [32]. The less stable As(III) form oxidises easily. In nature, the activity of microorganisms may contribute to changes of inorganic forms of As to volatile or non-volatile organic forms [28]. Some studies reported that the natural background level of arsenic in ground water is 5 $mg.dm^{-3}$ [25]. The most significant factors affecting particular forms of arsenic in the water environment are pH and the oxidation-reduction potential of the environment (Eh) [20, 21].

Inorganic forms of As are more toxic to humans than organic forms [10]. As(III) is organically bound and chemically or biochemically oxidizes to As(V). The As(V) form is more stable under aerobic condition; As(III) is more toxic, it causes chronic diseases and belongs to inhibitors of biochemical oxidation. Many mammals methylate inorganic arsenic to dimethylarsinic acid. This substance causes organ-specific toxicity and acts as a promoter of genesis of tumours in many organs [12]. The International Agency for Research on Cancer (I. A. R. C.) classified arsenic as a Group 1 human carcinogen. This element has carcinogenic, mutagenic and teratogenic effects on humans. Long-term exposure to arsenic can cause severe damage to an organism [19]. Due to its chemical structure, it has similar biochemical properties as phosphorus and can replace it in a certain way. It affects perniciously almost at the DNA level and destroys enzymes and proteins. Many epidemiological studies conducted throughout the world have demonstrated that the human intake of arsenic exceeding the limit value causes degenerative changes in optic and acoustic nerves, painful periphery polyneuropathy, encephalopathy, anaemia and pernicious tumours mainly of skin, kidneys, liver and lungs, leukaemogenesis and lymphoma [1]. Arsenic accumulates in bones, hair and nails. Permanent concentration of arsenic of 100 $mg.dm^{-3}$ is related to 1 : 200 lifelong possibility of the development of tumours that exceeds the annual probability of death due to a tumour disease. An acute toxicity was recorded after drinking water from a well with the arsenic content 1.3—20 $mg.dm^{-3}$ [14].

There are no published expert studies that would give more complex information on the properties of the mineral water from Gajdovka. Arsenic concentrations have been lately sporadically monitored. Moreover, there exists no overview of arsenic levels during the year, nor of potential effects of the seasonal changes, its relationship to particular components of mineral water, or its dependency on water levels in the nearby river Hornád.

This study focused on the determination of selected characteristics of the mineral water "Gajdovka" relevant to the health of its consumers.

CHARACTERISTICS OF THE SPRING

On the basis of the Slovak technical standard STN 86 8000, valid up to 2005, the mineral water from the spring Gajdovka was classified as "natural, low-mineralized, hydrogen carbonate-chloride, calcium-sodium-magnesite, carbonate, sulfuric water, hypotonic, cold (temperature approximately 13 °C) water" [5].

A new well with designation G-5, 30 m deep, of capacity 0.3 dm3.s^{-1} was drilled in 1995. On the basis of the analysis of its chemical composition and other properties, mineral water from this well was characterised as mineral water with deep circulation and long-term retention, metamorphosed, with significant influence of neogene sediments from which the chloride-sodium component of the water is supported. Its mineralisation is related to the solution of sedimentary carbonate rocks. These rocks also contain some iron minerals, such as pyrite (FeS_2) and arsenopyrite (FeAsS). Significant amounts of iron and arsenic comes from the hydrolytic decomposition of the mentioned minerals while free hydrogen sulfide is created. From the facts presented above, it shows that the component influencing the water quality the most is arsenic. After leaving the reduction environment of an original thermodynamic conditions, the contact of mineral water of deep circulation with air starts to eliminate amorphous ferrous sulphides (FeS and Fe2S3) that have adverse effect on the sensorial properties of the water. The listed properties classed the mineral water as healing waters with modified mode of use [13].

The spring is protected by a protective fence to prevent the possibility of its direct pollution and the water is pumped by a submersible pump. The original aroma of fresh water persists for twelve hours after sampling. Unaltered mineral water acquires earthy — petroleum odour 24 hours after sampling. This odour is caused by bacterial strains that survive in deep-circulation mineral waters and are hygienically harmless. Potential turbidity can be caused by the presence of iron in water that does not hinder its consumption [5].

MATERIALS AND METHODS

Sampling and processing of samples

Samples of mineral water for determination of basic indicators according to the Food Code [29] were taken in the years 2013—2015, always in October, and were analysed at the Geoanalytical Laboratory of the State Geological Institute of Dionýz Štúr in Spišská Nová Ves, Slovakia. All sampling vessels were provided by this laboratory.

All vessels intended for collection of samples were thoroughly washed and dried before use. The sample for the determination of mercury was collected in a glass vessel of volume 100 cm^3 containing 1.25 cm^3 of concentrated HNO_3. The sample for the determination of other metals was collected to a polyethylene vessel of volume 250 cm^3 containing 1.25 cm^3 of concentrated HNO_3. For the determination of H_2S, 250 cm^3 of water was collected to a glass vessel that contained 2.5 cm^3 of cadmium acetate of concentration 100 g.dm^{-3} and 1.25 cm^3 of 25 % w/w NaOH solution. To determine the relevant cations and anions, 2 dm^3 of water were collected in a glass vessel. Sample for the determination of the total mineralization of the water was collected in 1 dm3 vessel. Water samples for microbiologic analysis were collected in sterile glass vessels of volume 1 dm^3.

For regular monitoring of the concentrations of arsenic, iron and hydrogen sulfide in mineral water conducted in 2014, the samples were taken once per week, always on Wednesdays in the morning, stabilised and examined after transfer to a laboratory. In total, 51 samples of mineral water were taken and analysed.

To determine the overall mineralisation of water in 2014, 2 separate samples were collected in glass vessels with a volume of 1 dm^3. One sample (1 dm^3) was evaporated in a porcelain dish on a water bath (Sample 1) and another was allowed to evaporate freely at room temperature (Sample 2). The residues (fine crystalline matter) were then used for X-ray diffraction analysis and IR spectrometry.

Analytical methods

The analysis of the chemical composition of mineral water was made at an accredited Geoanalytical Laboratory of the State Geological Institute of Dionýz Štúr in Spišská Nová Ves, according to internal regulations of this laboratory.

X-ray diffraction powder analysis was made with a diffractometer XRD D2 PHASER (Bruker, Germany), using

CuK(α) radiation generated at 10 mA and 30 kV. The measurement was made in a range of 10—90 ° 2 Theta and evaluated by software Diffrac.EVA v. 2.1. To identify the phase, the database ICDD PDF (ICDD PDF-2 Release 2009) was used. Measurement conditions were the same for all samples.

For analysis of the infrared spectra of powder samples, an Alpha FT-IR Spectrometer ALPHA's Platinum ATR single reflection diamond ATR module (Bruker, Germany) was used. To determine particular metals, the methods of atomic emission spectrometry with inductively coupled plasma (AES-ICP), atomic absorption spectrometry with hydride technique (AAS-HG) and atomic absorption spectrometry with mercury analyser (AAS-AMA) were used.

Chlorides and sulphates were determined by ion chromatography (IC), carbonates by volumetric analysis and hydrogen sulfide by photometry.

The monitoring of arsenic and iron concentration during the year 2014 was conducted by the method of atomic absorption spectrometry with an electrothermic atomizer (AAS-ETA) using a SpektrAA 220 (Varian), with Zeeman background correction.

The hydrogen sulfide content in samples was determined by volumetric analysis with iodometric titration. The determination was carried out in triplicate.

The residues after evaporation of two 1 dm3 samples of water (Samples 1 and 2), obtained at determination of mineralization were subjected to X-ray diffraction analysis and IR spectrometry with the collaboration of the Department of Environmental Engineering, Faculty of Civil Engineering, Technical University of Košice.

Microbiological analysis involving 14 parameters was carried out in a microbiological laboratory of the Section of Microbiology and Environmental Biology of the Regional Authority of Public Health in Košice. The methods of membrane filtration and cultivation complied with relevant technical standards.

Information on the level of water in the river Hornád were obtained from the Slovak Water Management Company in Banská Štiavnica, Slovakia [27].

Statistical evaluation

One-way analysis of variance (ANOVA) was used for statistical evaluation of the results. The calculation was performed using Excel. The likelihood of the first type error, referred to as "P-value", was calculated by ANOVA. The effect of the season on the monitored parameters, namely the concentration of arsenic, iron, hydrogen sulphide, and level of water in the Hornad River were evaluated. Correlation between individual parameters was investigated. $P < 0.05$ was considered significant.

RESULTS

The analysis of residues after evaporation of 1 dm^3 of water on water bath and at room temperature (Samples. 1 and 2) showed that the composition of both samples was almost identical. In samples there were identified compounds of $CaCO_3$ (aragonite), NaCl (halite) and Na_2SO_4 (thenardite). In sample 2 also $MgCa(CO_3)_2$ (dolomite) was identified. The results of X-ray powder analysis, completed through the measurement of IR spectra of these samples in the range from 4000 cm^{-1} to 600 cm^{-1} confirmed the presence of anions CO_3^{2-} and SO_4^{2-} appertaining to compounds determined through the previous method in the analysed samples. Repetency assignment of particular absorption bands to inorganic anions was made on the basis of the literature [23]. Typical infrared absorption frequencies characterizing the presence of $(CO_3)^{2-}$ and $(SO_4)^{2-}$ anions in the samples are shown in Table 1.

The results of the analysis of the particular indicators determined at the Geoanalytical Laboratory of the State geological Institute of Dionýz Štúr in Spišská Nová Ves are presented in Table 2.

Table 1. Infrared absorption frequencies

Wavenumber [cm^{-1}]		**Assignment**
Sample No. 1	**Sample No. 2**	
1480.43 s	1480.15 s	$CO3^{2-}$
1421.24 vs	1424.64 vs	$CO3^{2-}$
1113.57 s	1111.27 s	$SO4^{2-}$
881.87 w	877.03 w	$CO3^{2-}$
853.17 vw	855.00 sp	$CO3^{2-}$
667.5 vw	668.29 vw	$SO4^{2-}$
	638.41 sp	$SO4^{2-}$
615.71s	614.76 s	$SO4^{2-}$

vw — very weak; w — weak; s — strong; vs — very strong; sp — sharp

Table 2. Determination of inorganic indicators in mineral water "Gajdovka" in the period of 2013—2015

Indicator	Limit [29] [mg.dm^{-3}]	Concentration [mg.dm^{-3}]			LOQ [mg.dm^{-3}]	Method
		2013	2014	2015		
Na	**800.0**	379 ± 37.9	364 ± 36.4	260 ± 26	0.05	AES-ICP
K	**–**	27.0 ± 2.7	25.4 ± 2.54	30.5 ± 3.05	0.1	AES-ICP
Ca	**≥ 20.0**	284 ± 19.9	264 ± 18.5	264 ± 18.5	0.2	AES-ICP
Mg	**200.0**	143 ± 10.0	115 ± 8.0	116 ± 8.12	0.2	AES-ICP
Fe	**10.0**	0.210 ± 0.021	0. 114 ± 0. 011	0.255 ± 0.026	0.007	AES-ICP
Mn	**2.0**	0.267 ± 0.04	0.250 ± 0.038	0.249 ± 0.037	0.002	AES-ICP
Al	**0.4**	0.04 ± 0.008	0. 0 ± 0.02	0.05 ± 0.01	0.02	AES-ICP
Cu	**2.0**	< 0.002	< 2.0	< 2.0	2.0	AES-ICP
Zn	**5.0**	0.003 ± 0.0006	< 0.002	< 0.002	0.002	AES-ICP
As (total)	**0.05 As(III)**	0.089 ± 0.009	0.073 ± 0.007	0.071 ± 0007	0.001	AAS
Cd	**0.003**	< 0.0003	< 0.0003	< 0.0003	0.0003	AES-ICP
Pb	**0.01**	< 0.005	< 0.005	< 0,005	0.005	AES-ICP
Cr	**0.05**	< 0.002	< 0.002	< 0.002	0.002	AES-ICP
Hg	**0.001**	< 0.0001	< 0,0001	< 0.0001	< 0.0001	AAS
H2S	**–**	4.39 ± 0.88	4.20 ± 0.84	5.27±1.05	0.01	P
Cl-	**500.0**	415 ± 20.8	406 ± 20.3	302 ± 15.1	1.0	IC
(CO3)2-	**–**	< 0.3	< 0.3	< 0.3	0.3	OA
(SO4)2-	**1 400.0**	255 ± 12.8	214 ± 10.7	218 ± 10.9	2.0	IC

LOQ — limit of quantification; IC — ion chromatography; AES-ICP — atomic emission spectrometry with inductively coupled plasma
AAS — atomic absorption spectrometry; OA — volumetric analysis; P — photometry

The determination of the total mineralization of water showed that the residue after evaporation in individual years was as follows: 2013: 2.548 g.dm^{-3}; 2014: 2.653 g.dm^{-3} and 2015: 2.629 g.dm^{-3}. The average weight of the residue was 2.610 g.

Microbiological analysis that focused on 14 indicators showed an absence of pathogenic microorganisms and indicators of faecal contamination. The water complied with relevant requirements. The monitored indicators, type of the method used (standard) and relevant results are summarised in Table 3.

The monitoring of the concentrations of arsenic, iron and hydrogen sulphide conducted throughout the year 2014 was conducted to determine variations in arsenic concentrations in mineral water throughout the year and to investigate the potential relationship between the concentrations of arsenic, iron and hydrogen sulfide. The levels of the river Hornád was monitored as another factor with possible influence on arsenic concentration in mineral water "Gajdovka". The results are presented in Tables 4a and 4b.

The minimal, maximal and average values of the concentrations of the analytes are presented in Table 5.

The average concentrations of arsenic in mineral water in particular months are presented in Table 6.

DISCUSSION

Arsenic usually gets into the environment in a natural way as the product of decomposition of minerals that

Table 3. Microbiological analysis of mineral water "Gajdovka" in 2014

Indicator	Unit/volume tested	Result	Type of method	Technical standard
Pathogenic microorganisms		not present	MF	STN ISO 6340
Escherichia coli	CFU/250 ml	0	MF	STN EN ISO 9308-1
Coliform bacteria	CFU/250 ml	0	MF	STN EN ISO 9308-1
Enterococci	CFU/250 ml	0	MF	STN EN ISO 7899-2
Pseudomonas aeruginosa	CFU/250 ml	0	MF	STN EN ISO 16266
Sporebearing sulphites reducing the anaerobic bacteria	CFU/50 ml	0	MF	STN EN 26461-2
Microorganisms cultivable at 21 °C ± 1 °C	CFU/1 ml	0	C	STN EN ISO 6222
Microorganisms cultivable at 37 °C ± 1 °C	CFU/1 ml	0	C	STN EN ISO 6222
Living organisms	individuals/ml	0	M	STN 757711
Dead organisms	individuals/ml	0	M	STN 757711
Ferrous and manganese bacteria	% coverage of the field of view	0	M	STN 757711
Ferrous and manganese bacteria	CFU/30 ml	not present	C	
Sulphur green bacteria	CFU/30 ml	not present	C	
Microscopic fungi (micromycetes)	individuals/ml	0	M	

C — cultivation method; MF — membrane filtration; M — microscopic method; CFU — colony forming unit

contain it, or through emissions from coal combustion, ore processing, extracts from sludge beds, mining piles and old mines. The most significant source of the contamination of ground water by arsenic are pit water flowing out of old mining works or water flowing from mining piles [31]. In the case of weathering of arsenopyrite containing mining mullock, the concentrations of arsenic in ground water may result in high local levels. As an example, we can mention the abandoned mine deposit Poproč, located near Košice. In this location the important source of contamination is the pit water from swamps named Agnes with a high concentration of arsenic (2.4 mg.dm^{-3}) and antimony (0.6 mg.dm^{-3}) [7]. Loredo et al. [22] stated that the concentration found in one mining location in Spain ranged from 4.1 to 5.6 mg.dm^{-3} of As. Arsenic is also part of some insecticides, phosphate fertilizers and detergents [6].

Nowadays, great attention is given to the issue of arsenic presence mainly in connection with contamination of drinking water and its sources [26]. In the past, the allowable arsenic concentration in drinking water was 50 mg.dm^{-3}. In 1993, WHO decreased this value to 10 mg.dm^{-3} on the basis of long-tern epidemiological studies. In Slovakia, the Regulation of the Government of the Slovak Republic No. 354/2006 of the Collection defines the requirements for water intended for human consumption and for quality check of this water. According to this regulation, the limit value of arsenic in drinking water is 10 mg.dm^{-3}. Observation of this limit can cause problems in some regions of Slovakia. It concerns especially the locations where the public water supplies are ground sources with higher content of arsenic that comes from the geological background. This results in the increased level of arsenic in drinking water, e. g. in Pohronský Bukovec in 2009 [15], in artesian wells in districts Nové Zámky and Šaľa in 2010 [11] and, unexpectedly, also in municipality Brehov in the district of Trebišov in 2015 [16]. In the last case, increased arsenic in ground water was probably related to andesite mining in this area.

Higher concentrations of arsenic in spring and min-

Table 4a. Levels of hydrogen sulfide, total arsenic and iron in mineral water in the period of January — June, 2014

Date of sampling month/day	H_2S [mg.dm^{-3}]	As (total) [mg.dm^{-3}]	Fe [mg.dm^{-3}]	Height of the river Hornád (cm)
1/18	5.49 ± 0.66	0.031 ± 0. 008	0.34 ± 0.04	103
1/15	4.61 ± 0.55	0.052 ± 0.013	0.45 ± 0.05	97
1/22	5.83 ± 0.70	0.120 ± 0.030	0.36 ± 0.04	112
1/29	5.03 ± 0.60	0.110 ± 0.028	0.49 ± 0.06	111
2/5	4.52 ± 0.54	0.032 ± 0.008	0.41 ± 0.05	111
2/12	6.43 ± 0.77	0.053 ± 0.013	0.42 ± 0.05	119
2/19	4.10 ± 0.49	0.057 ± 0.014	0.40 ± 0.05	139
2/26	5.14 ± 0.62	0.140 ± 0.035	0.32 ± 0.04	120
3/5	5.97 ± 0.72	0.056 ± 0.014	1.19 ± 0.12	113
3/12	5.70 ± 0.68	0.081 ± 0.020	0.28 ± 0.04	104
3/19	5.75 ± 0.69	0.089 ± 0.022	0.22 ± 0.03	112
3/26	5.41 ± 0.65	0.041 ± 0.010	0.24 ± 0.03	110
4/2	5.39 ± 0.65	0.049 ± 0.012	0.26 ± 0.03	108
4/9	5.19 ± 0.62	0.061 ± 0.015	0.20 ± 0.03	112
4/16	5.06 ± 0.61	0.062 ± 0.015	0.25 ± 0.03	110
4/23	4.87 ± 0.58	0.039 ± 0.009	0.17 ± 0.02	106
4/30	4.90 ± 0.59	0.043 ± 0.011	0.23 ± 0.03	118
5/7	4.64 ± 0.56	0.063 ± 0.016	0.25 ± 0.03	114
5/14	5.20 ± 0.62	0.055 ± 0.014	0.24 ± 0.03	188
5/21	6.92 ± 0.83	0.058 ± 0.015	0.23 ± 0.03	184
5/28	5.94 ± 0.71	0.058 ± 0.015	0.23 ± 0.03	188
6/4	4.25 ± 0.51	0.052 ± 0.013	0.35 ± 0.04	117
6/11	2.31 ± 0.28	0.050 ± 0.013	0.14 ± 0.02	113
6/18	1.13 ± 0.14	0.053 ± 0.013	0.24 ± 0.03	104
6/25	3.18 ± 0.36	0.061 ± 0.015	0.44 ± 0.05	106

eral waters do not occur frequently. Water considered to be mineral water is defined in Chapter 25 of the Food Code as clear, colourless to yellowy water, with mild silt content, free of mechanical impurities. It cannot have atypical sensory properties and must have stable chemical composition and stable physical properties [29]. Mineral water must meet the microbiological, biological, physical and chemical indicators of quality listed in the Food Code. In this material the highest limit values (HLV) for particular indicators are listed. HLV for As(III) in mineral water is 0.05 mg.dm^{-3}.

Mineral water Gajdovka was subject to chemical and microbiological analysis in accredited laboratories in the years 2013 to 2015, always in October. The average overall mineralisation was 2.610 g.dm^{-3}. This value is very close to the level of 2.646 g.dm^{-3} determined in 1996 [13]. Regarding the concentrations of particular indicators involved in mineralisation (Na, K, Ca, Mg, Fe, Cl^-, SO_4^{2-}), the biggest changes were observed in the levels of sodium (379 mg. dm^{-3} in 2013; 364 mg.dm^{-3} in 2014; 260 mg.dm^{-3} in 2015), iron (0.210; 0.114; 0.255 mg dm^{-3}) and chlorides (415; 406;

Table 4b. Levels of hydrogen sulfide, total arsenic and iron in mineral water in the period of July — December, 2014

Date of sampling month/day	H_2S [mg.dm^{-3}]	As (total) [mg.dm^{-3}]	Fe [mg.dm^{-3}]	Height of the river Hornád [cm]
7/2	2.92 ± 0.35	0.038 ± 0.010	0.22 ± 0.03	125
7/9	3.35 ± 0.40	0.050 ± 0.013	0.21 ± 0.03	145
7/16	4.39 ± 0.53	0.052 ± 0.013	0.18 ± 0.03	160
7/23	4.92 ± 0.59	0.040 ± 0.010	0.15 ± 0.02	145
7/30	4.53 ± 0.54	0.064 ± 0.016	0.09 ± 0.01	156
7/31	5.69 ± 0.68	0.040 ± 0.010	0.10 ± 0.01	154
8/6	4.80 ± 0.58	0.060 ± 0.015	0.15 ± 0.02	122
8/13	4.17 ± 0.50	0.066 ± 0.017	0.15 ± 0.02	138
8/20	3.93 ± 0.47	0.064 ± 0.016	0.15 ± 0.02	136
8/27	4.21 ± 0.50	0.064 ± 0.016	0.14 ± 0.02	125
9/3	4.62 ± 0.55	0.066 ± 0.017	0.18 ± 0.03	132
9/10	3.94 ± 0.47	0.041 ± 0.010	0.29 ± 0.04	133
9/17	4.20 ± 0.50	0.047 ± 0.011	0.30 ± 0.04	114
9/24	5.14 ± 0.62	0.062 ± 0.016	0.23 ± 0.03	115
9/30	4.00 ± 0.48	0.052 ± 0.013	0.18 ± 0.03	104
10/1	4.20 ± 0.50	0.055 ± 0.014	0.14 ± 0.02	104
10/8	3.55 ± 0.43	0.094 ± 0.024	0.19 ± 0.03	112
10/15	3.87 ± 0.46	0.055 ± 0.014	0.18 ± 0.03	99
10/22	3.66 ± 0.44	0.058 ± 0.015	0.18 ± 0.03	132
10/29	3.59 ± 0.43	0.067 ± 0.017	0.28 ± 0 04	135
11/5	4.51 ± 0.54	0.063 ± 0.016	0.19 ± 0.03	133
11/12	4.02 ± 0.48	0.100 ± 0.025	0.20 ± 0.03	118
11/19	5.03 ± 0.60	0.098 ± 0.024	0.30 ± 0.04	112
11/26	4.88 ± 0.59	0.052 ± 0.013	0.33 ± 0.05	116
12/3	4.99 ± 0.60	0.081 ± 0.020	0.46 ± 0.06	113
12/10	4.93 ± 0.59	0.140 ± 0.035	0.˝53 ± 0.06	109

Table 5. Minimal, maximal and average values of the indicators monitored in 2014

Indicator	Unit	Value		
		Minimal	Maximal	Average
Arsenic (As) (total)	mg.dm^{-3}	0.031	0.140	0.063
Iron (Fe)	mg.dm^{-3}	0.090	1.190	0.275
Hydrogen sulfide (H_2S)	mg.dm^{-3}	1.130	6.920	4.608

Table 6. Average concentrations of total arsenic and calculated concentration of As(III) in the particular months of 2014 and comparison with the limit value (0.05 mg.dm-3)

Month	Average value total As [mg.dm^{-3}]	80—90 % As(III) [mg.dm^{-3}]	Limit overload [%]
January	0.078	0.063—0.070	26—40
February	0.071	0.057—0.064	14—28
March	0.067	0.054—0.060	8—20
April	0.051	0.041—0.046	< limit
May	0.059	0.047—0.053	0—6
June	0.054	0.043—0.049	< limit
July	0.047	0.038—0.042	< limit
August	0.064	0.052—0.058	4—16
September	0.054	0.043—0.049	< limit
October	0.066	0.053—0.059	6—18
November	0.078	0.062—0.070	24—40
December	0.110	0.088—0.099	76—98

302 mg.dm^{-3}). Relatively little changes were observed in the case of calcium, magnesium, arsenic and sulphates (Table 2). Table 2 presents also the limit values for individual inorganic parameters. Except for arsenic, neither indicator exceeded the limit value set by the Food Code [27].

The results of microbiological analysis presented in Table 3 showed an absence of any determined pathogenic microorganisms in the mineral water in the monitored years.

The relevant Food Code (Third part, Chapter 25, Annex No. 1: Quality indicators for table water, infant water and mineral water) states that the limit value for arsenic content in mineral water is 0.05 mg.dm^{-3} As(III) and this is not the value of overall arsenic. The concern is obvious — As(III) is 25 to 60 times more toxic than As(V) [9]. The AAS method used for determination of As can be used only for determination of total arsenic in water samples. Thus, the results obtained in this study characterise the concentration of total arsenic in mineral water. Under anaerobic conditions of ground mineral water, the form As(III) prevails. Under aerobic or oxidising conditions, the As(III) form oxidizes easily to As(V). The analyses of ground water showed that the share of As(III) is 80 to 90 % in overall content of arsenic [11]. When we used this proportion to calculate As(III) from total arsenic, the limit value was exceeded during seven months of the year 2014, i. e. during January to March, August, and October to December (Table 6). Thus, the mineral water met the prescribed limit value for arsenic content during 5 months in the year. These months were mostly the summer months. The arsenic content of mineral water determined in the Geoanalytical Laboratory in 2013—2015, converted to As (III), also indicated that the limit value was exceeded (2013—0.071; 2014—0.058; 2015—0.057 mg. dm^{-3}).

The influence of the seasons on the monitored parameters (H_2S, arsenic, iron and the level of river Hornád) was investigated by one-way ANOVA. The results were divided into four groups according to four seasons, to be specific January—March, April—June, July—September, October—December. Significant differences between seasons were observed for parameters H_2S, Fe and the level of river Hornád ($P < 0.05$ for H_2S and the level of river; $P < 0.001$ for Fe). No significant differences were observed for arsenic. No correlation between particular indicators were detected.

Except for some periods of different length, the mineral spring Gajdovka was used from the second half of the 19th century to 1920s. The spring was often closed because the water did not comply with the hygiene criteria. The modern history of this spring started in 1995 when 30-metres deep new well, designated G-5, was drilled. This well with capacity of 0.3 litres per second is used up to this day.

The problem with arsenic in mineral water persisted until 2006 when technology based on sorbent BAYOXIDE E33 was introduced. The arsenic content was decreased significantly but the water quality was also changed. The average concentration of overall arsenic in finished water was 0.0108 mg dm^{-3} in 2006—2008 [5]. However, water was became excessively enriched with iron and precipitation of its oxides and hydroxides occurred. The characteristic hydrogen sulfide smell disappeared. This was the reason why this technology was abandoned in 2009 [5]. Due to the interest of the public in the spring, the mineral water was treated by mixing mineral water with drinking water. The drinking water source is located in the gravel floodplains of the river Hornad near the Gajdovka spring [13]. Chemical composition of this drinking water shows that it is the basic calcium-magnesium-hydrogen carbonate type. Mineral water and drinking water are mixed at a ratio 1 : 1 (v/v). This way diluted mineral water is supplied to the public.

However, the problems with exceeding the limit value of arsenic content in mineral water still persist. Dietzová et al. [5] estimated the health hazard for children and adults presented by mineral water containing arsenic. Model calculations were made according to the methodology US EPA [30]. The daily consumption of 0.3 dm^3 by children and 1 dm^3 by adults do not lead to exceeding the recommended reference dose of arsenic (RfD: 3.0×10^{-4} mg.kg^{-1} of mass per day). The risk of consumption of arsenic in mineral water from Gajdovka spring is thus acceptable when the water is consumed irregularly and the volume consumed does not exceed the recommended amount [5]. Spring visitors are informed about the recommended amounts of consumed mineral water by means of information tables located near the withdrawal point.

There are only few mineral waters in Slovakia with chemical composition and properties similar to "Gajdovka". The arsenic problem is relevant also to other springs. The springs in Gánovce (Filice), Hôrka and Čenčice in district Poprad belong among the mineral springs with repeatedly determined excess arsenic values [17]. Water in these locations can be used in small amounts. The problem with arsenic can arise when water from these springs are commonly used for drinking.

The presence of arsenic in ground water in the Košice surroundings is not rare. Three geothermal wells with designation GTD-1 to 3 were made near the municipality of Ďurkov in the years 1998—1999. These wells are 2252 m, more than 3210 and 3151 metres deep. The temperature at well head in particular wells is 123—125 °C. Geothermal water of the structure Ďurkov is a complex water-steam-solid phase system. The value of its mineralisation ranges from 25 to 32.dm^{-3}. This geothermal water has distinct characteristics of Na-Cl type with low representation of substance Na-HCO_3. Of all trace metals arsenic is found in the highest concentration in geothermal water. The maximal concentration was determined to be 36 mg.dm^{-3}. The main source of the high level of arsenic is considered to be the neovulcanites of mountain range Slánske vrchy. At convenient geochemical conditions, arsenic is able to pass to water solution from arsenopyrite at the presence of pyrite, as salty water is capable of dissolving these minerals, it is even by solving of these minerals by salt water [3]. High content of arsenic in geothermal water presents a big risk of environmental contamination.

The most known mineral water containing arsenic in the Czech Republic is "Bělovesská kyselka" near Náchod that was very popular in the past and was known under the name of "IDA". Arsenic concentration in water from this spring reached 1 mg.dm^{-3} [18]. Unlike the spring Gajdovka, its mineralisation is lower (950 mg.dm^{-3}) and it has a balanced concentration of Na, Mg, Ca and sulphates, with low content of iron and, on the contrary, high content of CO_2. Considering the high content of arsenic, this mineral water is not suitable for permanent consumption. The analyses of water in 2015 showed that concentration of arsenic in source IDA was 0.479 mg.dm^{-3}. After the water was treated by means of a device for elimination of arsenic, the mineral water IDA used today contains less than 0.01 mg.dm^{-3} of arsenic. Near Náchod, in Hronov, there are another two arsenic containing mineral springs. These springs are similar to Gajdovka in many aspects. The water is strongly mineralised (2 g.dm^{-3}) with a high content of CO_2 and with significant share of iron and hydrogen sulfide. The springs in Náchod and Hronov are the only arsenic containing mineral waters in the Czech Republic [18].

CONCLUSIONS

Mineral water Gajdovka is very popular among the inhabitants of Košice. Therefore, the monitoring of its quality is important. Particularly problematic is the content of arsenic, which is one of the toxic elements and can endanger

human health when consumed regularly. The results of the determination of arsenic in mineral water throughout the year 2014 confirmed that its concentration changes during a calendar year and is often at or above the limit set by relevant regulations. When calculating the As(III) form from the total arsenic it was found that the limit value was exceeded during seven months of the monitored year, i.e. in January to March, August, and October to December. The limit concentration for the iron content, which influences the sensory quality of mineral water, was not exceeded during this year. Statistical analysis of the monitored parameters, namely the concentration of arsenic, iron and hydrogen sulphide and the level of the river Hornad, showed that the season influences the content of iron, hydrogen sulfide and the level of the river Hornad but not the level of arsenic. No correlation between the individual monitored parameters was observed. With regard to the arsenic content, the Regional Public Health Authority based in Košice adopted certain rules for the consumption of mineral water Gajdovka. These rules are posted at the delivery point and indicate the recommendations for the use of this mineral water.

ACKNOWLEDGEMENT

This study was supported by the Slovak Grant Agency for Science (Grant No. 1/0563/15).

REFERENCES

1. **ATSDR — Agency for Toxic Substances and Disease Registry, 2007:** Toxicological profile for arsenic. *U. S. Department of Health and Human Services Public Health Service*. Division of Toxicology and Environmental Medicine/Applied Toxicology Branch 1600, Clifton Road NE Mailstop F-32 Atlanta, Georgia, 30333.
2. **Bodiš, D., Kordík, J., Slaninka, I., Malík, P., Liščák, P., Panák, D., et al., 2010:** Mineral waters in Slovakia — evaluation of chemical composition stability using both historical records and the most recent data. *Journal of Geochemical Exploration*, 107, 382—390.
3. **Bodiš, D., Vranovská, A., 2012:** Genesis of anomalous arsenic content in the Ďurkov hydro-geothermal structure (In Slovak). *Podzemná voda* (Groundwater), 18, 123—136.
4. **Dietzová, Z., Bratská, Z., 2010:** Estimation of health risk from water consumption from the freely accessible spring water in Košice (In Slovak). In *Environment and Health*. Proceedings of Scientific Work, Bratislava, 25—30.
5. **Dietzová, Z., Labancová, J., Bratská, Z., 2012:** Is the health risk from arsenic in a freely accessible mineral spring in Kosice acceptable? (In Slovak). *Using Experimental Methods to Protect the Health of the Population and the Environment*. Reviewed Proceedings of Scientific Works, Košice, 32—37.
6. **Ďurža, O., Khun, M., 2002:** *Environmental Geochemistry of Heavy Metals* (In Slovak). Faculty of Natural Sciences, UK Bratislava, 116 pp.
7. **Fľaková, R., Ženišová, Z., Jašová, I., Krčmář, D., 2009:** Water contamination with arsenic and antimony in abandoned deposit Poproč (In Slovak). *Podzemná voda* (Groundwater), 15, 132—148.
8. **Gajda spa:** http://gajdovka.webnode.sk/gajdove-kupele/www.cassovia.sk/zony/anicka.php3. (In Slovak). Accessed Nov. 15, 2017).
9. **Gürkan, R., Kir, U., Altunay, N., 2015:** Development of a simple, sensitive and inexpensive ion — pairing cloud point extraction approach for the determination of trace inorganic arsenic species in spring water, beverage and rice samples by UV-Vis spectrophotometry. *Food Chemistry*, doi:10.1016/j.foodchem.2015.01.142. Accessed Feb. 2, 2018.
10. **Hagarová, I., Žemberyová, M., 2005:** Determination of arsenic in biological and environmental samples by AAS techniques (In Slovak). *Chemické Listy* (Chemical Letters), 99, 578—584.
11. **Hegedűsová, A., Pavlík, V., Hegedűs O., 2010:** The occurrence of arsenic in artesian wells of selected sites (In Slovak). *Acta Universitatis Matthiae Bell*i, Ser. Chem., 12, 81—86.
12. **Hughes, M. F., Razo, L. M., Kenyon, N. E. M., 2000:** Dose dependent effects on tissue distribution and metabolism of dimethylarsinic acid in the mouse after intravenous administration. *Toxicology*, 143, 155—166.
13. **Hydrogeochemical report, 1996:** Košice-Anicka-hydrogeochemical evaluation min. water in G-5 borehole. 035/96. Geoconzult a.s.
14. https://euroclean.sk/slovnik-sk/arsen-ve-vode-jeho-odstraneni/ (In Slovak). Accessed Feb. 2, 2018.
15. http://www.topky.sk/cl/10/568940/V-pitnej-vode-v-Pohronskom-Bukovci-nasli-arzen (In Slovak). Accessed Feb. 2, 2018.
16. http://vysetrenie.zoznam.sk/cl/1000663/1470313/Slovaci-v-ohrozeni--Zakazane-pitie-vody-z-vodovodu--obsahuje-nebezpecny-arzen (In Slovak). Accessed Feb. 2, 2018.

17. https://spis.korzar.sme.sk/c/5596015/pramene-v-okoli-ganoviec-maju-vyssi-obsah-arzenu.html. (In Slovak). Accessed Feb. 2, 2018.

18. http://www.putujici.cz/?p=p_354&sName=Prameny-plne-arzenu. (In Slovak). Accessed Feb. 2, 2018.

19. IARC—International Agency for Research on Cancer, 1980: IARC monographs on the evaluation of the carcinogenic risk of chemicals to humans, Vol. 20, *Some Metals and Metallic Compounds*, IARC Lyon, 39—140.

20. Jurkovič, Ľ., Hiller, E., Slaninka, I., Kordík, J., Majzlan, J., 2006: *Geochemical Study of Contaminated River Sediments and Surface Waters and Experimental Assessment of Mobility As* (the catchment area of the Kyjov and Ondava stream, Poša wasteland, eastern Slovakia) (In Slovak). Workshop BO. http://www.banskeodpady.sk/files/Jurkovic%20et%20al%202006_Worshop%20BO. pdf. Accessed Nov. 15, 2017.

21. Jurkovič, L., Kordik, J., Slaninka, I., 2006: Geochemical study of arsenic mobility insecondarily influenced Kyjov Brook and Ondava River (Eastern Slovakia). *Slovak Geological Magazine*, 12, 31—38.

22. Loredo, J., Ordóñez, A., Baldo, C. and García-Iglesias, J., 2003: Arsenic mobilization from waste piles of the El Terronal mine, Asturias, Spain. *J. Geochemistry: Exploration, Environment, Analysis*, 3, 229—237.

23. Milata, V., Segľa, P., Gatial, A., Šima, J., Kováčik, V., 2009: *Spectral Tables for Solving Problems and Problems in Molecular Spectroscopy* (In Slovak). STU, Bratislava, 90 pp. http://www.banskeodpady.sk/files/Jurkovic%20et%20al%202006_Worshop%20BO.pdf. Accessed Nov. 15, 2017.

24. Piroš, A., 1999: Was Anna the pub owner ? *Cassovia.sk:* http://www.cassovia.sk/zony/anicka.php3. Accessed Nov. 15, 2017.

25. Pitter, P., 1999: *Hydrochemie* (In Czech). 3rd rev., Prague, Higher School of Chemical Technology, 568 pp.

26. Rapant, S., Krčmová, K., 2006: Potential health risk of arsenic contamination of groundwater of the Slovak. *Mineralia Slovaca*, 38, 29—36.

27. Slovak Water Management Company, 2014: *Measured Curve, Water Hornad-Kysak, Water Conditions 2014* (In Slovak). Banská Šiavnica.

28. Ševc, J., Čerňanský, S., 2003: Microbial methylation as a part of transformation processes and migration of arsenic under natural conditions. *Phytopedon* (Bratislava), 2, 60—68.

29. State Veterinary and Food Administration SR: Table: Water quality indicators, infant water and mineral water. In *Food Code* (updated on Jan. 31, 2017). Part III, Chapter 25, Appendix No. 1. http://www.svssr.sk/legislativa/kodex_03_25_01 asp. Accessed Nov. 15, 2017.

30. US EPA Integrated Risk Information *System, 1998: Risk Assesment-Multipathway Exposure*. Risksoft 2,0 /software/.

31. Ženišová, Z., Fľaková, R., Jašová, I. Cicmanová, S., 2009: Antimony and arsenic in waters affected by mining activities in selected areas of Slovakia (In Slovak). *Podzemná voda* (Groundwater), 15, 100—117. https://doi.org/10.1144/1467-7873/03-003. Accessed Nov. 15, 2017.

32. Žemberyová, M., Chromá, O., Shearman, A., Hagarová, I., 2007: Speciation of chromium and inorganic arsenic in waters using solid phase extraction and atomic absorption spectrometry (In Slovak). *Chemické Listy* (Chemical Letters), 101, 303—309.

Received March 15, 2018
Accepted May 15, 2018

sciendo

DOI: 10.2478/fv-2018-0020

FOLIA VETERINARIA, 62, 2: 85—91, 2018

INTERACTION OF THE FUNGICIDE TEBUCONAZOLE WITH HUMAN SERUM ALBUMIN: A PRELIMINARY STUDY

Staničová, J.[1, 3], Želonková, K.[1], Verebová, V.[1], Holečková, B.[2], Dianovský, J.[2]

[1]Institute of Biophysics
[2]Institute of Genetics
University of Veterinary Medicine and Pharmacy, Komenského 73, 041 81 Košice
Slovakia
[3]Institute of Biophysics and Informatics, First Faculty of Medicine, Charles University, Kateřinská 1, Praha
Czechia

jana.stanicova@uvlf.sk

ABSTRACT

The interactions between the fungicide tebuconazole and human serum albumin were investigated using fluorescence and circular dichroism spectroscopies. The experimental results showed that the fluorescence quenching of the protein by the tebuconazole molecule was a result of the formation of a ligand-protein complex with a binding constant of 8.51×10^3 l.mol^{-1} and the number of binding sites in the macromolecule was close to 1. These findings demonstrated the fact that although the binding affinity of tebuconazole to the protein may be slight, it was very similar to other triazole fungicides. In addition, tebuconazole stabilized the α-helical secondary structure of the human serum albumin due to the increase of the α-content in the protein macromolecule.

Key words: association constant; fluorescence spectroscopy; human serum albumin; interaction; tebuconazole

INTRODUCTION

Tebuconazole [1-(4-chlorophenyl)-4,4-dimethyl 3-(1,2,4-triazol-1-ylmethyl) pentan-3-ol] (Fig. 1) is a representative of triazoles that are a class of fungicides largely used in agriculture as crop protection products [3]. Their antifungal activity is due to their ability to inhibit the P450 enzyme, which blocks the conversion of lanosterol to ergosterol causing disruption of the fungal cellular wall [5]. But the inhibition potency of these triazole fungicides including tebuconazole (TB) is not limited to fungi; they may also inhibit other P450-mediated activities resulting in various adverse effects [21].

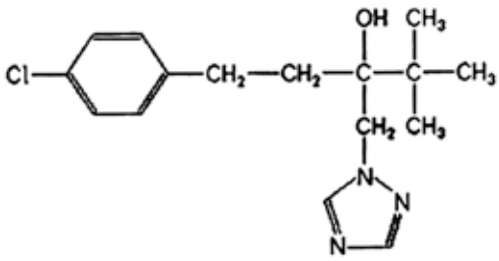

Fig. 1. The chemical structure of tebuconazole

TB is the triazole fungicide, which is applied on a number of crops such as grapes, rice, fruits, and vegetables because of its broad-spectrum antifungal activity. This fungicide had been classified by the US EPA as Group C-Possible Human Carcinogen [27]. TB is persistent in soils and presents moderate mobility [6]. It is classified as toxic to aquatic organisms and may cause long-term adverse effects in the aquatic environment [2]. The presence of TB in stream water has increased in recent years [18] and its concentrations detected in surface waters were up to 175—200 $\mu g.l^{-1}$ [7]. The results obtained by Liang et al. [17] indicated that exposure to TB could alter thyroid hormone levels as well as gene transcription in zebrafish larvae. Commercial formula Orius 25EW containing 25 % of tebuconazole applied in agriculture as a leaf and ear spray pesticide has been studied by Holečková et al. [12]. In this study, significant chromosomal aberrations in lymphocytes induced by the fungicide were discovered. Furthermore, TB-based fungicide induces sister chromatid exchange in bovine peripheral lymphocytes [26]. What's more, TB was found in human beings with the maximal concentrations of 19.2 $\mu g.l^{-1}$ and 2.22 $ng.kg^{-1}$ in urine and hair samples, respectively, from farm workers [9, 22].

In fact, because so little is known about the long-term toxicity of TB and other triazoles to vertebrates at this time, it is not possible to ascertain whether these molecules present a risk for mammalians chronically exposed to low doses. As a consequence, preliminary studies of interactions, in a broad sense, between TB and several proteins of interest, are one of the necessary steps toward an increased understanding of TB's toxicity on mammalians.

Human serum albumin (HSA) is the most abundant plasma protein and contributes significantly to many transport and regulatory processes. It forms about 60 % of the mass of human plasma proteins with a typical concentration of 40 $mg.ml^{-1}$ in the bloodstream [24, 10]. The protein binds to a wide variety of substrates such as metals, fatty acids, amino acids, hormones and an impressive spectrum of drugs [19].

Recently, several studies have been carried out to examine the toxic effects of pesticides at the protein level [23, 4, 32, 30] but information about the possible impact of triazoles on plasma proteins is still limited [29, 34]. At the same time, a binding of pesticides including triazoles to plasma proteins has toxicological importance as it can significantly affect their distribution and excretion in the organism [25]. When these fungicides penetrate into the bloodstream, they may bind to plasma proteins and subsequently induce some alternations of the protein structure and function.

The aim of this study was to obtain additional information about the interactive properties of TB in relation to plasma proteins with regard to the above mentioned frequent application of TB as a pesticide. These results may provide basic data for clarifying the binding mechanisms of TB with HSA and be helpful for food security and human health when TB is applied as an antifungal agent. Fluorescence and far UV circular dichroism spectroscopy (far UV CD) were used for a determination of the binding constant, mode of interaction between TB and human serum albumin molecules, and the effect of fungicide on the secondary structure of the HSA molecule.

MATERIALS AND METHODS

Tebuconazole (CAS Number 107534-96-3) was obtained from Sigma, and its grade was analytical standard. HSA (fatty acids free, globulin free, purity no less than 99 %) was purchased from Sigma and was used without further purification. To prepare stock solutions, TB was dissolved in 100 % ethanol in a concentration of 10^{-3} $mol.l^{-1}$ and a stock solution of HSA (concentration 5×10^{-4} $mol.l^{-1}$) was prepared in Tris-HCl (0.05 $mol.l^{-1}$ Tris + 0.1 $mol.l^{-1}$ NaCl) buffer, pH 7.4. Phosphate buffer (0.02 $mol.l^{-1}$, pH 7.4) was used for the CD spectroscopic measurements. Tris(hydroxymethyl)aminomethane, NaCl, HCl, and other reagents were all of analytical purity.

Fluorescence measurements were performed using a spectrofluorometer SHIMADZU RF 5301 PC in 1 cm quartz cuvette. The excitation wavelength was 295 nm and fluorescence was collected at 300—500 nm emission wavelengths using 5 nm/5 nm slits.

Complexes of TB/HSA for fluorescence spectroscopy were prepared by titration of TB into 2×10^{-6} $mol.l^{-1}$ HSA to have a final concentration of TB from 2×10^{-6} $mol.l^{-1}$ to 32×10^{-6} $mol.l^{-1}$.

Far UV CD spectroscopy experiments were carried out by means of a CD spectrometer Jasco J-815 in 0.1 cm quartz cuvette at room temperature and constant nitrogen flush. The spectra of HSA in the presence of TB were recorded in the range 200—270 nm with a scan rate of 50 $nm.min^{-1}$.

Three scans were accumulated for each spectrum, taking the average as the final data.

Complexes of TB/HSA for CD spectroscopy were prepared by the titration of TB into 3.75×10^{-6} mol.l^{-1} HSA to obtain a final concentration of TB from 3.75×10^{-6} mol.l^{-1}—1.875×10^{-5} mol.l^{-1}. The Tris-HCl buffer was replaced by phosphate buffer (0.02 mol.l^{-1}, pH 7.4) to eliminate the influence of Cl^- ions. The helical content of free and bound HSA was calculated from the mean residue ellipticity (MRE) values at 209 nm using the following equation

$$\% \alpha - \text{helix} = \frac{-\text{MRE}_{209\text{nm}} - 4\,000}{33\,000 - 4\,000} \times 100$$

Graphical presentations were evaluated by software Origin, versions 6.0 and 8.0.

RESULTS

Fluorescence spectroscopy is an effective method to study the interactions between small molecules and bio macromolecules. Fluorescence quenching refers to any process, which decreases the fluorescence intensity of a sample. The fluorescence of fluorophores within the HSA macromolecule may change when HSA interacts with other molecules, which could be reflected in the fluorescence spectra of HSA in the UV region. The changes in emission intensity value, and wavelength of emission maximum, respectively, are evaluated at experimental processing. Whereas the fluorescence intensity is influenced by a change in the polarity of the microenvironment of bio macromolecule as well as movement of charged groups in the vicinity of the fluorophores inside, hydrophobic changes in the microenvironment primarily dictate the shift in the emission maximum [14]. The shift in the emission maximum is a good index to evaluate any alternation in the hydrophobicity of the binding region [8]. Our emission fluorescence spectra of HSA in the absence and presence of TB are shown in Figure 2. It can be seen that the fluorescence intensity of the HSA decreases as a result of the increasing concentration of TB. This result points to moderate fluorescence quenching effect (Fig. 2 inset) but at the same time a remarkable deformation of emission spectra can be seen (Fig. 2). It looks like there was a blue shift observed at the highest TB concentration used in this study, which should point to any

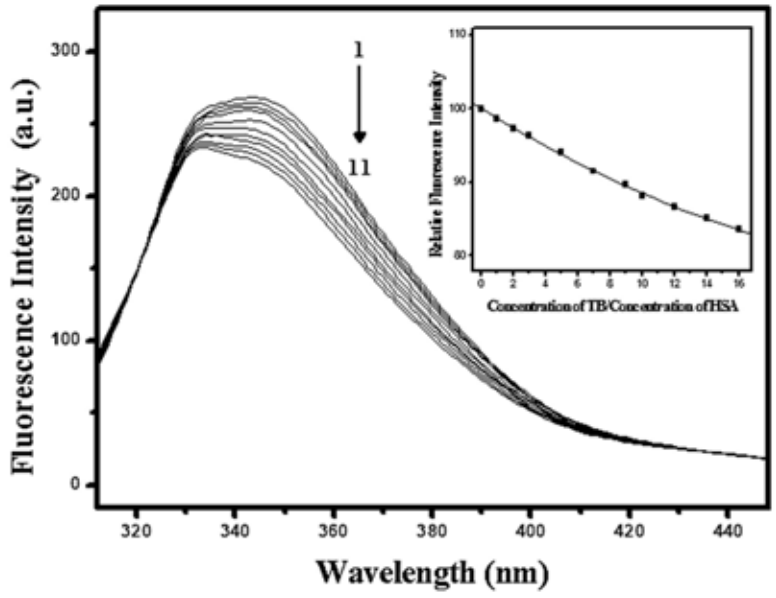

Fig. 2. Effect of tebuconazole on the fluorescence spectra of HSA

c(HSA) = 2 μmol.l^{-1}. Lines 1^{-1}1: c(TB) = 0; 2.0; 4.0; 6.0; 10.0; 14.0; 18.0; 20.0; 24.0; 28.0; 32.0 μmol.l^{-1}, respectively.
λ_{exc} = 295 nm; λ_{em} = 300—500 nm; pH = 7.4; T = 298 K
Inset: Fluorescence decrease of HSA upon TB binding at emission wavelength 344 nm

alternation in the hydrophobicity of the binding region of the HSA. However, the deformation of the emission spectrum in Fig. 2 cannot be regarded as the blue shift in the emission maximum but it probably presents a sum of two individual fluorescence spectra with maximum at 332 nm, and 351 nm respectively. Subsequently completed spectral deconvolution (not shown) has proven our above mentioned assumption. Considering a chemical structure of TB and hydrophobic cavity within the HSA macromolecule, two different modes of interaction between TB and the HSA can be assumed. At low concentration of TB, the TB molecules quench intrinsic fluorescence of HSA due to the interaction with the hydrophobic part of the protein showing a decrease in fluorescence intensity at 351 nm. On the other hand, at higher concentrations of the TB in complex, some TB molecules are inert and they enable the HSA macromolecule to have unchanged emission spectrum at 332 nm. Finally, we can assume there are two populations of the HSA macromolecules as a consequence of the interaction with TB at higher ratios.

A variety of molecular interactions can result in quenching, including excited-state reactions, molecular rearrangements, energy transfer, ground-state complex formation and collisional quenching [15]. The quenching mechanism can be described by the Stern-Volmer equation:

$$F0/F = 1 + kq\tau0[Q] = 1 + KSV\,[Q] \quad (1)$$

Where F0 and F are the fluorescence intensities of the protein in the absence and presence of the quencher (TB), respectively. [Q] is the concentration of the quencher, kq is the bimolecular rate quenching constant, τ0 is the average lifetime of the biomolecule without quencher about 10 ns for most biomolecules [16] and KSV is the Stern-Volmer constant. The inverse value of KSV represents the quencher (TB) concentration at which 50 % of the fluorophore intensity (HSA) is quenched.

The curve of (F0/F)-1 versus [Q] is shown in Fig. 3a. The corresponding kq and KSV constants for the TB/HSA complex were obtained by the fitting of the graphical representation of the Stern-Volmer equation. The quenching constants are summarized in Table 1.

Identification of binding parameters

If we assume static quenching then the association constant (KA) and the number of binding sites (n) in the bio macromolecule can be calculated by the following equation [31].

$$\log(F0/F-1) = \log KA + n\log[Q] \quad (2)$$

Fitting the plot of log(F0/F-1) versus log[Q] (so called Hill plot) for the interaction between the HSA and tebuconazole (Fig. 3b), the association constant and number of binding sites were obtained (Table 1).

To obtain more information on the binding of tebuconazole to HSA, circular dichroism spectroscopy was used to study the secondary structure of HSA and TB/HSA complex. CD is a sensitive technique to monitor the conforma-

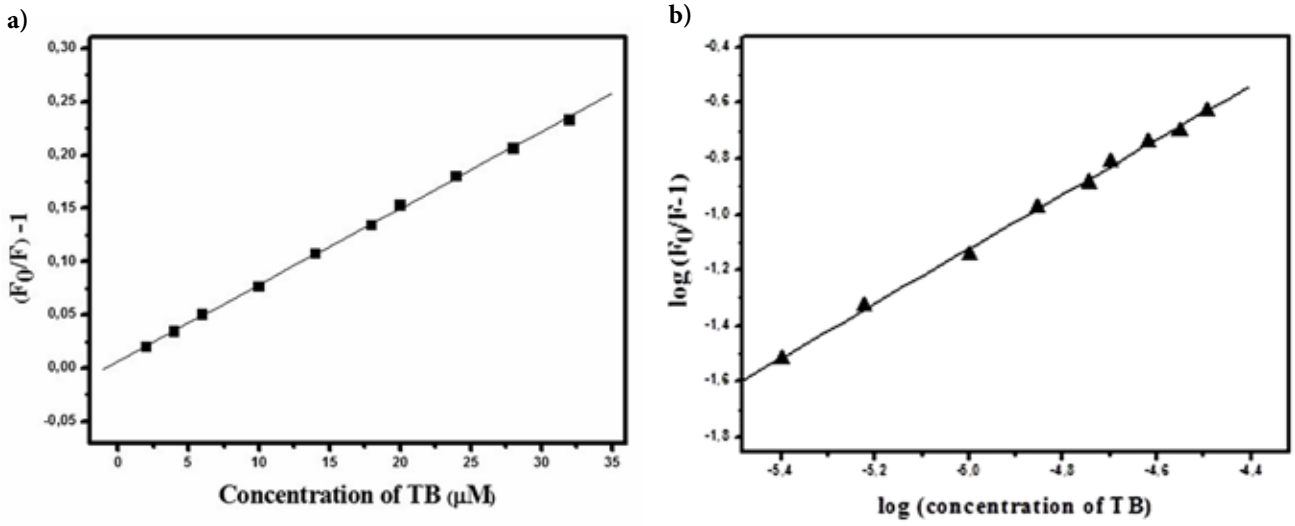

Fig. 3. a) Stern-Volmer representation of the fluorescence quenching of the HSA by tebuconazole; b) Hill plot for the determination of the binding parameters of the HSA interaction with TB
c(HSA) = 2 μmol.l^{-1}; λ_{exc} = 295 nm; λ_{em} = 344 nm, pH = 7.4;T = 298 K

Table 1. Bimolecular rate quenching constant (kq), Stern-Volmer quenching constant (KSV), association constant (KA) and number of binding sites (n) at the physiological conditions

T (K)	kq [l.mol^{-1}.s^{-1}]	KSV [l.mol^{-1}]	KA [l.mol	n
298	7.26×10^{11}	7.26×10^{3}	8.51×10^{3}	1.01

tional changes in proteins. Far UV CD measurements were performed in the presence of TB at different concentrations but the CD spectra stayed identical for the final concentration ratio 5/1 (Fig. 4).

As can be seen from Fig. 4, the CD spectra of HSA and the complex, respectively, display two negative bands in the ultraviolet region at 209 and 223 nm, characteristic of the α-helical structure of protein. The reasonable explanation is that the negative peak at 209 nm is contributed to $\pi \rightarrow \pi^*$ transition and 223 nm peak is contributed to $n \rightarrow \pi^*$ transfer for the peptide bond of α-helix [33].

As shown in Figure 4, TB alone (dotted line) does not show any optical activity in this region. The addition of TB to HSA leads to an increase in the CD signal without significant shift of the peaks indicating that the binding of TB to HSA induces an increase in the α-helical content of HSA. The α-helix content of HSA increased from 55% to 60% upon TB binding at a molar ratio of TB/HSA of 1/1 and 5/1, implying that the TB binding results in a conformation change that stabilizes the HSA structure by increasing its α-helical content. We assume that the increase of the α-helical content of HSA is realized at the expense of the random coil content when TB binds to the protein.

DISCUSSION

A better understanding of the interaction of the TB and other fungicides with various possible cellular targets is essential for the determination of their function in biological systems. The present contribution was focused on the results obtained in the study of TB associations with serum albumins represented by HSA.

The value of the association constant (Table 1) of the TB/HSA complex induced a slight binding affinity between the TB and the HSA. The interaction of four triazole fungicides (triadimefon, imazalil, myclobutanil, penconazole) with HSA has been reported in a comprehensive study by Zhang et al. [34]. The association constants determined by fluorescence quenching in this study range from 3.96×10^3 l.mol^{-1} (triadimefon) to 8.47×103 l.mol^{-1} (penconazole) [34]. Our association constant for the TB/HSA complex (8.51×103 l.mol^{-1}) falls into this interval very well. The number of binding sites for TB, which is close to 1 (Table 1) corresponded with those obtained by Zhang

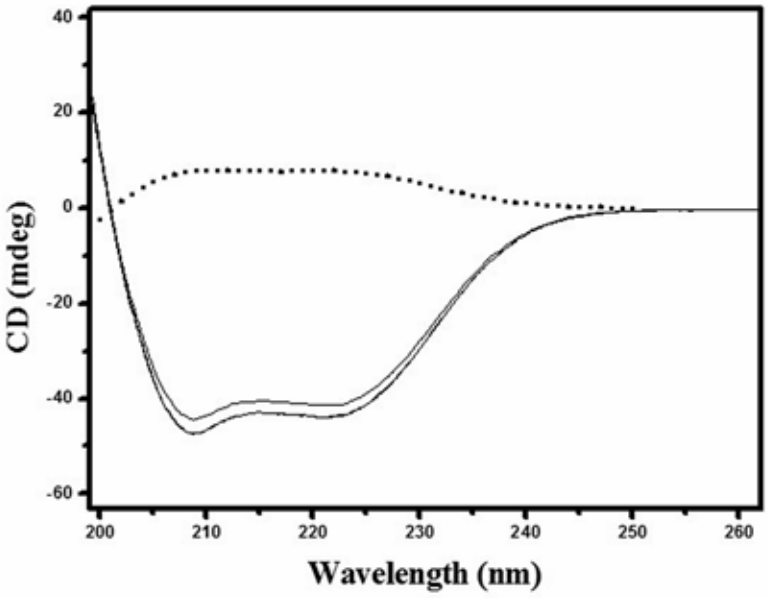

Fig. 4. Far UV CD spectra of HSA in absence and presence of TB
c(HSA) = 3.75 μmol.l^{-1}, c(TB) = 0; 3.75; 18.75 μmol.l^{-1}, phosphate buffer pH = 7.4

et al. [34]. Considering a chemical structure of all of the estimated triazole fungicides we may assume that both tebuconazole and penconazole molecules look similar. This fact can be one of many other reasons explaining their very similar binding affinity expressed by the association constants.

Comparing the binding affinities of other pesticides to HSA, we can consider the studies by Wang et al. [29] and Wang et al. [30]. They used the spectroscopic approach to find association constants for imidacloprid/HSA and thiacloprid/HSA. Both molecules represented the neonicotinoid insecticides currently being used in agriculture. Comparing the association constants of triazole and neonicotinoide pesticides we can declare that the binding affinity of triazole fungicides, including tebuconazole to HSA, is lower than those of neonicotinoides. But the differences are not very expressive.

It has previously been reported that the binding of certain ligands such as ciproflaxin [1], virstatin [13], phycocyanobilin [20] may cause a conformational change in HSA with an accompanying increase in its α-helical content and protein structural stabilization. This phenomenon is quite striking for protein-ligand systems with high affinities, e.g., binding of biotin to streptavidin causes the disappearance of the band arising from unordered structure in FT-IR spectra [11]. Surprisingly, an increase in the TB concentration causes the CD signal of the HSA to be increased, which indicates an increase of the helical secondary structure content in the HSA macromolecule. On the contrary, with the above mentioned knowledge about the tendency to increase the helical content in high binding affinity ligands, the binding affinity of TB to HSA is only slight. But Wang et al. [29] have obtained the same result for a slightly bound imidacloprid to HSA. The increase in negative ellipticity as shown in Fig. 4 might be due to the shielding of the peptide strand in the HSA macromolecule due to the increase in hydrophobicity on binding with TB [28]. This conclusion agrees with the result of the fluorescence quenching experiment.

The present study investigated the interaction of the triazole fungicide tebuconazole with HSA by spectroscopic methods. TB can interact with HSA *in vitro* under simulated physiological conditions. Considering a static mechanism of fluorescence quenching of HSA by the TB, we have determined the association constant which expresses the binding affinity between both molecules. The value of this constant indicates a slight binding affinity in comparison to other ligands, but it corresponds with the binding parameters of other triazole fungicides very well. Furthermore, the interaction of TB led to slight conformational changes of the HSA macromolecule.

ACKNOWLEDGEMENT

This study was supported by the project VEGA 1/0176/16.

REFERENCES

1. **Ahmad, B., Parveen, S., Khan, R. H., 2006:** Effect of albumin conformation on the binding of ciprofloxacin to human serum albumin: a novel approach directly assigning binding sites. *Biomacromolecules,* 7, 1350—1356.
2. **Bayer Cropscience Limited 2005:** Environmental information sheet Folicur® MAPP number 11278. *CPA Guidance Notes version 3.* ©EIS.
3. **Clausen, C. A., Yang, W. V., 2007:** Protecting wood from mould, decay, and termites with multicomponent biocide systems. *Int. Biodeter. Biodegr.*, 59, 20—24.
4. **Cui, Y., Guo, J. F., Xu, B. J., Chen, Z. Y., 2006:** Binding of chlorpyrifos and cypermethrin to blood proteins. *Pestic. Biochem. Phys.*, 85, 110.
5. **Di Renzo, F., Broccia, M. L., Giavini, E., Menegola, E., 2007:** Citral, an inhibitor of retinoic acid synthesis, attenuates the frequency and severity of branchial arch abnormalities induced by triazole-derivative fluconazole in rat embryos cultured *in vitro. Reprod. Toxicol.*, 24, 326—332.
6. **EFSA: Conclusion on the Peer Review of Tebuconazole 2008:** *EFSA Scientific Report,* 176, 1—109.
7. **Elsaesser, D., Schulz, R., 2008:** Mitigation of fungicide pollution in vegetated agricultural surface waters: GIS modelling and monitoring in the field. In *Conference Proceeding from the SETAC Europe 18th Annual Meeting*, SETAC, Warsaw, 406—407.
8. **Froehlich, E., Mandeville, J. S., Jenings, C. J., Sedaghat-Herati, R., Tajmir-Riahi, H. A., 2009:** Dendrimers bind human serum albumin. *J. Phys. Chem. B*, 113, 6986—6993.
9. **Fustinonu, S., Mercadante, R., Pollrdri, E., Rubino, F., Colosio, C., Moretto, A., 2012:** Biomonitoring human exposure to tebuconazole. *Toxicol. Lett.*, 211, S51.
10. **Gelamo, E. L., Silva, C. H. T. P., Imasato, H., Tabak, M., 2004:** On the hydrodynamics and temperature dependence

of the solution conformation of human serum albumin from viscometry approach. *Biochim. Biophys. Acta*, 1700, 24.

11. **Gonzáles, M., Bagatolli, L. A., Echabe, I., Arrondo, J. L. R., Argarana, C. E., Cantor, Ch. R., Fidelio, G. D., 1997:** Interaction of biotin with streptavidin. *J. Biol. Chem.*, 272, 11288—11294.
12. **Holečková, B., Dianovský, J., Šiviková, K., Mesarč, M., 2010:** Detection of chromosomal aberrations in cattle cells after conazole fungicide treatment. *Toxicol. Lett.*, 196S, S37—S351.
13. **Chatterjee, T., Pal, A., Chatterjee, B. K., Chakrabarti, P., 2012:** Interaction of virstatin with human serum albumin: spectroscopic analysis and molecular modelling. *PloS ONE*, 7, e37468.
14. **Khana, N. C., Tokuda, M., Waisman, D. M., 1986:** Conformational changes induced by binding of divalent cations to calregulin. *J. Biol. Chem.*, 261, 8883—8887.
15. **Lakowicz, J. R., 1983:** Quenching of Fluorescence. In **Lakowicz, J. R.:** *Principles of Fluorescence Spectroscopy*, Plenum Press: New York, NY, USA, 199—227.
16. **Lakowicz, J. R., Weber, G., 1973:** Quenching of fluorescence by oxygen: a probe for structural fluctuations in micro molecules. *Biochemistry*, 12, 4161—4170.
17. **Liang, Y., Mengli, C. H., Yihua, L., Wenjun, G., Guonian, Z., 2013:** Thyroid endocrine disruption in zebrafish larvae following exposure to hexaconazole and tebuconazole. *Aquat. Toxicol.*, 138—139, 35—42.
18. **Montuelle, B., Dorigo, A., Berard, B., Volat, A., Bouchez, A., Tlili, A., Gouy, V., Pesce, S., 2010:** The periphyton as a multi metric bio indicator for assessing the impact of land use on rivers: an overview of the ArdiSres-Morcille experimental watershed (France). *Hydrobiologia*, 657, 123—141.
19. **Peters, T. Jr., 1995:** Ligand binding by albumin. In **Peters, T. Jr.:** *All about Albumin.* Academic Press, San Diego, 76—132.
20. **Radibratovic, M., Minic, S., Stanic-Vucinic, D., Nikolic, M., Milcic, M., Cirkovic Velickovic, T., 2016:** Stabilization of human serum albumin by the binding of phycocyanobili, a bioactive chromophore of blue-green alga spirulina: Molecular dynamics and experimental study. *PloS ONE*, 11, DOI:10.1371/journal.pone.0167973.
21. **Robinson, J. F., Tonk, E. C. M., Verhoef, A., Piersma A. H., 2012:** Triazole induced concentration-related gene signatures in rat whole embryo culture. *Reprod. Toxicol.,* 34, 275—283.
22. **Schummer, C., Salquébre, G., Briand, O., Millet, M., Appenzeller, B. M. R., 2012:** Determination of farm workers' exposure to pesticides by hair analysis. *Toxicol. Lett.,* 210, 203—210.
23. **Silva, D., Cortez, C. M., Bastos, J. C., 2004:** Methyl parathion interaction with human and bovine serum albumin. *Toxicol. Lett.*, 147, 53.
24. **Sugio, S., Kashinma, A., Mochizuki, S., Noda, M., Kobayashi, K., 1999:** Crystal structure of human serum albumin at 2.5 Å resolution. *Protein Eng.*, 12, 439.
25. **Sulkowska, A., Maciazek-Jurczik, M., Bojko, B., Rownicka, J., Zubik-Skupien, I., Temba, E., et al., 2008:** Competitive binding of pheylbutazone and colchicines to serum albumin in multidrug therapy: a spectroscopic study. *J. Mol. Struct.,* 881, 97.
26. **Šiviková, K., Dianovský, J., Holečková, B., Galdíková, M., 2010:** Effects of two selected fungicides on the frequency of SCI in bovine peripheral lymphocytes. *Toxicol. Lett.,* 196S, S37—S351.
27. **U. S. Environmental Protection Agency (U. S. EPA), 2006:** Chemicals Evaluated for Carcinogenic Potential. Office of Pesticide Programs, *U.S. Environmental Protection Agency,* Washington, DC.
28. **Varshney, A., Ansari, M., Zaidi, N., Ahmad, E., 2014:** Analysis of binding interaction between antibacterial ciprofloxacin and human serum albumin by spectroscopic techniques. *Cell Biochem. Biophys.,* DOI 10.1007/s12013-014-9863-1.
29. **Wang, C., Li, Y., 2011:** Study on the binding of propiconazole to protein by molecular modeling and a multi spectroscopic method. *J. Agr. Food Chem.,* 59, 8507—8512.
30. **Wang, Y., Tang, B., Zhang, H., Zhou, Q., Zhang, G., 2009:** Studies on the interaction between imidacloprid and human serum albumin: Spectroscopic approach. *J. Photoch. Photobio. B.,* 94, 183—190.
31. **Xiang, G. H., Tong, C. L., Lin, H. Z., 2007:** Nitroaniline isomers interaction with bovine serum albumin and toxicological implications. *J. Fluoresc.*, 17, 22804—22809.
32. **Yan, C. N., Mei, P., Guan, Z. J., Liu, Y., 2007:** Studies on the thermodynamics features of the interaction between imidacloprid and bovine serum albumin. *Chin. J. Chem.*, 25, 1085.
33. **Yang, P., Gao, P., 2002:** *The Principle of Bioinorganic Chemistry,* Science Press, Beijing, 322—342.
34. **Zhang, J., Zhuang, S., Tong, C. H., Liu, W., 2013:** Probing the molecular interaction of triazole fungicides with human serum albumin by multi spectroscopic techniques and molecular modeling. *J. Agr. Food Chem.*, 61, 7203—7211.

Received March 29, 2018
Accepted May 18, 2018